Departamento de Genética
Universidad de Sevilla

# Role of ribosomal proteins eL40 and eS12 in the biogenesis and function of yeast ribosomes

*Memoria presentada para aspirar al grado de*
*Doctor en Biología*

**V.° B.°: El director de la Tesis** | **El doctorando**

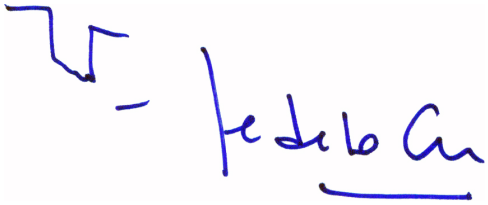

**Jesús de la Cruz Díaz**

**Sara Martín Villanueva**

This work was funded by a FPI fellowship from the Spanish Ministry of Economy and Competitiveness (BES-2014-069646), by project grants from the Spanish Government (BFU2013-42958-P and BFU2016-75352-P), and a short-term fellowship from the Spanish Ministry of Economy and Competitiveness (EEBB-I-2017-12401).

A mis abuelos,

por creer siempre en mi.

# INDEX

**1. RESUMEN** ..... 1

**2. INTRODUCTION** ..... 5

- The ribosome: Composition, evolution and function ..... 7
- Ribosomal proteins in *S. cerevisiae* ..... 9
- Ribosome biogenesis in *S. cerevisiae* ..... 11
  - Transcription and processing of pre-rRNAs ..... 13
  - Assembly of the SSU: Binding and dissociation of the 90S pre-ribosome ..... 16
  - Assembly of the SSU: Nucleocytoplasmic stages ..... 18
  - Nucleolar and nucleoplasmic assembly of the large r-subunit ..... 20
  - Cytoplasmic stages of the large r-subunit ..... 23
- Folding, transport and degradation of ribosomal proteins ..... 24
- Ubiquitin and ubiquitin-like proteins ..... 27
  - Ubiquitination and deubiquitination ..... 29
  - Functions of ubiquitination and the ubiquitin code ..... 31
  - Ubiquitin synthesis: ubiquitin genes ..... 33
  - Role of ubiquitin in r-proteins eL40 and eS31 ..... 36

**3. OBJECTIVES** ..... 38

**4. RESULTS** ..... 43

**CHAPTER 1 – The ubiquitin moiety of Ubi1 is required for proper production of ribosomal protein eL40 in *Saccharomyces cerevisiae*** ..... 45

- INTRODUCTION ..... 47
- RESULTS ..... 53
  - Generation of *ubi1* mutants for the phenotypic analysis of the ubiquitin-L40A fusion protein ..... 53
  - The *ubi1Δub* ubiquitin deletion mutant displays a slow-growth phenotype ..... 54
  - The *SMT3*-S-*eL40S ubi2Δ* mutant displays a slow-growth phenotype ..... 56

- Role of the ubiquitin and SUMO moieties on the expression levels of eL40A.....57
- The genomic *ubi1Δub*-HA and *SMT3-S-eL40A*-HA mutations affect 60S r-subunit biogenesis and translation.....58
- Expression *in trans* of free ubiquitin fails to rescue the deficiencies of the *ubi1Δub*-HA *ubi2Δ* and *SMT3-S-eL40A*-HA *ubi2Δ* mutants.....61
- Ubiquitin and SUMO modestly prevent eL40 or S31 protein aggregation.....63

• DISCUSSION.....67

• MATERIALS AND METHODS.....71

**CHAPTER 2 – Role of the beak ribosomal protein eS12 in ribosome biogenesis and function in *Saccharomyces cerevisiae*** .....77

• INTRODUCTION.....79

• RESULTS.....83

- Loss of eS12 results in a severe growth defect.....83
- Loss of eS12 leads to a strong 40S r-subunit shortage.....85
- Deletion of *RPS12* impairs rRNA processing.....85
- The *rps12Δ* deletion mutant accumulates the 20S pre-rRNA in the cytoplasm.....89
- The accumulated 20S pre-rRNA is not efficiently incorporated into translating ribosomes in *rps12Δ* cells.....91
- Dynamics of the *trans*-acting factors Enp1 and Ltv1 during 40S r-subunit biogenesis in the *rps12Δ* and *ubi3Δ* mutants.....94
- The absence of eS12 or eS31 induces an increase in translational misincorporation.....98

• DISCUSSION.....101

• MATERIALS AND METHODS.....105

**5. GENERAL DISCUSSION**.....113

**6. CONCLUSIONS**.....120

**7. BIBLIOGRAPHY**.....124

# 1. RESUMEN

Uno de los procesos más importantes que se dan en las células de todos los seres vivos es la traducción proteica, proceso en el que la información contenida en el ARN mensajero (ARNm), que actúa como molde, se utiliza para dar lugar a proteínas mediante la formación de enlaces peptídicos entre aminoácidos. Este proceso es catalizado por los ribosomas, complejos ribonucleoproteicos presentes en todos los organismos. Los ribosomas están compuestos por dos subunidades, una subunidad grande (60S en eucariotas) y una subunidad pequeña (40S en eucariotas).

La síntesis de ribosomas se encuentra rigurosamente regulada porque es un proceso esencial y complejo que supone una gran gasto energético para la célula. La biogénesis de ribosomas está altamente conservada en eucariotas, donde se inicia en el nucléolo, continúa en el nucleoplasma y finaliza en el citoplasma. Gracias a este alto grado de conservación, en esta tesis se ha trabajado con la levadura *Saccharomyces cerevisiae*, el organismo modelo más utilizado para el estudio de este proceso a lo largo de los años. En este organismo, la biogénesis de ribosomas consiste en el ensamblaje de forma ordenada de las 33 proteínas ribosómicas de la subunidad pequeña con el ARN ribosómico (ARNr) 18S para dar lugar a la subunidad 40S madura y de las 46 proteínas ribosómicas de la subunidad grande con los ARNr 25S, 5.8S y 5S, formando la subunidad 60S madura, que al unirse en el citoplasma constituyen el ribosoma completo 80S, competente para la traducción. Además de los ARNr y las proteínas ribosómicas, en este proceso intervienen más de 200 factores que no formarán parte del ribosoma maduro. Aunque se ha estudiado el papel que ejercen estos factores y las proteínas ribosómicas en la biogénesis de ribosomas, aún queda por dilucidar la contribución de algunos de ellos. En esta tesis, haciendo uso de herramientas genéticas y bioquímicas, se ha llevado a cabo la caracterización funcional de las proteínas ribosómicas eL40, eS31 y eS12 de *S. cerevisiae*.

Las proteínas ribosómicas eL40 y eS31 tienen una peculiaridad: de forma natural, ambas se traducen como un precursor fusionadas a ubiquitina. La ubiquitina es una proteína altamente conservada implicada varios procesos celulares, con un papel importante en degradación proteica. En prácticamente todos los organismos eucariotas, la ubiquitina se genera por corte proteolítico de precursores de poli-

ubiquitina o, curiosamente, fusionada a las proteínas ribosómicas eL40 y eS31. El papel específico que desempeña la fusión de ubiquitina en estas proteínas ribosómicas y, en concreto, cómo afecta a la biogénesis de ribosomas ha sido objeto de estudio en esta tesis. Los resultados indican que se ve reducida la expresión de eL40 en ausencia de la fusión de ubiquitina, afectando negativamente al crecimiento celular y a la cantidad de subunidades ribosómicas 60S, de manera similar a lo descrito anteriormente para eS31. Curiosamente, un incremento en la dosis de eL40 suprime estos fenotipos. Esto nos sugiere que la fusión de ubiquitina podría servir como chaperona molecular para facilitar la expresión y el plegamiento de eL40 y eS31.

Por otro lado, se ha analizado el papel del pico ribosómico en la biogénesis y función de los ribosomas. El pico es una estructura exclusiva de eucariotas que se encuentra en la cabeza de la subunidad pequeña del ribosoma y está formada por las proteínas eS12, eS31 y eS10. A través de la caracterización funcional de eS12 y eS31 se ha investigado la contribución del pico a la biogénesis de ribosomas. La ausencia de ambas proteínas provoca defectos similares y muy drásticos en el crecimiento celular. La biogénesis de ribosomas también se ve afectada ya que observamos un déficit de subunidades ribosómicas 40S y fallos en el procesamiento citoplasmático del precursor de ARNr 20S. Además, los resultados sugieren que ambas proteínas son primordiales para que la elongación traduccional se lleve a cabo de forma eficiente. Teniendo en cuenta todos estos datos, consideramos que la formación del pico ribosómico es un pre-requisito para la maduración y función de las subunidades ribosómicas 40S.

# 2. INTRODUCTION

## THE RIBOSOME: COMPOSITION, EVOLUTION AND FUNCTION

Ribosomes are the molecular organelles that universally catalyse the protein synthesis, process also known as translation. During translation, the messenger RNA (mRNA) serves as a template to produce proteins. Hence, ribosomes are essential organelles with an important task in gene expression: the decoding of the genetic code in all organisms (Wool, 1979).

Mature ribosomes consist of two subunits, one large (LSU) and one small (SSU), which both are composed of ribosomal RNAs (rRNAs) and proteins (r-proteins) associated through a network of intermolecular bridges. Both r-subunits fulfil different tasks in protein synthesis: the LSU catalyses the peptide bond formation and the SSU is responsible for the decoding process (Schmeing and Ramakrishnan, 2009). In prokaryotes, the LSU and SSU are also called 50S and 30S, respectively; the interaction of these subunits forms the 70S ribosomes (Davis and Williamson, 2017). In turn, in eukaryotes, mature ribosomes known as 80S are composed of large 60S subunits and small 40S subunits **(Figure 1)**. Furthermore, mitochondria and chloroplasts have their own ribosomes. In the budding yeast *Saccharomyces cerevisiae*, the eukaryote model organism used in this Thesis work, the LSU is composed of rRNAs 25S, 5.8S and 5S and 46 r-proteins, whereas the SSU consists of the rRNA 18S and 33 r-proteins (Ben-Shem et al., 2011).

Over the last years, cryogenic electron microscopy (cryo-EM) and crystallography studies have provided crucial information about the structure, function and synthesis of ribosomes (Ben-Shem et al., 2011; Klinge et al., 2012). From the structures, we learnt that the r-proteins are mostly distributed on the solvent-surface of the ribosome, whereas the rRNAs are mainly present in the intersubunit interface, where the functional activities of the ribosome reside (Wilson and Doudna Cate, 2012). Four structural domains that are sequentially assembled are distinguished in the SSU: the body, the platform, the head and the beak **(Figure 1A)**. The beak region is under study in this Thesis work **(see chapter 2)**. In the LSU there is a central protuberance, where the peptidyltransferase centre (PTC) is present and the L1 and acidic r-stalks **(Figure 1B)** (Ben-Shem et al., 2011). Although apparently monolithic, the LSU is really

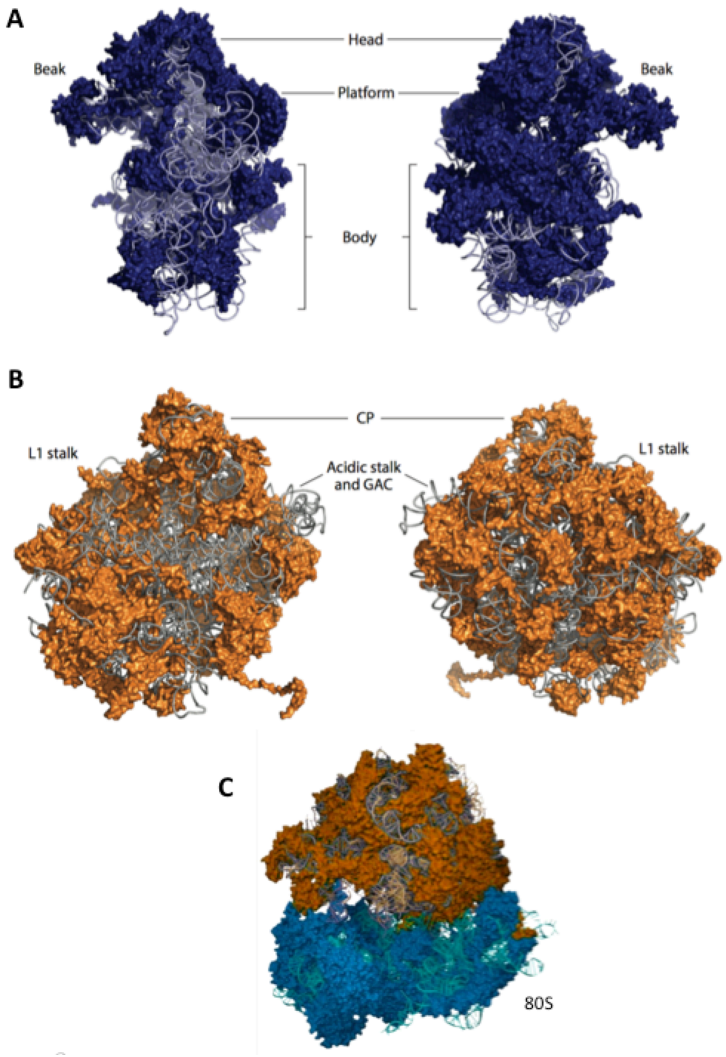


**FIGURE 1. Crystal structure of ribosomal subunits from *S. cerevisiae*. (A)** The subunit interface (left) and the solvent-exposed surface (right) of the small subunit. **(B)** The subunit interface (left) and the solvent-exposed surface (right) of the large subunit. **(C)** Association of 40S and 60S subunits through intermolecular bridges to form the complete 80S ribosome. Both ribosomal subunits are composed of r-proteins and rRNAs. The 60S r-proteins are coloured in orange and the 40S r-proteins are coloured in blue. The rRNAs are coloured in grey. CP, central protuberance; GAC, GTPase-activation center. Adapted from (de la Cruz et al., 2015).

partitioned into sections that assemble sequentially.

The composition and the structure of r-subunits are well conserved in evolution, being eukaryotic ribosomes larger and more complex than those from prokaryotes. Prokaryotic and eukaryotic ribosomes share a common core, which is in charge of the fundamental reactions during the translation process **(Figure 2)**. However, there are kingdoms-specific elements such as different r-proteins and specific extension

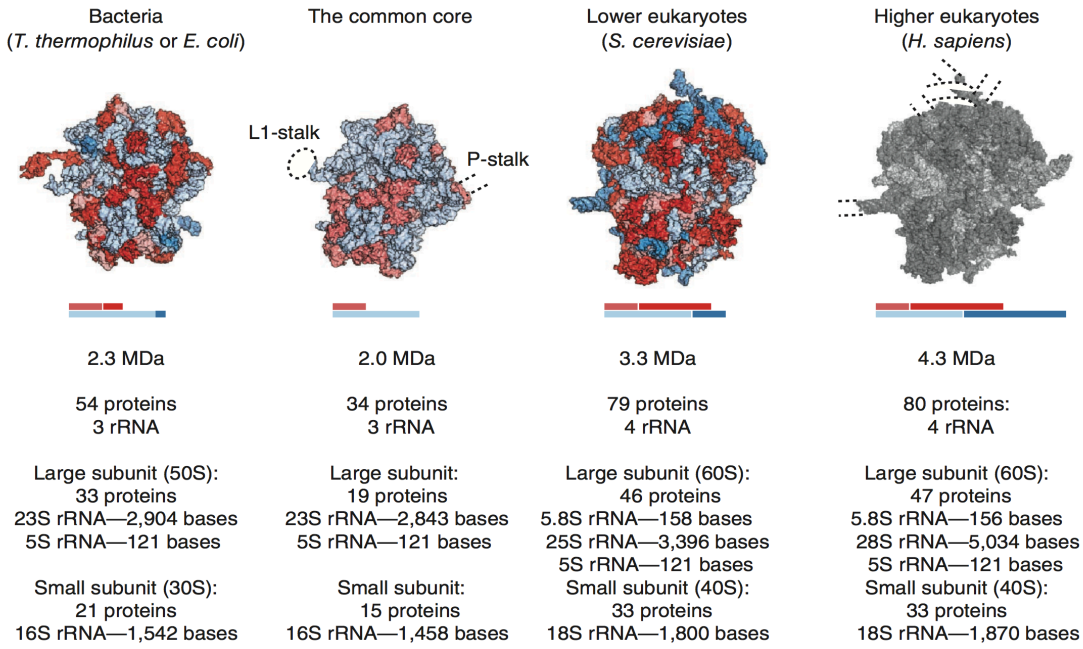


**FIGURE 2. Composition of bacterial and eukaryotic ribosomes and the common core.** The conserved ribosomal core between bacteria and eukaryotes is composed of RNA (light blue) and proteins (light red). Domain-specific proteins, extensions and protein insertions (dark red), and extension segments in ribosomal RNA (dark blue) are shown. Dashed lines correspond to flexible elements from higher eukaryotes. Adapted from (Melnikov et al., 2012).

segments in rRNAs and r-proteins (Melnikov et al., 2012; Melnikov et al., 2018). Thus, ribosomes grow in size upon transition from bacteria to eukaryotes. Translation initiation is quite different between distinct kingdoms; thus, most of eukaryotic-specific elements of the SSU are involved in this process.

### RIBOSOMAL PROTEINS IN *S. cerevisiae*

The r-proteins have some peculiarities; generally, most r-proteins are small, basic (except proteins of the acidic stalk) and have intrinsically disordered domains. Their basic nature is important to neutralize the negative charges of the rRNAs, given that practically all r-proteins directly interact with rRNA in mature ribosomes. Mostly, r-proteins are distributed on the solvent-surface of the ribosome (Ben-Shem et al., 2011). However, most eukaryotic r-proteins also contain long specific extensions that can penetrate deeply into the ribosome **(Figure 3)**. Some of these extensions are important to stabilize rRNA junctions or to mediate contacts between ribosomes and

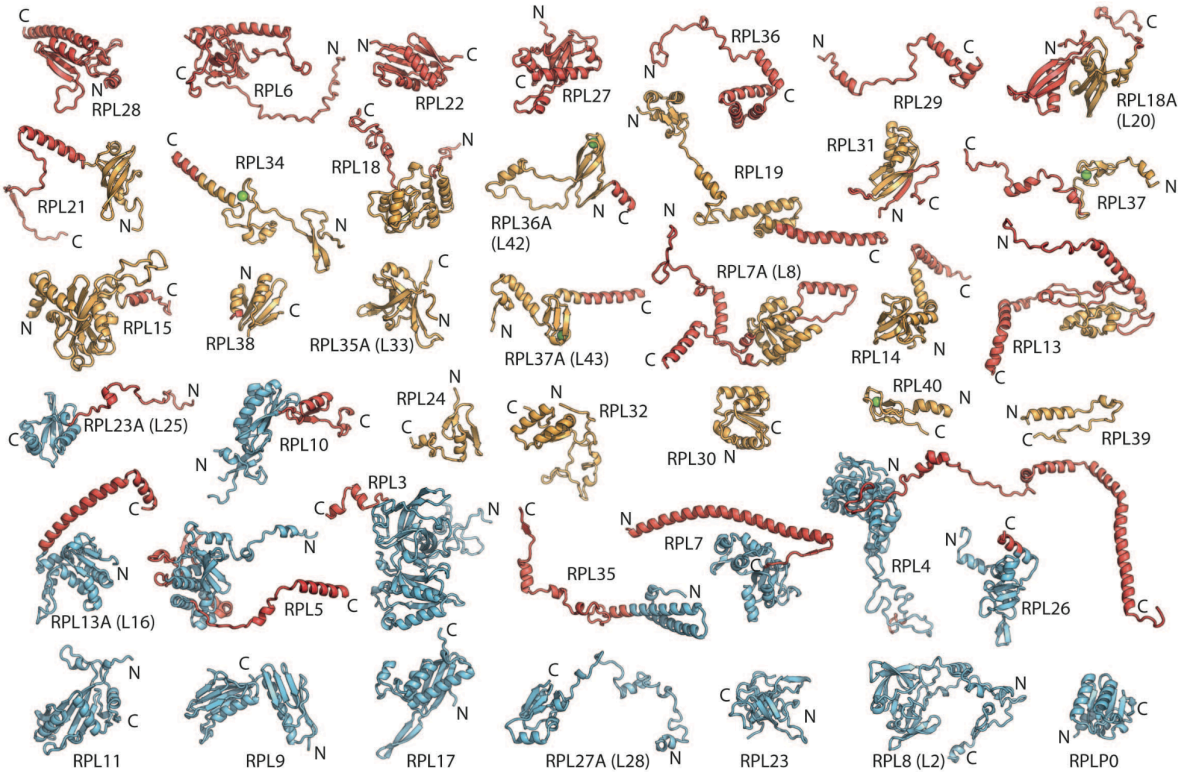


**FIGURE 3. Ribosomal proteins of the large ribosomal subunit**. The large r-subunit of *Tetrahymena thermophila* contains 42 r-proteins. Six of them are eukaryotic-specific and 16 are present in all domains of life. Eukaryotic-specific extensions and proteins are depicted in red. Protein cores found in all kingdoms are depicted in light blue and proteins with archaeal homologs are in gold. The positions of the N- and C-terminal ends are indicated. The human nomenclature is used and the yeast homolog is shown in parentheses when the yeast nomenclature differs. Adapted from (Klinge et al., 2011).

their ligands (Melnikov et al., 2018). Furthermore, these extensions can serve as nuclear localization signals to deliver the r-proteins to the nucle(ol)us, where ribosome biogenesis takes place, or as chaperones binding site to help their transport through the nuclear pore complex (NPC), offering simultaneous protection predominantly against protein aggregation (e.g. (Fernández-Pevida et al., 2016) (Pillet et al., 2015)). In mammal cells, additional roles have been described for these extensions. For example, extension of uL13 (formerly L16) controls translation of inflammatory mRNAs (Mazumder et al., 2003) and extensions of uL5 and uL18 (formerly L11 and L5 respectively) control programmed cell death through inhibition of the oncoprotein Mdm2, which prevents ubiquitination of p53 (Deisenroth and Zhang, 2010).

As mentioned before, there are 79 r-proteins in *S. cerevisiae*; 59 of these r-proteins are encoded by two paralogous genes (Kellis et al., 2004). Usually, the amino

acid sequences from both paralogues are very similar but not identical and the effects of deleting one of the two genes are different; thus, it has been suggested the possibility of paralogue-specific functions (Chaillou, 2019). Assembly of a specific paralogue r-protein or its counterpart results in heterogeneous ribosome populations, which have been speculated to be able to perform different cellular physiological roles. Changes in the ribosome composition can occur at additional levels: posttranslational modifications of r-proteins, alternative forms of rRNAs and post-transcriptional modifications of rRNAs, as well as binding to other non-ribosomal proteins (Genuth and Barna, 2018). Given this heterogeneity, the idea of specialized ribosomes has recently arisen (Chaillou, 2019). This specialization could imply a new level of regulation of gene expression.

## RIBOSOME BIOGENESIS IN *S. cerevisiae*

Ribosome synthesis is a very important cellular task. Yeast cells produce around 2000 ribosomes per minute in exponential growth conditions (Warner, 1999). This process consumes a lot of cellular resources as it requires the synthesis of rRNAs, r-proteins and the function of 76 small nucleolar RNAs (snoRNAs) and more than 200 non-ribosomal *trans*-acting proteins, also known as ribosome assembly factors (Woolford and Baserga, 2013). These factors provide speed, accuracy, timing and directionality to the ribosome synthesis process and participate in its regulation.

Ribosome biogenesis starts in the nucleolus, where pre-rRNAs are produced and nascent pre-ribosomal particles are formed **(Figure 4)**. These pre-ribosomal particles travel through the nucleoplasm to the cytoplasm, where the last maturation steps take place (Woolford and Baserga, 2013). This route is enormously dynamic, since many factors and proteins must associate and further dissociate upon performing their respective functions. Moreover, a large number of structural rearrangements occur. Ribosome biogenesis must be rigorously regulated as defects in ribosome assembly have deleterious consequences. In fact, dysregulation of ribosome assembly have been closely linked to human diseases (Teng et al., 2013).

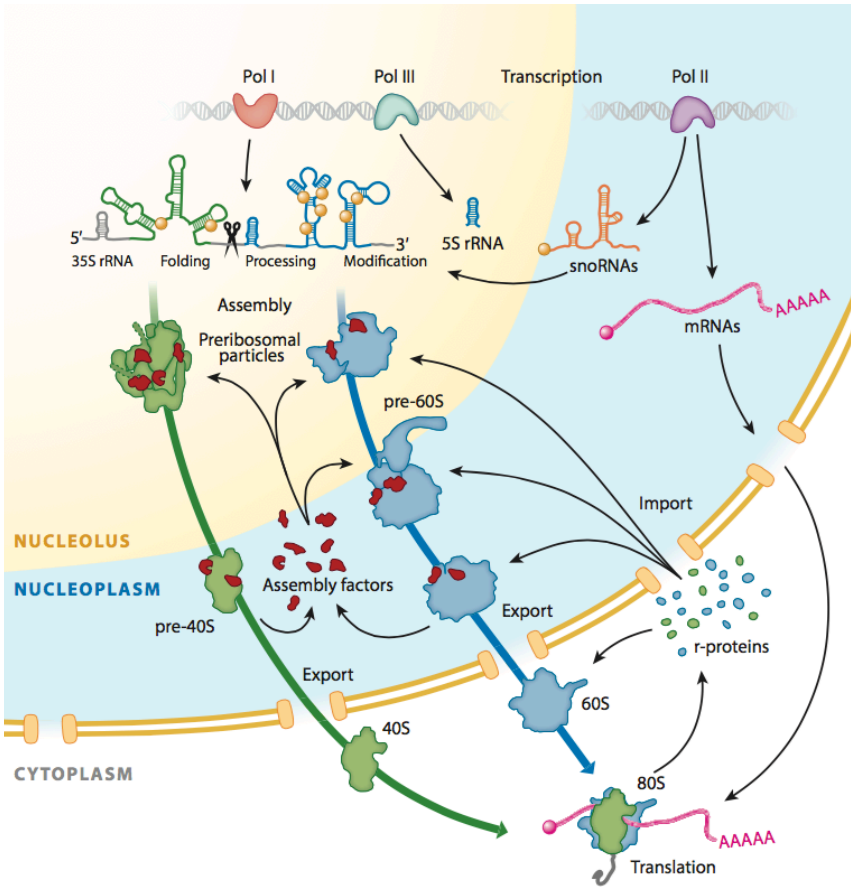


**FIGURE 4. Eukaryotic ribosome assembly route.** Eukaryotic ribosome assembly begins with the transcription of the rDNA in the nucleolus by the RNA polymerase I, which transcribes the 35S pre-rRNA and the RNA polymerase III, which transcribes the 5S rRNA. On the other hand, the RNA polymerase II synthesizes the snoRNAs and the mRNAs that translate into the r-proteins. Ribosome assembly factors and r-proteins associate with the nascent pre-rRNAs to form pre-ribosomal particles. 40S and 60S r-subunits undergo apparently independent maturation pathways in which many different assembly factors transiently associate. Pre-ribosomal subunits travel across the nucleoplasm to the cytoplasm, where the last assembly factors dissociated and the mature 80S ribosome acquires functionality. Adapted from (Bassler and Hurt, 2018).

Ribosome production depends on nutrient availability, adaptation to stress and the capability to progress through the cell cycle. The TORC1 and protein kinase A (PKA) signalling pathways mediate this regulation **(Figure 5)**. These pathways control the level of both pre-rRNAs and r-proteins transcriptionally and post-transcriptionally (de la Cruz et al., 2018).

The first step in ribosome biogenesis is the transcription of the ribosomal DNA (rDNA). In *S. cerevisiae*, there are around 150 tandem repeats of the rDNA transcription unit located in chromosome XII **(Figure 6)**. Each transcriptional unit

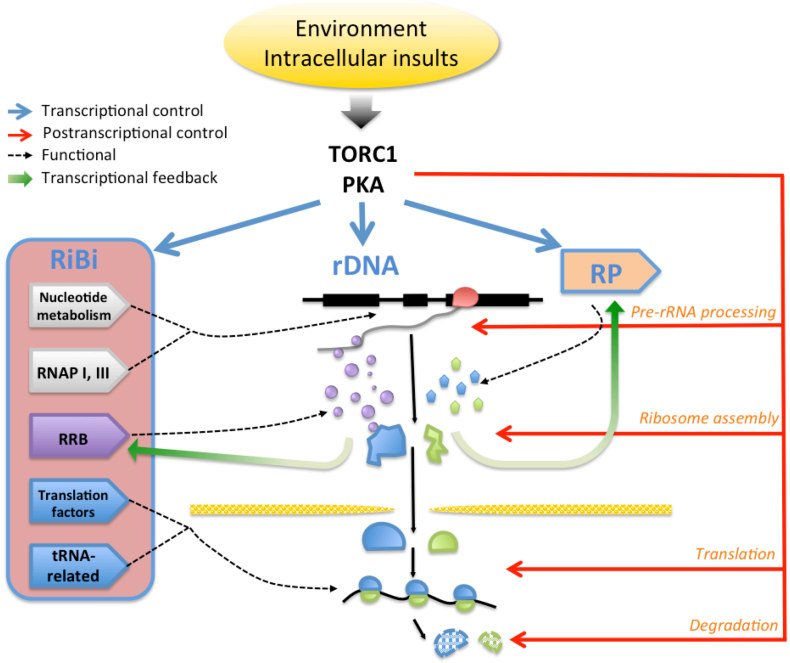


**FIGURE 5. Regulation of ribosome biogenesis in *S. cerevisiae*.** The TORC1 and PKA pathways regulate ribosome biogenesis at different levels. They control the transcription of ribosomal proteins (RP) and ribosomal biogenesis (RiBi) regulons and rDNA. Post-transcriptionally, they regulate pre-rRNA processing, ribosome assembly, translation and the degradation of r-subunits. Furthermore, a feedback system specifically regulates r-protein and rRNA and ribosome biosynthesis (RRB) genes. Adapted from (de la Cruz et al., 2018).

contains the pre-rDNA unit 35S (that will be processed to produce the mature 18S, 5.8S and 25S rRNAs) and 5S rDNA unit (Nomura et al., 2004). Despite the high copy number of these repeats, only about half of the 150 rDNA copies are actively transcribed simultaneously under exponential growth conditions, while the other copies are maintained inactivated. Growth conditions can modulate this proportion since rDNA is highly transcribed when nutrients are abundant but certain environmental stresses like a depletion of nutrients leads to lower transcription level of rDNA. The high number of copies could serve as a protection against mutations, thus, maintaining genome integrity (Ide et al., 2010).

### Transcription and processing of pre-rRNAs

In yeast, the RNA polymerase III (RNAP III) transcribes the 5S rRNA in a precursor form. This precursor will be processed exonucleolytically at its 3' end by the exonuclease Rex1 and, this mature 5S rRNA will be part of the large subunit (Ciganda

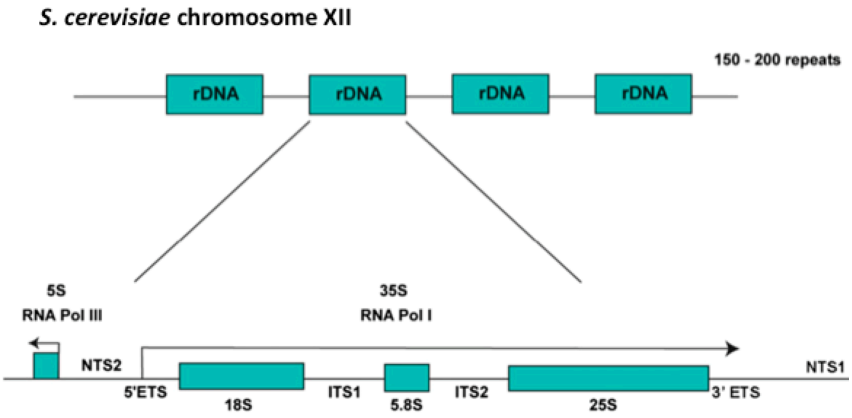


**FIGURE 6. Organization of the rDNA locus in *S. cerevisiae*.** About 150 tandem repeats of rDNA are located in the chromosome XII. Each unit is transcribed by the RNA polymerase I (RNA pol I) as a 35S precursor of rRNAs. 5S rRNA is independently transcribed by the RNA polymerase III (RNA pol III). 35S pre-rRNA is processed to generated the mature 18S, 5.8S and 25S rRNAs. These regions are flanked by two external transcribed spacers (5' ETS and 3' ETS) and by two internal transcribed spacers (ITS1 and ITS2). There are two non-transcribed spacers (NTS) that separated 5S and 35S regions. Adapted from (Woolford and Baserga, 2013).

and Williams, 2011). On the other hand, RNA polymerase I (RNAP I) transcribes the 35S pre-rRNA species. This precursor contains the mature 18S, 5.8S and 25S pre-rRNAs for the large subunit (Nomura et al., 2004). Moreover, 35S pre-RNA contains external and internal transcribed spacers (ETS and ITS respectively) that are exo- or endonucleolytic cleaved. **Figure 7** summarizes the pre-rRNA processing pathway.

Processing of pre-rRNA can occur post-transcriptionally or co-transcriptionally (Fernández-Pevida et al., 2015). In the post-transcriptional way, a complete 35S pre-rRNA is synthesized as it is present in the early 90S pre-ribosomal particle. However, in exponentially growing cells, about 70% of pre-rRNAs undergo co-transcriptional cleavage, before transcription of 35S pre-rRNA is completed (Koš and Tollervey, 2010).

Pre-rRNA processing starts in the nucleolus, in the context of pre-ribosomal particles and it is a multi-step process. Initially, the 35S pre-rRNA unit is cleaved at $A_0$ (to generate 33S pre-rRNA) and $A_1$ (to generate 32S pre-rRNA) sites practically simultaneously (Hughes and Ares, 1991). Then, cleavage at site $A_2$ in ITS1 produces 20S and 27S$A_2$ pre-rRNAs under exponential growth conditions (Koš and Tollervey, 2010). Separately, these precursors will continue 40S and 60S r-subunits maturation

pathways, respectively. In contrast, under unfavourable growth conditions, processing occurs post-transcriptionally and cleavage at site $A_3$ in ITS1 by RNase MRP tends to occur prematurely, producing the 23S pre-rRNA. Productive maturation of pre-ribosomal particles containing this alternative precursor is controversial (Kos-Braun et al., 2016).

Pre-40S ribosomal particles containing the 20S pre-rRNA are exported to the cytoplasm, where endonucleolytic cleavage at site D by the endonuclease Nob1 take place to produce mature 18S rRNA (Fatica et al., 2003). On the other hand, $27SA_2$ pre-rRNA processing is more complex and two alternative maturation pathways can occur

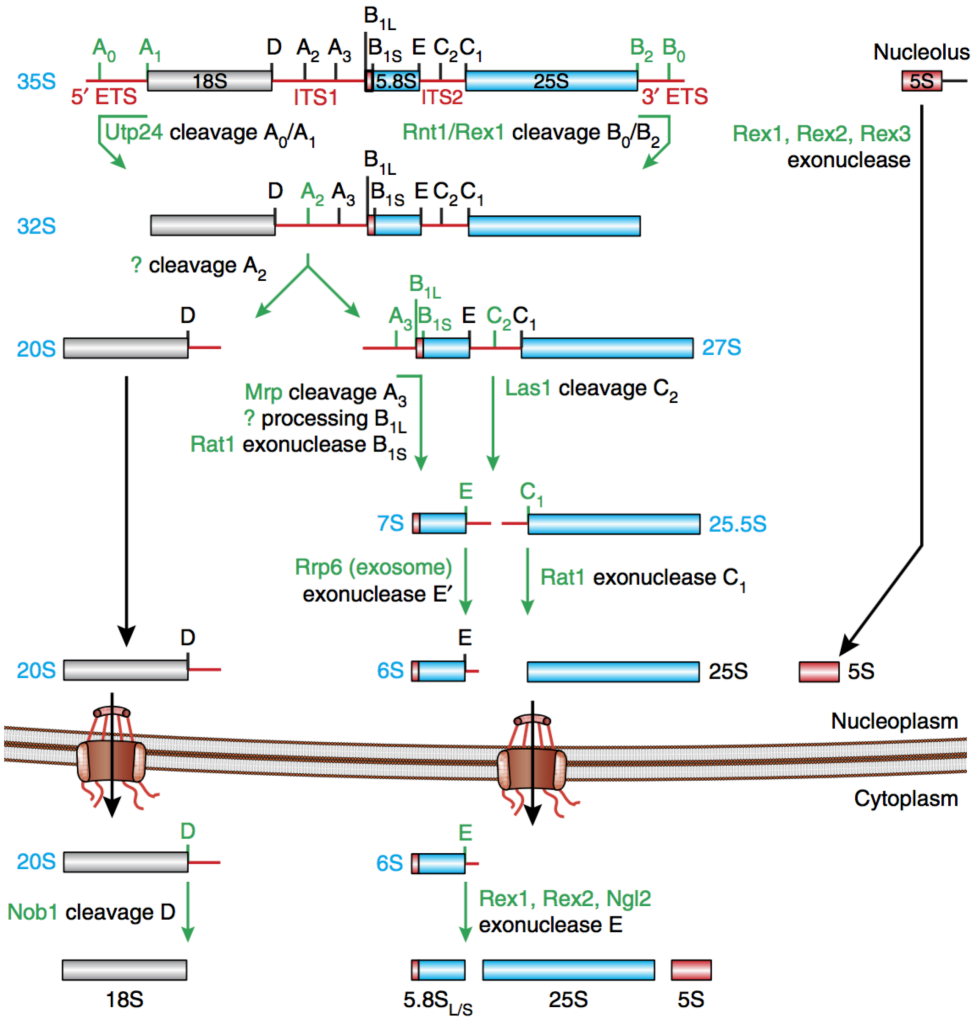


**FIGURE 7. Pre-rRNA processing pathway in *S.cerevisiae*.** Main steps in pre-rRNA processing and main pre-rRNA intermediates are shown. The enzymes and the corresponding processing sites are indicated in green. Note that some nucleases have been not identified yet (question marks). Pre-rRNA intermediates are indicated in blue. Adapted from (Peña et al., 2017).

in the nucleolus. About 85% of $27SA_2$ pre-rRNA is first cleaved at the $A_3$ site by the endonuclease RNase MRP and then, the $27SB_S$ pre-rRNA is produced by exonucleolytic cleavage at the $B_{1S}$ site (Chu et al., 1994). By contrast, about 15% of $27SA_2$ pre-rRNA is cleaved at the $B_{1S}$ site generating the $27SB_L$ pre-rRNA (Faber et al., 2006). Next maturation processes are identical for both 27SB pre-rRNAs. Endonucleolytic cleavage by Las1 at the $C_2$ site separates the 25.5S and $7S_S$ or $7S_L$ pre-rRNAs (Gasse et al., 2015). Finally, the 25.5S pre-rRNA is processed to mature 25S rRNA by the exonucleases Rat1 and Rai1 (Fromm et al., 2017). The 7S pre-rRNAs are 3'-5' processed exonucleolytically in several steps by the exosome and other nucleases; the processing of the last precursors ends in the cytoplasm where mature $5.8S_S$ and $5.8S_L$ rRNAs is produced (Thomson and Tollervey, 2010).

Inside pre-ribosomal particles, where the pre-rRNA processing reactions take place, there are many other elements in addition to pre-rRNAs. These particles contain r-proteins and non-ribosomal factors (snoRNAs and proteins) (Kressler et al., 2010). Some of these factors are nucleases that are directly involved in pre-rRNA processing. However, other factors have indirect or unknown roles in pre-rRNA processing. It has been described that some factors are implicated in covalent modifications of rRNA that can occur co-transcriptionally. Some snoRNPs (small nucleolar ribonucleoproteins) can catalyse pseudouridylation or 2'-O-ribose methylation of pre-rRNA, which are important rRNA modifications for rRNA function or structure (Sharma and Lafontaine, 2015). On the other hand, binding of r-proteins can be important to stabilize or re-fold rRNA by altering the RNA structure (Woodson, 2008).

**Assembly of the SSU: Binding and dissociation of the 90S pre-ribosome**

The first stable pre-ribosomal particle identified was the early 90S (also known as SSU processome) that seems to contain the entire 35S pre-rRNA. Recent cryo-EM studies have managed to determine the structure of early pre-ribosomal particles (Chaker-Margot et al., 2016; Kornprobst et al., 2016; Sun et al., 2017). These cryo-EM studies have provided information about the earliest steps of 40S r-subunit assembly **(Figure 8)**, which are sequential and occur co-transcriptionally. Many transient factors are involved in the assembly of the small r-subunit (Klinge and Woolford, 2019).

During the transcription of the 35S pre-rRNA, the modules UtpA and UtpB, are first recruited to the nascent 5'-ETS to form the 90S pre-ribosomal particle. First, the UtpA complex interacts with the 5'-ETS and recruits the U3 snoRNP (U3 snoRNA, Nop1/fibrillarin, Nop56, Nop58 and Snu13) and the UtpB complexes (Pérez-Fernández et al., 2007). Both complexes, UtpA and UtpB, act as molecular chaperones and provide an encapsulated environment for 18S rRNA subdomains preventing their premature folding (Hunziker et al., 2016). U3 snoRNA has an important role since it base-pairs with 5'-ETS and the pre-18S rRNA resulting in a reduction of conformational freedom of pre-rRNA, which is crucial for the exact timing of the endonucleolytic processing that occurs at sites $A_1$ and $A_2$. (Barandun et al., 2018). Subsequent associations of modules occur after these initial sequential steps. The UtpC complex, which is situated at the top part of the 90S pre-ribosome, allows the recruitment of a first set of 40S r-proteins and other factors located in the outer regions of the 90S pre-ribosomal particle such as the enzymes GTPase Bms1, the methyltransferase Emg1, the acetyltransferase Kre33 and helical-repeat-containing proteins (Barandun et al., 2018).

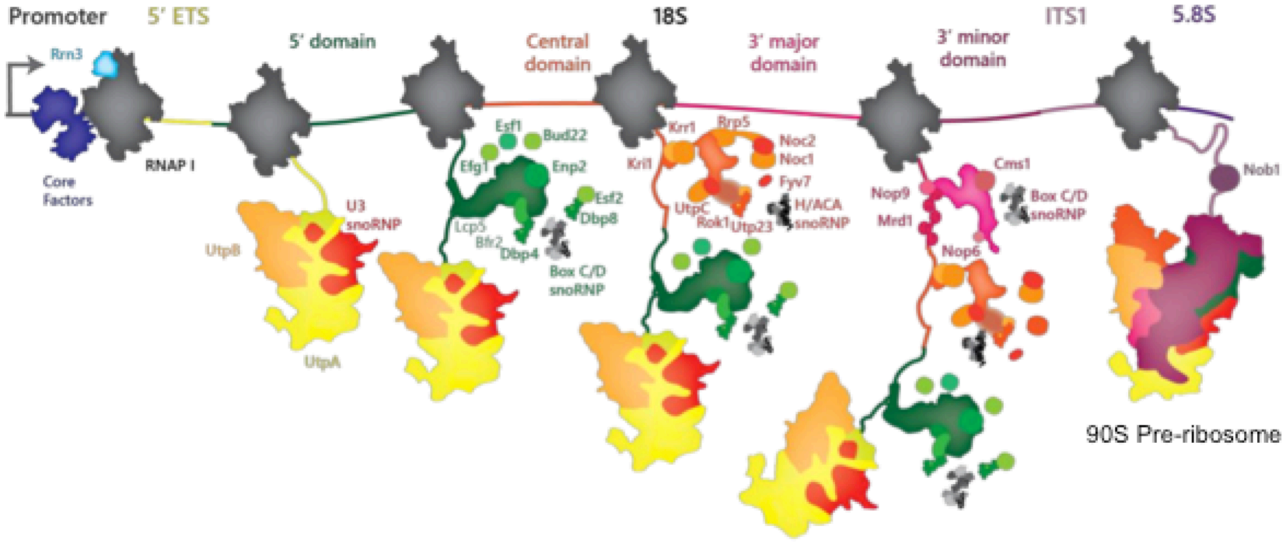


**FIGURE 8. Co-transcriptional assembly of the 90S pre-ribosome.** Schematic representation of early events of small subunit assembly in the nucleolus. The nascent 35S pre-rRNA transcribed by RNAPI recruits early 90S modules (e.g., UTP-A, UTP-B, U3 snoRNP). Then, other transient components are associated in a sequential manner and the rRNA is compacted to form the 90S pre-ribosome. Factors are coloured correspondingly with their recruitment stage. Adapted from (Chaker-Margot, 2018).

In the final form of the 90S pre-ribosome, distinct conformational changes induce 35S pre-rRNA processing at sites $A_1$ and $A_2$. The nuclease Utp24 has been suggested to catalyse cleavage at these sites (Wells et al., 2016). These cleavages result in the release of an earliest pre-40S particle containing the 20S pre-rRNA from its scaffold in the 90S pre-ribosomal particle, splitting the maturation pathways of both ribosomal subunits, which only meet again in the cytoplasm.

**Assembly of the SSU: Nucleocytoplasmic stages**

In early pre-40S particles, the 5' and central domains of 18S rRNA (body and platform regions) are nearly maturated, whereas the 3' major domain (head and beak regions) appeared partially immature. Moreover, the major 40S r-subunit translation-active sites are not formed yet (Johnson et al., 2017). Nuclear pre-40S r-particles are rapidly exported to the cytoplasm through the nuclear pore complex (NPC). However, prior to this export, the remodelling of the 3'domain of 18S rRNA to form the head of the mature 40S r-subunit is necessary (Bassler and Hurt, 2018).

The recruitment of several assembly factors is also required to facilitate the translocation of pre-40S r-particles to the cytoplasm. Some of these factors probably associate after the $A_2$ cleavage (like Ltv1, Tsr1 and Rio2) but other factors are also found in very early pre-ribosomal particles (like Enp1 and Pno1) (Barandun et al., 2017). Moreover, it has been found that some of these factors recruit the exportin Crm1 in the presence of RanGTP to facilitate the nuclear export to pre-40S r-particles (Moriggi et al., 2015).

An important step during the transition from the nucleolus to the cytoplasm is the formation of the beak region. The apical region of the beak, which includes a remodelled helix H33 of 18S rRNA and the r-proteins eS12 and eS31 located at their mature positions, have been identified in early 90S r-particles (Sun et al., 2017). Prior to nuclear export, the binding of r-protein uS3 to the beak is reorganized by phosphorylation of a subcomplex composed of uS3, Enp1 and Ltv1, mediated by the kinase Hrr25 and increasing the flexibility of the head region (Johnson et al., 2017). Once in the cytoplasm, release of Ltv1 and Enp1 is mediated by

phosphorylation/dephosphorylation allowing the stable incorporation of r-protein uS3, which is necessary to stabilize the interface between the body and the head and for the cytoplasmic assembly of eS10 (Collins et al., 2018). Moreover, after or during the beak formation, ATP hydrolysis by Rio2 triggers the rotation of the head likely to its mature position (Ferreira-Cerca et al., 2012).

In the cytoplasm, quality-control mechanisms are necessary to ensure the production of translation-competent 40S r-subunits **(Figure 9)** (Peña et al., 2017). Dissociation of some assembly factors is needed to further maturate the small subunit as these factors apparently block the binding sites of some r-proteins and translation factors (Scaiola et al., 2018). For example, Dim1, Rio2 and Tsr1 prevent premature interactions of pre-40S r-particles with eIF1A and the 60S r-subunit (Peña et al., 2017). Finally, release of Rio2 and Tsr1 factors recruits Rio1 and the GTPase eIF5B (Fun12) allowing the interaction of pre-40S r-particles with mature 60S r-subunits to generate an 80S-like particle (McCaughan et al., 2016). Furthermore, release of some assembly factors is coordinated with the cleavage of the 20S pre-rRNA and the accommodation of the last r-proteins. The RNA-binding protein Pno1 blocks the eS26 final binding site until very late stages in the maturation pathway and, together with Nob1 inhibit the binding of the translation initiation factor eIF3. In the context of the 80S-like particle, in order to acquire translation competence, Pno1 is released by the ATPase Rio1, which enables the cleavage at the D site of the 20S pre-rRNA by the endonuclease Nob1 since Pno1 masks the Nob1 cleavage site at the 3' end in the 18S rRNA (Scaiola et al., 2018). Then, Pno1 is replaced by the ribosomal protein eS26 with the help of Tsr2 and late assembly factors are removed (Lebaron et al., 2012). Assembly of eS26 is controversial since some studies indicate that eS26 is already present in the 90S pre-ribosome, which could suggest that some r-proteins can interact weakly with the pre-rRNAs in early stages, however, these interactions are stronger across the maturation pathway (Peña et al., 2016). Altogether, these quality control steps ensure that only properly assembled 40S r-subunits enter into translation.

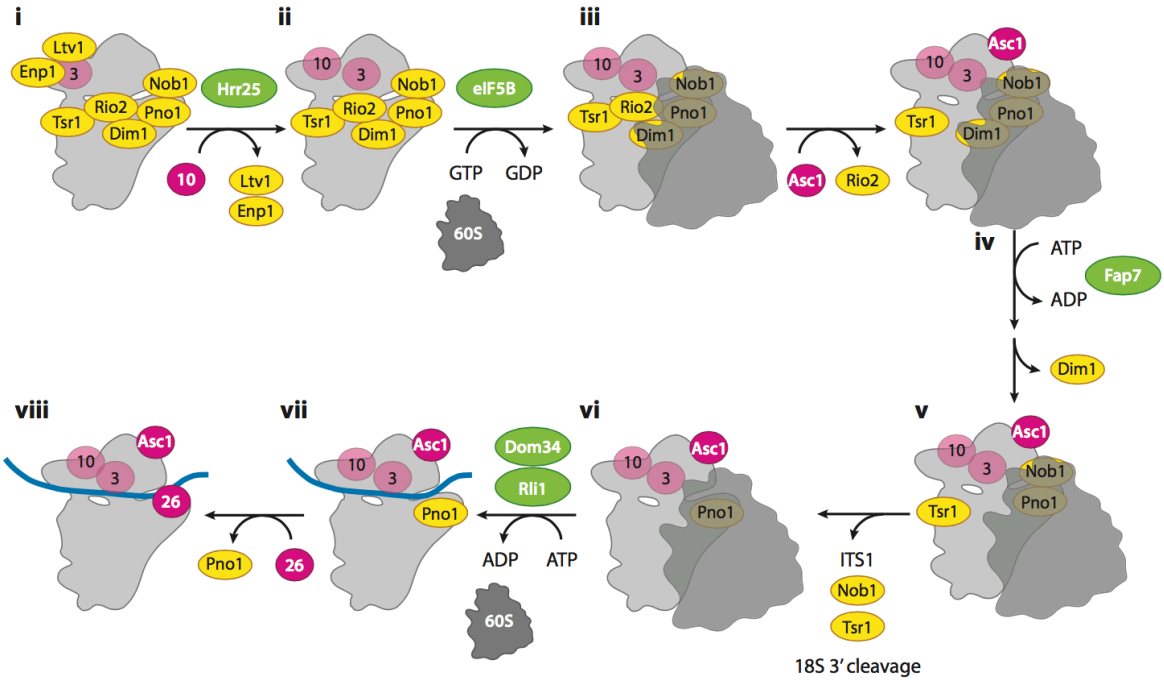


**FIGURE 9. Model for intermediate and late events in 40S subunit maturation pathway in *S. cerevisiae***. The late assembly reactions including association and dissociation of late assembly factors and the formation of 80S-like particles are shown. Final cleavage at D site of 18S rRNA performed by the endonuclease Nob1 is also shown. This reaction could occur in late 80S-like particles (illustrated in the figure) or after dissociation of the late pre-40S particle from the 60S subunit. Stably bound assembly factors are coloured in yellow and transiently bound assembly factors/translation factors are in green. The r-proteins are shown in magenta, mRNA in blue, pre-40S r-subunits in light grey and 60S r-subunits in dark grey. Adapted from (de la Cruz et al., 2015)

### Nucleolar and nucleoplasmic assembly of the large r-subunit

The structure and the assembly of the large subunit are more complex than that of pre-40S r-particles. Rather than the characteristic encapsulated environment of rRNA domains in the small pre-particle, rRNA domains of 60S r-subunit maturate in a modular fashion and they are intertwined in the mature large subunit (Klinge and Woolford, 2019). Only the very first steps of 60S r-subunit assembly seem to occur co-transcriptionally, but we lack cryo-EM structures for these earliest stages.

As mentioned before, assembly of 60S r-subunit starts with the cotranscriptional $A_2$ cleavage in the 90S pre-ribosome. However, before this cleavage could generate pre-60S particles, the assembly factor Rrp5 seems to be necessary to initiate the assembly of the large r-subunit given that binding of Rrp5 in ITS1 is necessary for $A_2$ and $A_3$ cleavages, and it may coordinate assembly of both r-subunits (Eppens et al.,

1999). During nucleolar stages, the pre-rRNA is folded into a more compact conformation guided by scaffolds formed by several assembly factors like Rrp5, Mak21, Noc2 and Nop4 (Granneman et al., 2011) (Hierlmeier et al., 2012). Other assembly factors (Npa1, Npa2, Rsa8 and Nop8) and RNA helicases (Dbp2, Dbp3, Dbp6, Dbp7, Dbp9 Mak5 and Prp43) participate in very early stages to stabilize and/or to remodel RNAs or RNPs and stay associated with the pre-60S r-particle until their removal in the nucleus or the cytoplasm (Rodríguez-Galán et al., 2013) (Rosado et al., 2007) (Joret et al., 2018).

The functional regions of 60S r-subunits known as the GTPase activating centre (GAC), peptidyltransferase centre (PTC) and the peptide exit tunnel (PET) start to emerge in the nucleolus by the assembly of r-proteins and cycles of association/release of assembly factors (Kater et al., 2017). Finally, functional PTC and PET regions are constructed upon the transition of pre-60S subunits from the nucleolus to the nucleoplasm, where more protein exchange events take place to remove those factors that block the formation of the mature structure of rRNA helices (Wu et al., 2016).

The formation of the PTC and the PET is coupled with the cleavage of ITS2 at the $C_2$ site, which is catalysed by the endonuclease Las1 (Gasse et al., 2015). Previously, the remodelling of the rRNA domains near ITS2 is required. It does so by releasing nearby assembly factors like Ytm1 and Erb1, which is mediated by the AAA-ATPase Rea1 (Miles et al., 2005). Once ITS2 is cleaved by Las1, Nop53 is positioned where Erb1 was previously located and recruits the helicase Mtr4 (Thoms et al., 2015). Binding of Mtr4 makes the 7S pre-rRNA accessible for channelling into the exosome, which finally processes ITS2 once it is cleaved (Fromm et al., 2017).

The central protuberance is also stabilized upon transition from the nucleolus to the nucleoplasm **(Figure 10)**. This structure includes the 5S rRNA and r-proteins uL5 and uL18 (known as the 5S RNP). However, it is not clear when and how the 5S RNP is incorporated into early pre-60S r-particles. Some studies suggest that the importin Syo1 helps the assembly of the 5S RNP and this complex is incorporated into the pre-60S particle with assistance of the assembly factors Rpf2 and Rrs1 (Zhang et al., 2007)

(Calviño et al., 2015) (Kressler et al., 2012). Before nuclear export of pre-60S particles, these two assembly factors are released and the 5S RNP rotates 180º to reach its mature conformation, serving as a checkpoint (Leidig et al., 2014). Others structural rearrangements occur in the central protuberance and some factors like the AAA-ATPase Rea1 stabilize the rotated state (Barrio-García et al., 2015). ATP hydrolysis by Rea1 induces the release of the GTPase Nog2, which permits the association of the export factor Nmd3 and recruits the exportin Crm1/Xpo1 (Matsuo et al., 2014). Nmd3 aids the compaction of the pre-ribosomal particle facilitating its translocation and it seems to prevent premature tRNA incorporation (Sengupta et al., 2010). Others export factors are also recruited to mediate the efficient translocation of pre-60S particles across the NPC, but only if these checkpoints are passed. For example, release of the assembly factor Mrt4 enables binding of the export factors Mex67 and Mtr2, which is coupled with the maturation of the emerging P r-stalk (Sarkar et al., 2016).

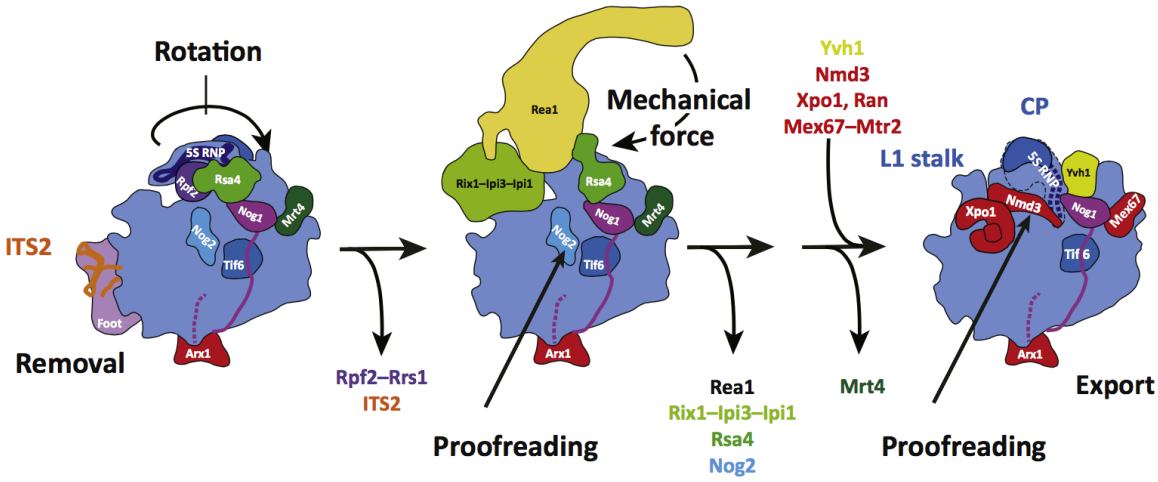


**FIGURE 10. Model of nuclear pre-60S r-subunit maturation events.** Simplified representation of successive nuclear proofreading steps for acquisition of export competent large pre-60S r-subunits. The first particle contains the characteristic "foot" structure (ITS2 in orange) and the 5S RNP is in its pre-mature conformation. Next, the exonucleolytic degradation of the ITS2 and the rotation of the 5S RNP occurs. The AAA-ATPase Rea1 and the Rix1 subcomplex sense the correct 5S RNP position. The ATPase activity induces the activation and release of the GTPase Nog2, a prerequisite for the recruitment of the export adaptor Nmd3, which is recognized by the exportin Crm1/Xpo1 in a RanGTP-dependent manner. The export factor Mex67–Mtr2 is recruited close to the nascent P r-stalk. Adapted from (Kressler et al., 2017).

### Cytoplasmic stages of the large r-subunit

Once pre-60S particles emerge in the cytoplasm, the pre-rRNA 6S is processed to the mature 5.8S rRNA, last r-proteins are incorporated and the remaining assembly factors are dissociated in a coordinated way. At this stage, GTPases and ATPases drive the release of these factors in a hierarchical pathway **(Figure 11)** (Peña et al., 2017).

The first step in the cytoplasmic maturation is the recruitment and activation of the AAA-ATPase Drg1 by the assembly factor Rlp24, which induces the replacement of Rlp24 by eL24, its homologous r-protein (Kappel et al., 2012). Then, the maturation pathway bifurcates into events centered at the PET or at the joining surface. On one hand, Ssa1-4, Rei1 and Jjj1 are required for the dissociation of Arx1 and Alb1 from the PET (Greber et al., 2016).

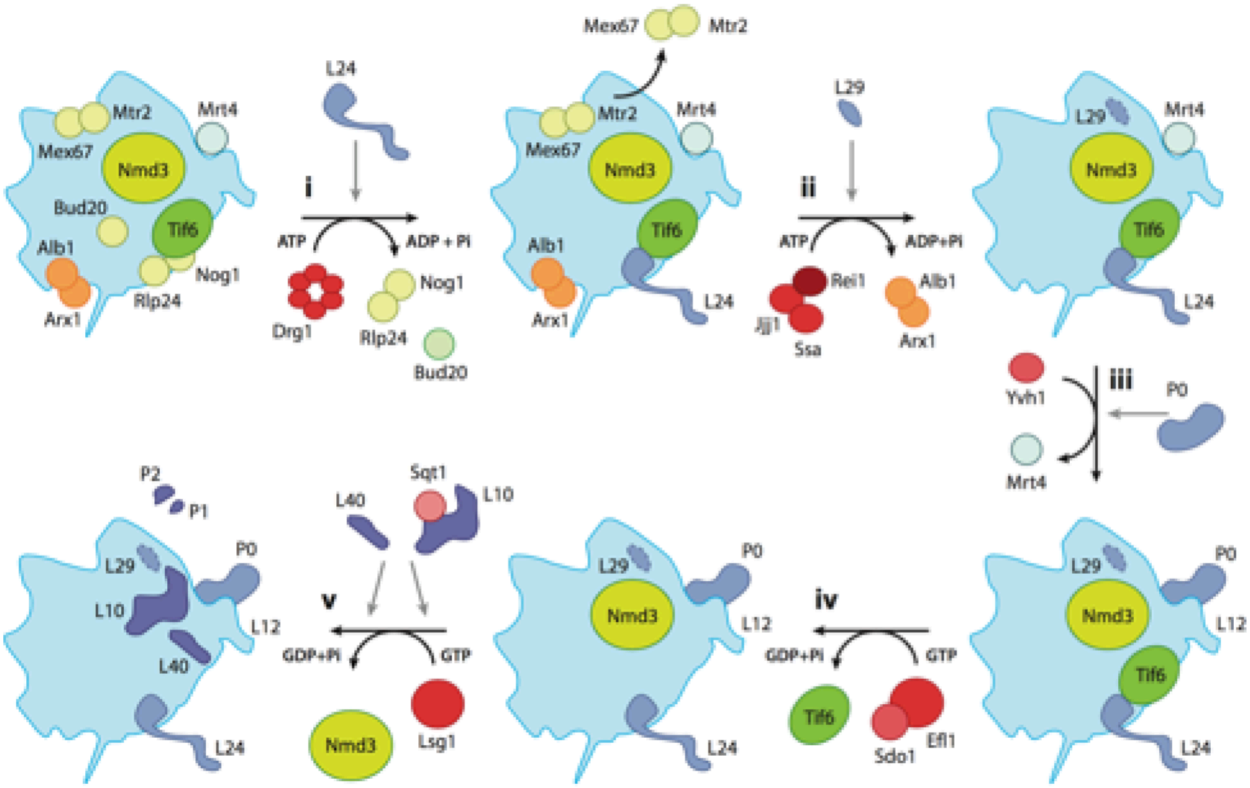


**FIGURE 11. Cytoplasmic maturation of pre-60S ribosomal particles**. In last steps of 60S subunit maturation, adaptors and assembly factors are sequentially released to enable assembly of the remaining r-proteins. Note that the order of some steps is approximate. Finally, release of Nmd3 allows the 60S r-subunits to gain translation competence. In the last step, 60S r-subunits gain translation competence by release of Nmd3 and finally, acidic r-proteins P1 and P2 assemble when both mature ribosomal subunit are joined and committed to translation. Adapted from (de la Cruz et al., 2015).

On the other hand, last steps on the joining face are unclear since there are controversial studies. Some studies suggest that the release of Nog1 is coupled to the release of Drg1 (Loibl et al., 2014). However, recent results indicate that the release of either factor is uncoupled from the other and that the N-terminus of the export adaptor Nmd3 could activate the release of Nog1 (Zhou et al., 2019). Once Nog1 is released, Nmd3 helps the incorporation of the r-protein uL16 (formerly L10), which in turn is necessary for the release of Nmd3. Moreover, timing of the binding of the biogenesis factor Yvh1 is unclear. This factor promotes P stalk assembly by displacing Mrt4; it has been proposed that Yvh1 is required in the nucleoplasm for recruitment of the export factors Mex67-Mtr2, previously to the nuclear pre-60S r-particle export (Sarkar et al., 2016). However, recent findings suggest that binding of Yvh1 into pre-60S r-particles is blocked until Nog1 is released in the cytoplasm (Zhou et al., 2019). Finally, some factors are recruited at the P stalk to test-drive before starting the translation process. Incorporation of the r-protein uL16 activates the GTPase Efl1 to release Tif6 (eIF6), which is a pre-requisite for subunit joining (Ma et al., 2017). If these cytoplasmic steps have been completed successfully, functional centres could participate in protein synthesis.

## FOLDING, TRANSPORT AND DEGRADATION OF RIBOSOMAL PROTEINS

Ribosomal proteins are synthetized in the cytoplasm but most of them are incorporated into nucle(ol)ar pre-ribosomal particles, so they have to travel to the nucleus to reach their assembly sites. However, as mentioned before, r-proteins have particular features: most of them are basic, contain intrinsically disorder domains and long extensions rich in lysine and arginine (Jäkel et al., 2002). Due to these characteristics, r-proteins have a high tendency to aggregate. For this reason, different cellular mechanisms have evolved to protect newly synthesized r-proteins from aggregation and to ensure their safe delivery (Peña et al., 2017) (Pillet et al., 2017).

In eukaryotes, molecular chaperones are involved in the folding of nascent proteins (*de novo* folding). A group of these molecular chaperones interact with

ribosomes, binding close to the PET and includes two distinct ribosome-associated chaperone categories: the nascent polypeptide-associated complex (NAC) and the Hsp70•Hsp40-based ribosome-associated complex (RAC) (Albanèse et al., 2006). In *S. cerevisiae*, RAC is composed by the catalytically-inactive Hsp70 homolog Ssz1 and the Hsp40 protein Zuo1. RAC heterodimer binds to the Hsp70 paralogue Ssb1 or Ssb2 to form the chaperone triad or Ssb-RAC complex (Zhang et al., 2017). In this complex, Ssb binds the nascent polypeptides to their proper co-translational folding and RAC acts as a regulator of the process by stimulating the ATPase activity of Ssb (Leidig et al., 2013). Most r-proteins can be folded by this general chaperone system **(Figure 12A)**. Previous studies have revealed that these ribosome-anchored chaperone systems play a crucial role in stabilizing the aggregation-prone species of r-proteins in the cytoplasm since the simultaneous deletion of NAC and SSB/RAC results in the aggregation of more than 50 r-proteins (Koplin et al., 2010).

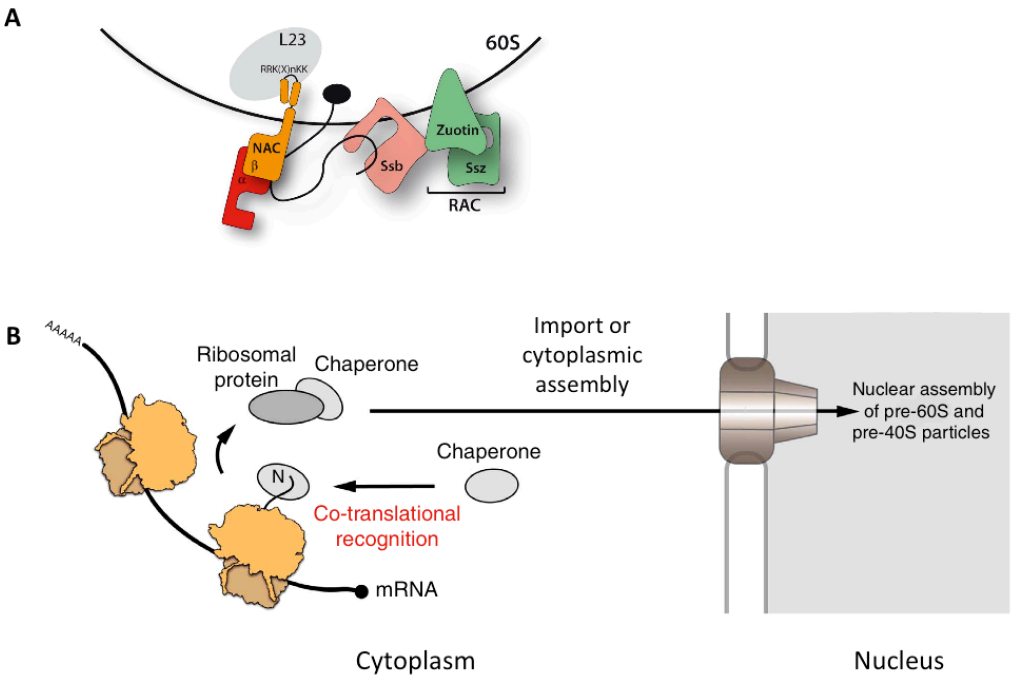


**FIGURE 12. Models for ribosomal proteins folding. (A)** Scheme of the dual system nascent polypeptide-associated complex (NAC) and the ATP-dependent Hsp70 SSB/ribosome-associated complex (SSB/RAC). Both machineries associate with ribosomes and contact with emerging nascent polypeptides (black line). These ribosome-associated chaperones are implicated in *de novo* folding of r-proteins. Adapted from (Koplin et al., 2010) **(B)** Model for the co-translational capturing of ribosomal proteins by their specific dedicated chaperone. Some dedicated chaperones interact co-translationally to their specific r-protein partner proteins to prevent their aggregation. Moreover, dedicated chaperones can promote nuclear import and/or assist assembly of r-proteins into pre-ribosomal particles. Adapted from (Pausch et al., 2015).

Apart from these general chaperone machineries, importins also stabilize r-proteins. Importins are a group of proteins that mediate the nuclear import of proteins by recognition of their nuclear localization signals (NLS). In yeast, principal importins that transport r-proteins are karyopherins Kap104, Kap123 and Pse1 (Rout et al., 1997). For r-proteins, due to their high tendency to aggregate, importins are also required to act as chaperones protecting them from aggregation (Jäkel et al., 2002). However, importins release their cargo into the nucleus so further mechanisms may be required to ensure protection of r-proteins until they reach their assembly site.

Apparently, these mechanisms are not enough to ensure optimal expression of r-proteins, and indeed, specific r-proteins require exclusive systems. Recently, a new group of proteins called dedicated chaperones has been uncovered. These proteins interact specifically with newly synthesized r-proteins to prevent their aggregation, promote their nuclear import and/or assist their assembly into pre-ribosomal particles (Pillet et al., 2017). Until today, dedicated chaperones for eleven r-proteins have been found: uS3, uS5, eS6, uS11, eS26, uL3, uL4, uL14, uL16, uL5 and uL18, but more are expected to be discovered. In some cases, dedicated chaperones can bind to their r-protein partners co-translationally until the r-protein assembles into pre-ribosomal particles **(Figure 12B)** (Pausch et al., 2015). However, a class of dedicated chaperones termed “escortins” only bind to their r-protein partners after their import into the nucleus and guide them through the nucleus to their assembly site (Pillet et al., 2017). For example, the escortin Tsr2 associates with eS26 after its nuclear import, thereby dissociating the eS26-importin complex in a RanGTP-independent manner, and assists in its assembly into 90S pre-ribosomal particles (Schütz et al., 2014).

Interestingly, unassembled r-proteins are rapidly degraded to maintain their cellular homeostasis. Recently, a degradation pathway termed ERISQ, for *Excess RIboSomal protein Quality control*, has been described in which the HECT-domain E3 ubiquitin ligase Tom1 participates (Sung et al., 2016a). It seems that Tom1 ubiquitinates residues of unassembled r-proteins that are normally inaccessible as they are concealed in the mature ribosome. This type of ubiquitination targets these r-proteins for proteasome-dependent degradation. Other mechanisms are related to

ribosome metabolism; thus, in stress conditions, 40S r-subunits are located in stress granules (known as P-bodies) and they are degraded by autophagy (Grousl et al., 2009). Moreover, upon nutrient starvation, mature ribosomes are selectively degraded by a process regulated by ubiquitination and referred to as ribophagy (Kraft et al., 2008).

## UBIQUITIN AND UBIQUITIN-LIKE PROTEINS

Proteins are subject to a high variety of post-translational modifications. Among these protein modifiers, one of the most studied is ubiquitin. Ubiquitin is a small and globular protein of 76 amino acids present in all eukaryotes. Actually, ubiquitin was originally named "ubiquitous immunopoietic polypeptide" and is one of the most highly conserved eukaryotic proteins known (Goldstein et al., 1975). The most common function of ubiquitin is tagging proteins for proteasome-mediated degradation. The proteasome is a large multi-subunit complex of proteases and regulatory proteins shaped as a capped cylinder and inside of which proteins are digested (Finley et al., 2012). However, ubiquitin can also act as a non-proteolytic signal in the regulation of diverse cellular processes including DNA repair, transcription, and trafficking of membrane proteins (Kwon and Ciechanover, 2017).

Several other proteins structural and evolutionarily related to ubiquitin have been discovered. Like ubiquitin, these proteins contain a β-grasp fold and are known as ubiquitin-like proteins (UBLs) (Cappadocia and Lima, 2018). Some of these proteins are able to be conjugated to others proteins, in a similar way as ubiquitin. The functions of UBLs include diverse processes such as nuclear protein transport, DNA repair, autophagy, chromosome replication, etc.

Despite ubiquitin, UBLs are present not only in eukaryotes but have also been found in prokaryotes (Iyer et al., 2006). However, not all UBL families are found in all eukaryotes. In yeast, several UBLs have been described **(Figure 13)**, for example, Smt3, Rub1, Urm1, which drive modifications known as SUMOylation, NEDDylation and urmylation, respectively, or Atg8 and Atg12, factors that participate in autophagy. The

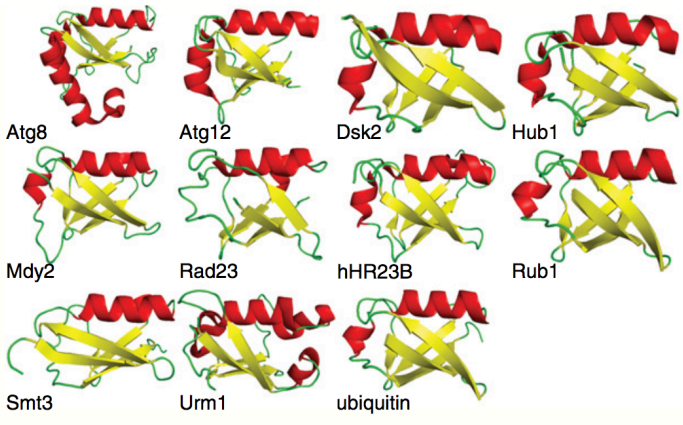


**FIGURE 13. Ubiquitin-like domains.** Structural models of the ubiquitin-like domain of different proteins from *S. cerevisiae.* The conserved β-grasp fold is depicting in all cases. Adapted from (Yu et al., 2016).

UBL-targets are not always proteins; for example, Atg8 is conjugated to the phospholipid phosphatidylethanolamine (Ichimura et al., 2000), and Urm1 can act as a sulphur carrier in a tRNA modification pathway (Wang et al., 2011).

Among these UBLs, the SUMO (Small Ubiquitin-like MOdifier) family has gained importance in last years. SUMO is highly conserved in all eukaryotes but the number of SUMO genes is variable. For example, in *S. cerevisiae*, only one essential SUMO gene, *SMT3*, has been identified, while in humans at least four SUMO genes have been found.

Structurally, the main difference between an ubiquitin and a SUMO molecule resides in a N-terminal extension of the SUMO protein that is not present in ubiquitin. The sumoylation process is analogous to the ubiquitination one but the enzymes that participate in both processes are different. Like ubiquitination, sumoylation is a reversible process. SUMO deconjugation (desumoylation) is catalysed by ULP proteases, which in yeast are known as Ulp1 and Ulp2 (Cappadocia and Lima, 2018).

SUMO is involved in various cellular processes, such as nuclear transport, cell-cycle progression, protein trafficking, stress response, etc. Rather than promoting protein degradation like the ubiquitin moiety, the SUMO attachment blocks the proteasomal degradation by competing with ubiquitination (Wilson, 2017). Thus,

sumoylation seems to enhance protein stability. However, another class of enzymes called SUMO-targeted ubiquitin ligase (STUbL) have been discovered. These enzymes recognize sumoylated proteins as targets for ubiquitination. This activity results in a hybrid signal, indicating that SUMO and ubiquitin can cooperate with each other (Nie and Boddy, 2016).

There are also proteins that contain UBL domains as part of its primary sequence. These UBL domains are not usually processed and confer properties similar to those from a transferable UBL, being especially important to establish or maintain specific protein interactions (Hochstrasser, 2000). Interestingly, some ribosome assembly factors harbour UBL domains important for ribosome biogenesis. For example, the pre-60S assembly factors Rsa4 and Ytm1 contain N-terminal UBL domains that directly interact with the factor Rea1. These associations are required for the ATP-dependent dissociation of some pre-ribosomal factors (Ulbrich et al., 2009).

**Ubiquitination and deubiquitination**

As stated above, ubiquitin can be reversibly conjugated to proteins as a post-translational modifier in a process called ubiquitination. The ubiquitination reaction is mediated by the cooperative action of three types of enzymes: the ATP-dependent E1 ubiquitin-activating enzyme, the E2 ubiquitin-conjugating enzyme, and the E3 ubiquitin ligase **(Figure 14)** (Finley et al., 2012; Pickart, 2001). Commonly, ubiquitination results in the formation of an isopeptide bond between the C-terminal glycine (Gly) of the ubiquitin and the amino group of a specific lysine (Lys) of the target protein (Pickart, 2001).

Ubiquitin itself has seven lysine residues (K6, K11, K27, K29, K33, K48, and K63), all of which can be conjugated to a second ubiquitin molecule (Peng et al., 2003), leading to the formation of topologically distinct polyubiquitin chains. Alternatively, in the N-terminal methionine (M1), an ubiquitin molecule can also be attached, at least in higher eukaryotes (Fennell et al., 2018).

In yeast, there is only one E1 enzyme (Uba1) responsible for activation of ubiquitin. However, there are multiple E2 and E3 enzymes that generate ubiquitin

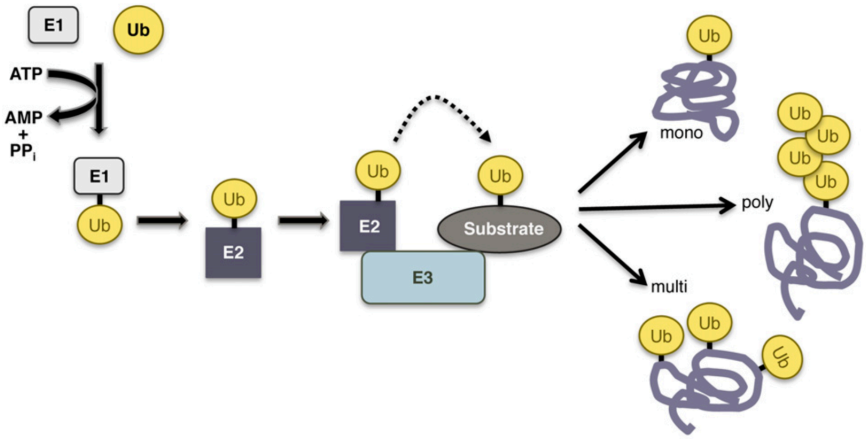


chains. These enzymes determine the architecture of the ubiquitin chain and define the linkage type (Finley et al., 2012). Regarding the diversity of possible combinations,

**FIGURE 14. Scheme of the ubiquitination process.** Ubiquitin conjugation involves the cascade of the E1–E2–E3 enzymes. This process can generate monoubiquitinated proteins or multi- or poly-ubiquitinated proteins if more than one round of ubiquitination are performed. Adapted from (Finley et al., 2012).

many receptors with several ubiquitin-binding domains (UBDs) have been described. These receptors play a key role in decoding ubiquitin signals (Kwon and Ciechanover, 2017).

Like other post-translational modifications, ubiquitination is a reversible process. Removal of ubiquitin can be performed in a single step by deubiquitinating enzymes (DUBs). These enzymes hydrolyse the linkage between ubiquitin and their substrates, as well as between ubiquitin molecules themselves (Finley et al., 2012). In yeast, 20 DUBs have been identified but this number varies in different organisms, for example, there are around 100 DUBs in humans. Despite the certain degree of redundancy found among DUBs, there are mechanisms of regulation by which some DUBs have highly diversified functionality and require substrate specificity, for example depending on the recognition of the ubiquitin chain (Mevissen and Komander, 2017).

Deubiquitination is necessary to recycle ubiquitin since DUBs recover ubiquitin molecules from the modified proteins. Therefore, action of DUBs is required to maintain the levels of free ubiquitin in the cell. Indeed, defects in deubiquitination cause reduced ubiquitin levels (Finley et al., 2012). Hence, deubiquitinases are key

enzymes, being necessary to regulate their localization, abundance and catalytic activity (Mevissen and Komander, 2017). In conclusion, the regulation of all ubiquitin-dependent processes requires a strict interplay between "writers" (e.g. E1/ E2/E3s), "erasers" (e.g. DUBs) and "readers" (e.g. proteins with UBD) (Ohtake and Tsuchiya, 2017).

### Functions of ubiquitination and the ubiquitin code

Originally, ubiquitination was thought to target only a set of substrates. However, nowadays it is understood that ubiquitin plays an important role in many biological processes. Indeed, it has been considered that the nature of the ubiquitination controls the fate of the protein target in the cell **(Figure 15)** (Finley et al., 2012).

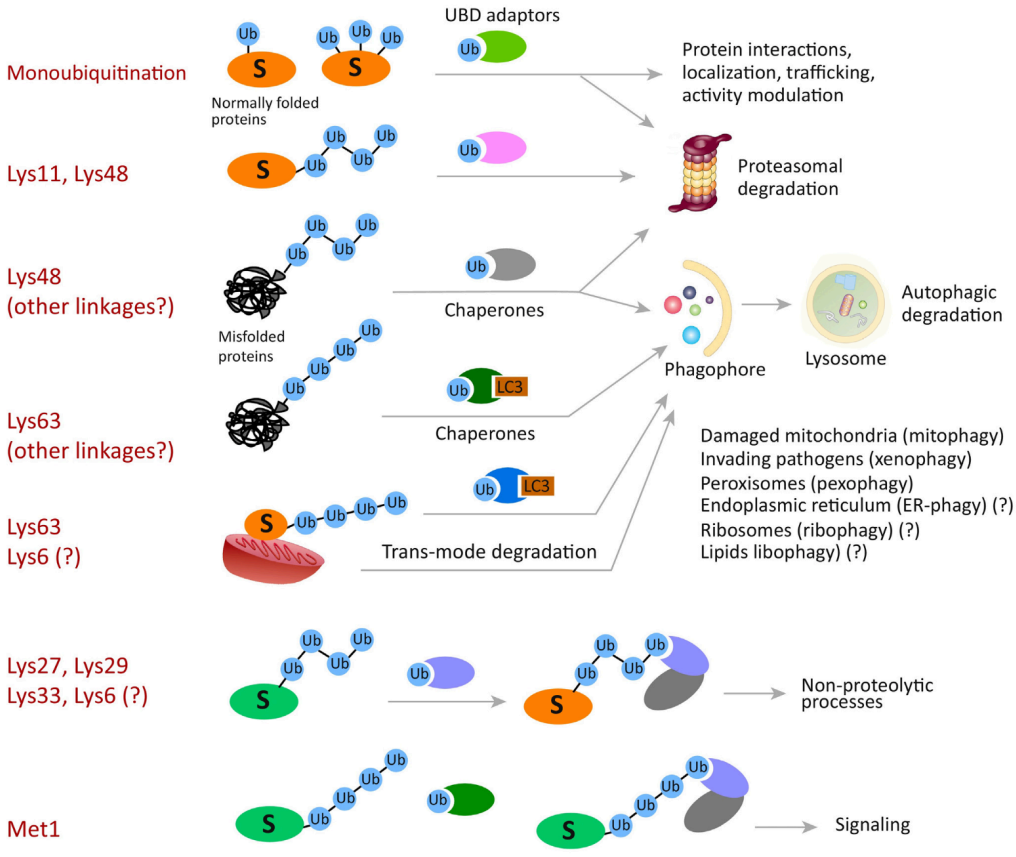


**FIGURE 15. Many cellular processes depend on ubiquitination.** Ubiquitin linkages are recognized and interpreted by a class of ubiquitin-binding domains (UBDs) of specific adaptors, which decipher the ubiquitin code. In general, different ubiquitin chains are important in various biological processes. The physiological fate of the modified targets depends on the poly-ubiquitin attachment. In general, Lys48 and Lys11 linkages are related with proteasomal degradation of normally folded short-lived proteins, whereas Lys48 and Lys63 linkages are involved in the degradation of misfolded proteins. However, relatively little is known about the functions of atypical linkages such Lys6, Lys27, Lys29, Lys33, and Met1. S, substrate for ubiquitination. Adapted from (Kwon and Ciechanover, 2017).

As mentioned before, ubiquitin plays an important role in protein degradation. Two different proteolytic pathways can mediate degradation of misfolded proteins: the proteasome system and autophagy. These two systems have been considered as independent degradative systems. However, ubiquitination links both systems because it acts as a degradation signal not only in the proteasome system but also in the autophagy process. It appears that these two systems are bi-directionally related: they work in a networked manner coordinated by ubiquitination (Ji and Kwon, 2017). Given this dynamic interplay, new models suggest that "the ubiquitin code" is not sufficient to make the decision between these two protein degradation pathways (Zientara-Rytter and Subramani, 2019).

The most prominent linkage is Lys48, critical for protein degradation by the proteasome. On other hand, Lys63 linkage serves as an autophagic degradation signal and can modulate non-degradative processes, such as DNA repair and protein transport (Finley et al., 2012; Kwon and Ciechanover, 2017). Atypical linkages related with protein degradation can also be found; for example, Lys6 can facilitate autophagic degradation, and Lys11 and Lys29 linkages act as proteasomal degradation signals, alone or in combination with Lys48 and Lys63 linkages (Ji and Kwon, 2017).

In addition to proteolytic processes, ubiquitin linkages can mediate non-proteolytic processes (for a Review, see (Kwon and Ciechanover, 2017)). Attachment of just one ubiquitin (mono-ubiquitination) has been long thought to signal protein interaction, localization, and activity modulation but not proteolysis. However, recent evidences show that mono-ubiquitination can also act as a proteolytic signal (Braten et al., 2016). In multi-ubiquitination, more than one molecule of ubiquitin is linked to several independent lysine residues in one protein. Nevertheless, in poly-ubiquitination, one or more molecules of ubiquitin are added to the previously conjugated ubiquitin to the target protein (Finley et al., 2012). Moreover, recent studies show that ubiquitin can be conjugated with ubiquitin-like modifiers (such as SUMO and NEDD8) or small molecular chemicals (such as acetate and phosphate), generating a huge variation in linkages **(Figure 16)** (Kwon and Ciechanover, 2017). The diversity of processes that are regulated is extraordinary, even when considering just

ubiquitin-protein modifications. For example, atypical Lys27 linkage acts as a scaffold in protein-protein interactions and it is important in the DNA damage response since it marks damaged DNA sites (Gatti et al., 2015); Lys33 linkage modulates membrane protein trafficking; and linear ubiquitination (Met1-linked ubiquitin chains) which is important in cell death signalling cascades and to regulate immunity (Fennell et al., 2018).

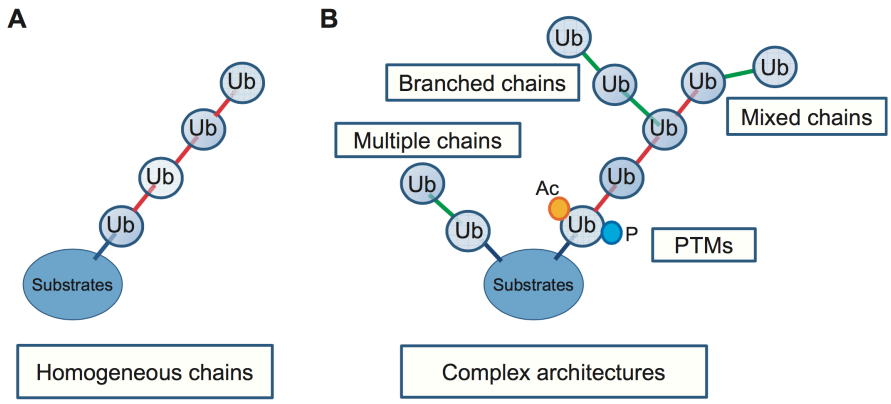


**FIGURE 16. Scheme of ubiquitin chain architectures. (A)** Poly-ubiquitin chains can be linear if several ubiquitin molecules are bound using the same type of linkage. These homogenously linked poly-ubiquitin chains have been studied extensively. **(B)** Complex poly-ubiquitin chain architectures with acetylated or phosphorylated ubiquitin, ubiquitin-like modifiers and heterotypic chains that include branched as well as mixed chains have emerged but they have been less well-studied. Ac, acetylation; P, phosphorylation. Adapted from (Ohtake and Tsuchiya, 2017).

### Ubiquitin synthesis: ubiquitin genes

Ubiquitin is produced *de novo* by the proteolytic maturation of two kinds of precursor forms; the first one consists of a head-to-tail poly-ubiquitin protein and the second one is a N-terminal ubiquitin fused to r-proteins eL40 and eS31. The precursor protein has to be proteolytically processed to make the C-terminal Gly-Gly motif available for conjugation.

In *S. cerevisiae,* ubiquitin is encoded by four different genes: *UBI1*, *UBI2*, *UBI3* and *UBI4* **(Figure 17)** (Özkaynak et al., 1987). *UBI4* encodes a poly-ubiquitin precursor of five tandem repeats of ubiquitin. This gene is apparently the main ubiquitin source in stationary phase or in stress conditions (Finley et al., 1987). The repetitive structure of the *UBI4* gene gives an advantage to cells to quickly produce large amounts of

ubiquitin in response to stress (Gemayel et al., 2017). On the other hand, *UBI1*, *UBI2* and *UBI3* encode for a linear fusion of a sole ubiquitin moiety with r-proteins (Finley et al., 1989). These genes generate most cellular ubiquitin in exponential growth conditions. *UBI1* and *UBI2* are paralogous genes and, in this case, ubiquitin is fused to the 60S r-protein eL40A and eL40B, respectively. In turn, the *UBI3* gene encodes for a single ubiquitin moiety fused to the 40S r-protein eS31. In humans, there are also four genes encoding for ubiquitin: *UBB* and *UBC* (poly-ubiquitin genes), *UBA80* (ubiquitin fusion with eS31) and *UBA52* (ubiquitin fusion with eL40).

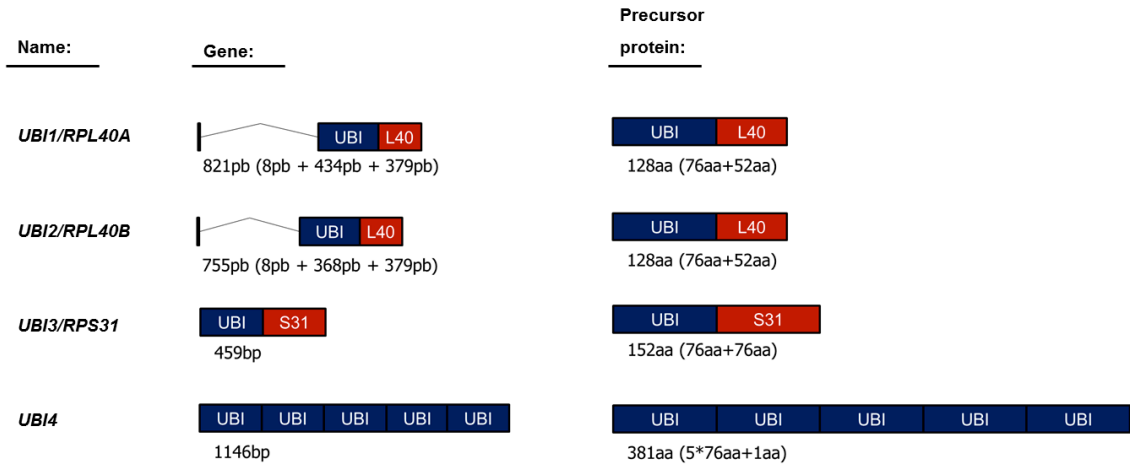


**FIGURE 17. Schematic representation of the *UBI* genes in *S. cerevisiae*.** The *UBI1* and *UBI2* genes encode for a single N-terminal ubiquitin moiety fused to the 60S r-protein eL40. *UBI3* gene has the same structure than *UBI1/2* but the ubiquitin molecule is fused to the 40S r-protein eS31. *UBI4* consists of a 5 head-to-tail repeats of ubiquitin. Adapted from Antonio Fernández Pevida Thesis work.

Ubiquitin appears to be fused with r-proteins across the life kingdoms. This could be the result of a smart strategy of linking protein synthesis and degradation to maintain protein homeostasis. However, this scenario could have been selected on any r-protein in different organisms. Instead, most eukaryotes, like yeast, curiously share r-proteins eL40 and eS31 as the only proteins fused to ubiquitin. Furthermore, orthologues of both r-proteins are present in eukaryotes and in archaea but not in bacteria. It is not clear why evolution has selected these r-proteins as the main (almost exclusive) r-proteins fused to ubiquitin. Indeed, certain authors have proposed that ubiquitin can act as a co-translational chaperone that facilitates the synthesis and assembly of these particularly small r-proteins into the ribosome (Finley et al., 1989;

Lacombe et al., 2009). This hypothesis correlates with the evolutionary origin of the ubiquitin system previously proposed by Varshavsky (Varshavsky, 2012). Given that in prokaryotes ubiquitin-like proteolytic pathways have been found but not the *bona fide* ubiquitin system, Varshavsky proposed that primordial ubiquitin (i.e. a protein containing the ubiquitin fold) served as an incipient N-terminal co-translational chaperone of polypeptides. This function might account for its initial spread in the eukaryotic kingdom through DNA recombination and positive selection.

Interestingly, only a few rare exceptions to the general ubiquitin fusion arrangement have been found in some organisms. For example, a poly-ubiquitin precursor is fused to the ribosomal protein eL40 in *Trypanosoma cruzi* (Swindle et al., 1988). In the protozoa *Giardia lamblia* and *Entamoeba histolytica*, ubiquitin is rarely encoded by mono-ubiquitin genes (Krebber et al., 1994) (Wostmann et al., 1996). Moreover, in *G. lamblia*, the r-protein eS31 is fused to an ubiquitin-like protein that surprisingly remains uncleaved in the mature ribosome (Catic et al., 2007). The r-protein eS31 is also fused to an ubiquitin-like protein in the nematodes *Caenorhabditis elegans* and *C. briggsae*. Therefore, in certain organisms, the ubiquitin moiety has diverged into ubiquitin-like proteins (Jones and Candido, 1993). For example, in mammals the ribosomal protein eS30 is synthetized as a fusion protein with an ubiquitin-like protein that, in this case, is post-translational cleaved (Gietz and Sugino, 1988). The rare algae *Chlorarachniophytes* are another exception; in these organism, there is an unexpected diversity of genes fused to ubiquitin such as the r-proteins eL40 and eS31, the r-proteins P1 and P2, actin, a nickel superoxide dismutase, etc. (Sibbald et al., 2019). Moreover, in this alga the ubiquitin moiety has been detected in the N-terminal, C-terminal or even in an internal position.

Remarkably, while ubiquitin is extremely conserved during the eukaryotic evolution, there is a high diversity in the ubiquitin system. Moreover, eukaryotic genomes keep identical copies of the ubiquitin gene despite its redundancy (Zuin et al., 2014). It has been proposed that frequent recombination events in the poly-ubiquitin locus generated new copies of ubiquitin (or ubiquitin-like modifiers) and serve to maintain the high degree of similarity. On the other hand, the ubiquitin sequence in

the ubiquitin fusion gene with eS31 is variable between lower eukaryotes (Catic and Ploegh, 2005). However, this moiety is maintained in those organisms probably because this arrangement confers some positive advantages.

### Role of ubiquitin in r-proteins eL40 and eS31

As mentioned before, in most eukaryotes ubiquitin is fused to eukaryotic-specific r-proteins eL40 and eS31. This raises the question of whether the ubiquitin moiety might play a direct role in the synthesis, assembly, and/or function of these two r-proteins. However, the exact contribution of the ubiquitin moiety to ribosome biogenesis has been poorly studied. The r-protein eL40 is an essential protein that associates in the cytoplasm with late pre-60S r-particles, whereas eS31 is a quasi-essential r-protein of the small r-subunit that assembles in the nucleus (Fernández-Pevida et al., 2016; Fernández-Pevida et al., 2012). Interestingly, both r-proteins are located in the joining surface of its respective subunit, close to the elongation factors binding site **(Figure 18)** (Ben-Shem et al., 2010).

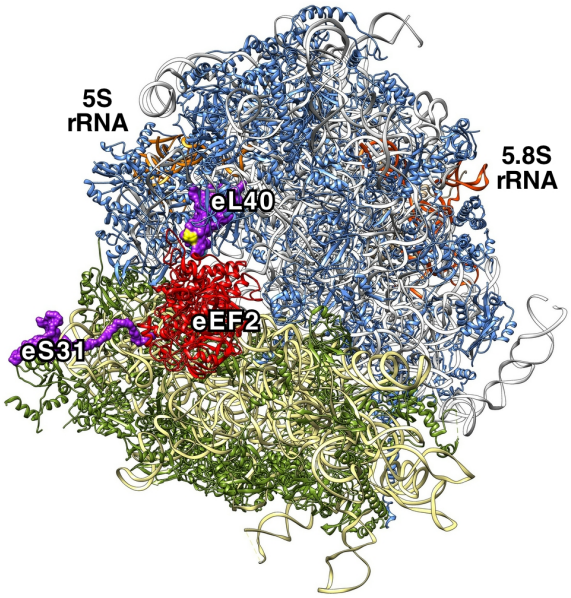


**FIGURE 18. Positions of r-proteins eL40 and eS31 in mature ribosomes from *S. cerevisiae*.** Ribosomal proteins eL40 and eS31 within the large and small r-subunit, respectively, have been highlighted in purple. The remaining r-proteins are coloured in blue (large r-subunit) or green (small r-subunit); 25S rRNA is coloured in pale grey, 5.8S and 5S rRNAs in orange, and 18S rRNA in pale yellow. Position of eEF2 (red) in the 80S ribosome is indicated. Adapted from (Martín-Villanueva et al., 2019).

Previous studies suggest that the proteolytic maturation of these Ubi precursors occurs very rapidly, likely co-translationally; indeed, the precursor proteins could never be detected under wild-type conditions (Fernández-Pevida et al., 2016; Finley et al., 1989). We have previously demonstrated that the proteolytic maturation of the Ubi precursors is required for proper assembly of r-proteins eS31 and eL40 into 40S and 60S r-subunits, respectively since non-cleaved Ubi3 or Ubi1 variants confer lethal phenotypes when expressed as the sole source of eS31 or eL40 (Lacombe et al., 2009) (Martín-Villanueva et al., 2019). Moreover, non-cleaved variants of Ubi3 or Ubi1 can be incorporated into pre-ribosomal particles only when there is no competition with the processed wild-type r-proteins. These studies also indicate that Ubi3-containing r-particles are slightly impaired in translation initiation, whereas the Ubi1-containing r-particles delay their cytoplasmic maturation and compromise the efficiency of translation elongation; this is probably due to the fact that the unprocessed ubiquitin could be interfering with the recruitment and function of the elongation factors eEF1A and eEF2, which bind in close proximity to eL40 (Lacombe et al., 2009) (Martín-Villanueva et al., 2019).

We have also studied the consequences of deleting the N-terminal ubiquitin moiety of the Ubi3 precursor. The ubiquitin deletion mutant *ubi3Δub* shows slow-growth phenotype, a shortage of 40S r-subunit and 18S rRNA content defects, which are suppressed by its increased dosage (Finley et al., 1989; Lacombe et al., 2009). These results reveal that the ubiquitin moiety is important but not essential for the functional integrity of eS31. Accordingly, it has been proposed that the ubiquitin moiety could act as a chaperone to facilitate the correct folding, thus, contributing to the efficient synthesis of r-proteins eS31 and eL40. In agreement with this hypothesis, practically all r-proteins tend to aggregate in the absence of the ribosome-associated Ssb-RAC and NAC chaperone complexes, with the apparent exception of eS31 and eL40 (Koplin et al., 2010). Additionally, the proteolytic removal of ubiquitin from eS31 and eL40 could serve to couple the supply of ubiquitin to the production and/or function of ribosomes, integrating and coordinating the synthesis and degradation of proteins in eukaryotes. One of the objectives of this work is to further examine the effects of deleting the N-terminal ubiquitin moiety of the Ubi1 precursor.

# 3. OBJECTIVES

The aim of our group is to deepen the knowledge on the function of selected *trans*-acting factors and r-proteins from both r-subunits in the ribosome biogenesis process of the model eukaryote *S. cerevisiae.* Specifically, in this Thesis Work, I have explored the role of a pair of particular r-proteins eL40 and eS31, which are synthesized as precursors fused to an ubiquitin molecule, in ribosome biogenesis and function. The precise objectives of this work are:

1. Study the role of the ubiquitin moiety fused to the eL40 r-protein in the biogenesis of yeast ribosomes. More specifically, we aim to analyse how the absence of this *cis*-acting ubiquitin moiety or its replacement by the ubiquitin-like protein Smt3 affects the expression and assembly of eL40 in 60S r-subunits.

2. Assess the contribution of the so-called beak region of 40S r-subunits in yeast ribosome synthesis and function, through the phenotypical analysis of mutants lacking the r-proteins eS12 and eS31, alone or in combination.

# 4. RESULTS

# CHAPTER 1

# The ubiquitin moiety of Ubi1 is required for proper production of ribosomal protein eL40 in *Saccharomyces cerevisiae*

## INTRODUCTION

Ubiquitin is a small eukaryotic protein of 76 amino acids whose name (i.e., it occurs *ubiquitously*) results from its extremely evolutionary conservation (Iyer et al., 2006). Ubiquitin functions as a reversible post-translational modifier of proteins to regulate many different cellular processes such as DNA repair, chromatin dynamics, cell cycle regulation, membrane and protein trafficking, endocytocis, autophagy, but most notably proteasome-dependent protein degradation (Kwon and Ciechanover, 2017; Pickart, 2001). Normally, the conjugation of ubiquitin to other proteins involves the formation of an isopeptide bond between the α-carboxyl group of the C-terminal glycine of an ubiquitin molecule with an ε-amino group of a specific lysine residue within the target protein (Kwon and Ciechanover, 2017; Pickart, 2001). This process is known as ubiquitination and involves three sequential steps: activation, conjugation and ligation, which are performed by E1s or ubiquitin-activating enzymes, E2s or ubiquitin-conjugating enzymes and E3s or ubiquitin ligases, respectively. The reversal of this modification, deubiquitination, is catalysed by specific proteases named deubiquitinating enzymes (Amerik and Hochstrasser, 2004).

In most eukaryotes studied, ubiquitin is encoded by two groups of genes: (i) the first one comprises genes encoding a single copy of ubiquitin fused to r-proteins, commonly eL40 and eS31. Ubiquitin fusions to other r-proteins, such as P1 or P2, and even to non-ribosomal proteins, such as actin, have been reported in diverse genera of the rare single-celled algae of the class *chlorarachniophyceae* as *Bigelowiella natans* (Archibald et al., 2003). (ii) The second class includes genes that encode a polyubiquitin precursor protein, which consists of a polymer of several tandem ubiquitin monomers (e.g. (Baker and Board, 1987; Callis et al., 1995; Gemayel et al., 2017; Özkaynak et al., 1987)). For both classes, free *de novo* ubiquitin is synthesized by proteolytic maturation from the corresponding precursor proteins. Only rarely, ubiquitin is encoded by mono-ubiquitin genes, as occurring in the protozoa *Giardia lamblia* and *Entamoeba histolytica,* or in algae as *Guillardia theta* and *B. natans* (Krebber et al., 1994; Sibbald et al., 2019; Wostmann et al., 1996).

In *S. cerevisiae,* but also in mammals, ubiquitin is encoded by four different genes (Finley et al., 1989). The yeast *UBI4* gene (equivalent to human *UBB* and *UBC* genes) encodes a polyubiquitin precursor protein of five head-to-tail repeats of ubiquitin. Expression of *UBI4* occurs when cells enter the stationary phase or when they are exposed to several stresses including heat shock, oxidative stress, exposure to DNA-damaging agents or nutrient depletion (Cheng et al., 1994; Finley et al., 1987; MacDiarmid et al., 2016; Özkaynak et al., 1987; Simon et al., 1999; Treger et al., 1988). The paralogous *UBI1* and *UBI2* yeast genes (equivalent to human *UBA52* gene) encode a single ubiquitin moiety fused to the 60S r-proteins eL40A and eL40B, respectively. In turn, the yeast *UBI3* gene (equivalent to human *RPS27A/UBA80* gene) codes for a single copy of ubiquitin fused to the 40S r-protein eS31 (Finley et al., 1989; Özkaynak et al., 1987). In active growing yeast cells, most of the ubiquitin originates from these three r-protein fusion genes (Finley et al., 1987), and their expression is differentially repressed by starvation or by stress conditions (Fraser et al., 1991).

There are other proteins that share the ubiquitin fold; these proteins are also able to undergo conjugation to substrate proteins through an equivalent isopeptide bond to that involving ubiquitin, which also occurs by an analogous process than ubiquitination (for a review, see (Pickart, 2001; Pickart and Eddins, 2004)). Among these proteins, known as ubiquitin-like modifier proteins, SUMO (small ubiquitin-related modifier) is the broadest spread member within eukaryotes (Pickart and Eddins, 2004). Four SUMO genes coding for different monomeric SUMO isoforms have been identified in mammals, while yeast harbours a single essential gene, *SMT3*, which encodes the SUMO protein called Smt3 (Johnson, 2004). Sumoylation of target proteins regulates various cellular processes by modulating the localization or activity of the SUMO-modified substrate proteins. In contrast to ubiquitination, sumoylation seems to enhance the stability of the target proteins (review in (Johnson, 2004; Muller et al., 2001)). This latter feature has been biotechnologically exploited to increase the yield of recombinant proteins in *Escherichia coli*; thus, the N-terminal fusion of a single SUMO moiety to recombinant proteins that normally fail to proper fold and precipitate as inclusion bodies significantly improves their stability and solubility (e.g. (Lee et al., 2008; Peroutka Iii et al., 2011)). Similarly, expression of N-terminal fusions of ubiquitin

to recombinant proteins has been found to augment their yield and increase their solubility (Baker, 1996; Butt et al., 1989; Ecker et al., 1989). However, whether N-terminal fusions of SUMO or ubiquitin moieties to given proteins could act physiologically as *in vivo* molecular chaperones for proper folding and efficient expression of the fused proteins remains obscure (see discussion of ref. (Graciet et al., 2006)).

We are interested in understanding the contribution of the ubiquitin moiety within the Ubi1/2 and Ubi3 proteins to ribosome biogenesis and function. Experimental evidence indicates that while eS31 is a quasi-essential r-protein that assembles in the nucleus, most likely into early 90S pre-ribosomal particles (Fernández-Pevida et al., 2016; Sun et al., 2017), eL40 is an essential r-protein that associates in the cytoplasm with late pre-60S r-particles (Fernández-Pevida et al., 2012; Kruiswijk et al., 1978). Under wild-type conditions, the Ubi1/2 and Ubi3 precursor proteins could so far never be detected, suggesting that their proteolytic maturation occurs very rapidly, likely co-translationally, and therefore before the assembly of the respective r-proteins into pre-ribosomal particles (Fernández-Pevida et al., 2016; Finley et al., 1989; Lacombe et al., 2009). We have previously studied the consequences of introducing mutations in the intersection between both ubiquitin and eS31 within the Ubi3 precursor, and ubiquitin and eL40 within the Ubi1 precursor that partially or totally impair ubiquitin removal (Lacombe et al., 2009; Martín-Villanueva et al., 2019). The obtained results indicate that the presence of ubiquitin hinders the assembly of the respective r-proteins into pre-ribosomal particles, consequently, assembly of either eS31 or eL40A is favoured over that of non-cleaved Ubi3 or Ubi1, respectively (Lacombe et al., 2009; Martín-Villanueva et al., 2019). Moreover, non-cleaved Ubi3 or Ubi1 variants confer lethal phenotypes when expressed as the sole source of eS31 or eL40, respectively. Only in these circumstances (e.g. depletion of either wild-type r-protein eS31 or eL40 counterparts), these mutant proteins get incorporated into nascent pre-ribosomal particles (Lacombe et al., 2009; Martín-Villanueva et al., 2019). Strikingly, while Ubi3-containing r-particles are partially impaired in translation initiation but can finally engage in translation (Lacombe et al., 2009), Ubi1-containing r-particles delay their cytoplasmic maturation (i.e. Tif6

recycling), prevent r-subunit joining and hinder translation elongation (Martín-Villanueva et al., 2019). In addition, we and others have shown that the ubiquitin moiety of the Ubi3 precursor can be deleted without causing a deleterious phenotype to the corresponding *ubi3Δub* mutant, as long as the unfused eS31 r-protein is expressed at elevated dosage (Finley et al., 1989; Lacombe et al., 2009). In contrast, expression of eS31 from an integrated *ubi3Δub* allele into its natural chromosomal locus conferred a pronounced slow-growth (sg) phenotype and a shortage of 40S r-subunits (Finley et al., 1989; Lacombe et al., 2009). Thus, the N-terminal ubiquitin moiety of Ubi3 has an important role during the efficient synthesis of eS31 and hence influences its subsequent assembly and the overall levels of 40S r-subunits. In this study, we performed an equivalent analysis with an *ubi1Δub* allele, which encodes an ubiquitin-free Ubi1ΔUb precursor protein. As above, when the sole cellular source of eL40 comes from a single-copy *ubi1Δub* allele expressed from its genomic locus, cells showed a pronounced sg phenotype and a deficit of 60S r-subunits; both defects are fully suppressed by increasing the gene dosage of the *ubi1Δub* allele from a *CEN* plasmid. Therefore, as for Ubi3, it appears that the ubiquitin moiety of Ubi1 is important for the efficient accumulation of the corresponding eL40A product protein. Importantly, expression of an N-terminal Smt3-fused eL40A variant protein as sole source of eL40 leads to a mildly but significantly improvement of cell growth, especially at high temperatures. Finally, we have evaluated the aggregation status of HA-tagged eL40A protein expressed either from a genomic *UBI1*-HA, a *ubi1Δub*-HA or a *SMT3-eL40A*-HA allele, and compared it to that of HA-tagged eS31 expressed either from a genomic *UBI3*-HA or a *ubi3Δub*-HA allele. As results, we found practically no differences in the aggregation status of the HA-tagged eL40 protein derived from the ubiquitin-free Ubi1ΔUb-HA precursor when compared to that from an UBI1-HA precursor in cells also containing a *ubi2Δ* mutation. However, we could find both, a clear tendency for enhanced aggregation of the HA-tagged eS31 derived from the *ubi3Δub*-HA allele compared to that from the *UBI3-HA* allele and for reduced aggregation of eL40A-HA when expressed from the Smt3-eL40A-HA precursor compared to that from Ubi1Δub-HA. Herein, these results are discussed on the context of the possible role of N-terminal ubiquitin moiety fused to eS31 and eL40 as

molecular chaperones to facilitate the correct folding and efficient synthesis of these two r-proteins.

## RESULTS



### Generation of *ubi1* mutants for the phenotypic analysis of the ubiquitin-L40A fusion protein

Yeast eL40 is an essential r-protein of 52 amino acids that is encoded by two independent paralogous genes, *UBI1* (*RPL40A*; YIL148W) and *UBI2* (*RPL40B*; YKR094C). As previously mentioned, in practically all eukaryotes, eL40 as well as the r-protein eS31 (*UBI3* gene), are produced as C-terminal parts of ubiquitin-fused precursor proteins. We have previously studied the effects of impairing the ubiquitin removal within Ubi1 and Ubi3 precursors by using mutants where the efficiency of this removal was reduced (Lacombe et al., 2009; Martín-Villanueva et al., 2019). However, to date, only experimental data concerning the phenotypic consequences of expressing a genomic *ubi3Δub* allele, which lacks the region coding for the ubiquitin moiety, are available (Finley et al., 1989; Lacombe et al., 2009). To explore the role of the N-terminal fused ubiquitin moiety within Ubi1/2 precursors, we constructed two different mutants **(Figure 1)**. First, we generated a mutant replacing the endogenous wild-type *UBI1* copy with an *ubi1Δub* mutant, which harbours a deletion of the ubiquitin moiety from the Ubi1 precursor. To allow efficient translation of the construct, an ATG start codon was inserted just downstream the 5' *UBI1* untranslated sequence; thus, the corresponding eL40A protein started with an N-terminal methionine not present in the natural eL40A. Second, we replaced the endogenous *UBI1* allele with a *SMT3-S-eL40A* allele, where the ubiquitin coding region was exchanged with a Smt3 (hereafter SUMO) coding region. To facilitate cleavage of the SUMO moiety, we inserted a serine codon at the junction between the coding regions of Smt3 and eL40A. In both constructs, as well as in a genomic wild-type *UBI1* copy, we also added an in-frame C-terminal single HA epitope for western detection.

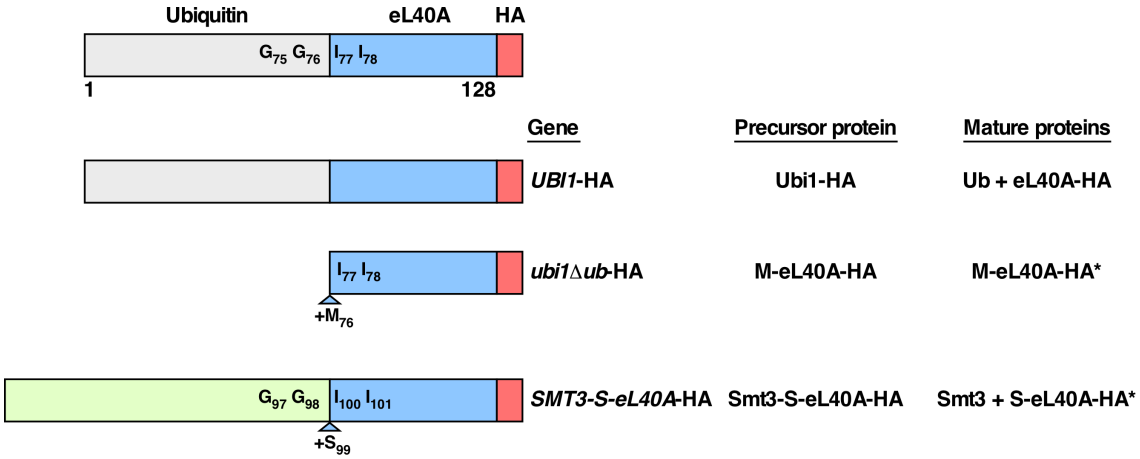


**FIGURE 1. Schematic representation of the genomic constructs used in this study.** Ubi1 consists of an N-terminal ubiquitin moiety fused to the r-protein eL40A. A peptide bond between the C-terminal glycine of ubiquitin (G76) and the N-terminal isoleucine of eL40A (I77) connects the two proteins. Relevant residues and *ubi1* mutant variants thereof used in this study are also indicated. The relevant constructs, precursor and mature protein names are also indicated. The asterisk denotes that the exact nature of the mature proteins derived from these precursor proteins has not been studied; thus, the indicated mature proteins correspond to the most likely products. A C-terminal 1xHA tag was added for western detection of the Ubi1 and/or eL40 protein variants.

## The *ubi1Δub* ubiquitin deletion mutant displays a slow-growth phenotype

For the functional analysis of the generated mutants, we first examined the growth phenotype associated with the deletion of the ubiquitin moiety from the Ubi1 precursor **(Figure 2)**. As eL40 is encoded by two independent paralogous genes, we performed this analysis both in the presence or the absence of a functional eL40B r-protein (wild-type *UBI2* or *ubi2Δ* background, respectively). As previously described (Fernández-Pevida et al., 2012; Martín-Villanueva et al., 2019), the presence of the HA epitope slightly affected growth when eL40A-HA is the sole source of eL40, especially at low temperatures. In agreement, doubling times of ca. 1.8 h, 2.0 h and 3.0 h were obtained in liquid YPD at 30 ºC for the wild-type W303-1A strain, and the isogenic *ubi2Δ* and *UBI1*-HA *ubi2Δ* mutants, respectively. As also discussed (Martín-Villanueva et al., 2019), this is likely due an adverse effect of the extra amino acids on the interaction environment of the C-terminus of eL40A within the ribosome. **Figure 2** also shows that deletion of the ubiquitin moiety has no effect on cell growth when the *UBI2* gene is present. However, the *ubi1Δub*-HA *ubi2Δ* mutant, in which the sole cellular source of eL40 comes from the single-copy expression of a ubiquitin-free eL40A r-protein, showed a severe sg phenotype, at all tested temperatures. Compared with the previous strains, the *ubi1Δub-HA ubi2Δ* mutant doubled every 5.5 h in liquid YPD at 30 ºC.

It has been previously shown that increased dosage of the *ubi3Δub* allele suppresses its growth defect phenotype (Finley et al., 1989; Lacombe et al., 2009). Thus, to address whether a similar situation occurred upon an increased dosage of the *ubi1Δub* allele, we cloned either the wild-type *UBI1*-HA or the mutant *ub1Δub*-HA allele on YCplac111, a low-copy-number *CEN LEU2* plasmid (Gietz and Sugino, 1988), and transformed a shuffle *ubi1Δ ubi2Δ* strain (TAY001 strain; see **Table 1**). After plasmid pHT4467Δ-UBI1 (*URA3 ADE3*) shuffling on 5-FOA-containing plates, cells were analysed on YPD plates. As shown in **Figure 2**, expression of the *ub1Δub*-HA allele from a *CEN* plasmid was able to significantly ameliorate the growth defect of the *ubi1Δub-HA ubi2Δ* strain to apparently the wild-type extend. This is in agreement with previous data showing that the expression of a *ubi1Δub* allele from a strong promoter also complemented the lethal phenotype of a *ubi1Δ ubi2Δ* strain to the wild-type extend (Finley et al., 1989). We conclude that the ubiquitin moiety of Ubi1 is required for optimal cell growth when its expression is driven from a single-copy allele.

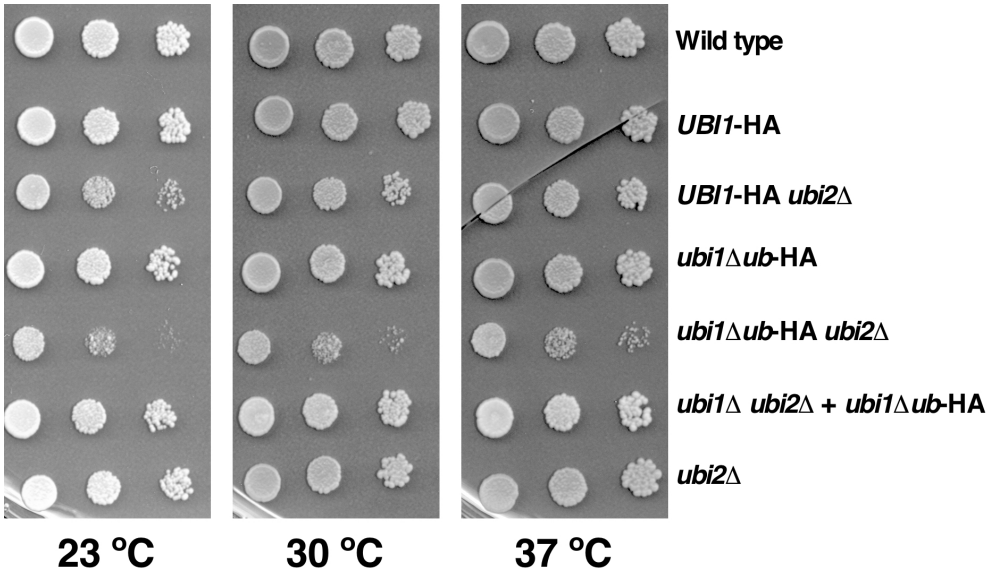


**FIGURE 2. The genomically integrated *ubi1Δub*-HA allele confers a slow-growth phenotype**. Growth analysis of the indicated strains, either expressing a C-terminally HA-tagged Ubi1 (*UBI1*-HA) or an Ubi1Δub (*ubi1Δub*-HA) variant protein from the *UBI1* genomic locus or from a centromeric plasmid (+ *ubi1Δub*-HA), in a wild type *UBI2* or a *ubi2Δ* null mutant background**.** Strains W303-1A (Wild type), SMY113 (*UBI1*-HA), SMY256 (*UBI1*-HA *ubi2Δ*), SMY107 (*ubi1Δub*-HA), SMY257 (*ubi1Δub*-HA *ubi2Δ*), SMY215 [YCplac111-ubi1Δub-HA] (*ubi1Δ ubi2Δ +* ubi1Δub-HA) and JDY922 (*ubi2Δ*) were spotted in fivefold serial dilution steps onto YPD plates, which were incubated for 4 days at 22 ºC or for 3 days at 30 ºC and 37 ºC.

**The *SMT3*-S-*eL40S ubi2Δ* mutant displays a slow-growth phenotype**

The small ubiquitin-like modifier SUMO shares an overall three-dimensional structure very similar to ubiquitin and possess, as ubiquitin, a C-terminal glycine residue (e.g. (van der Veen and Ploegh, 2012)). Thus, we reasoned that if ubiquitin had a *cis*-acting function affecting that of the eL40 protein, the replacement of the ubiquitin moiety in Ubi1 by the SUMO molecule should not drastically impair the function of eL40 if properly processed. To this aim, we first analysed the consequences in growth of replacing the ubiquitin moiety of the Ubi1 precursor by the ubiquitin-like modifier SUMO. As above, we used both the *UBI2* and *ubi2Δ* backgrounds. As shown in **Figure 3**, when the wild-type *UBI2* allele is present, the strain displays apparent wild-type growth. Interestingly, the *SMT3*-S-*eL40A*-HA *ubi2Δ* strain, where the sole source of eL40 comes from the precursor Smt3-S-eL40A-HA, shows a mild but significant improvement of the cell growth if compared with that of the isogenic *ubi1Δub ubi2Δ* counterpart, which is especially evident at higher temperatures. Consistently, compared to other *ubi1* strains, the *SMT3*-S-*eL40A*-HA *ubi2Δ* strain doubled every 4.0 h in liquid YPD at 30 ºC. As above, increasing the gene dosage of *SMT3*-S-*eL40A*-HA by

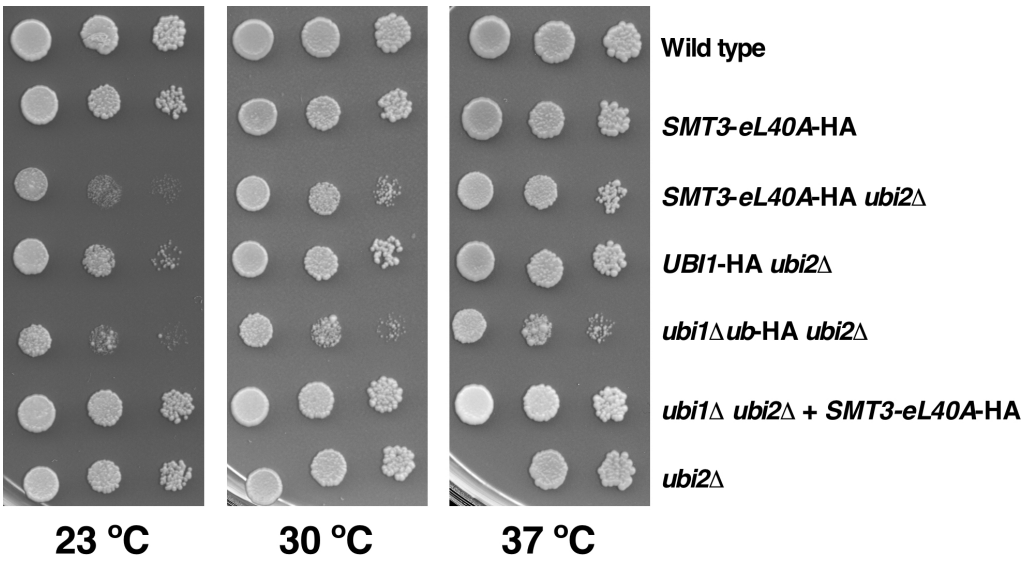


**FIGURE 3. The genomically integrated *SMT3-eL40A* allele permits better growth than the *ubi1Δub*-HA one.** Growth analysis of the indicated strains, either expressing a C-terminally HA-tagged Ubi1 (*UBI1*-HA) or a fusion Smt3-eL40A (*SMT3-eL40A*-HA) variant protein from the *UBI1* genomic locus or from a centromeric plasmid (+ *SMT3-eL40A*-HA), in a wild type *UBI2* or a *ubi2Δ* null mutant background**.** Strains W303-1A (Wild type), SMY218 (*SMT3-eL40A*-HA), SMY258 (SMT3-*eL40A*-HA *ubi2Δ*), SMY256 (*UBI1*-HA *ubi2Δ*), SMY257 (*ubi1Δub*-HA *ubi2Δ*), SMY216 [YCplac111-SMT3-eL40A-HA] (*ubi1Δ ubi2Δ +* SMT3-eL40A-HA) and JDY922 (*ubi2Δ*) were spotted in fivefold serial dilution steps onto YPD plates, which were incubated for 4 days at 22 ºC and for 3 days at 30 ºC and 37 ºC.

the use of a low-copy-number plasmid is suppressing the sg phenotype linked to the genomic single-copy *SMT3*-S-*eL40A* allele. We conclude that SUMO is able to partially compensate the loss of the *cis*-acting role of the ubiquitin moiety of Ubi1 on eL40A.

**Role of the ubiquitin and SUMO moieties on the expression levels of eL40A**

The fact that the sg phenotype linked to the expression of either the *ubi1Δub*-HA or *SMT3*-S-*eL40A*-HA alleles as the sole source of cellular eL40 r-protein was suppressed by increasing the copy-number of the respective alleles, strongly suggests that the ubiquitin-coding tail of the *UBI1* gene facilitates the expression of eL40A r-protein. To test this hypothesis, we monitored the expression levels of the eL40A-HA protein in the different used strains by western blotting. As shown in **Figure 4**, the protein levels of eL40A-HA significantly decreased in the *ubi1Δub-HA ubi2Δ* strain, compared with the expression of wild-type eL40A-HA r-protein from the *UBI1*-HA allele. As expected, an increased dosage of the *ubi1Δub-HA* allele restores the protein levels of eL40A-HA **(Figure 4, lane 5)**. Together, these results indicate that the ubiquitin moiety of Ubi1 is required for the efficient production of the eL40 r-protein.

To assess the efficiency of Smt3-S-eL40A-HA cleavage into SUMO and eL40A-HA, western blot analyses using anti-HA antibodies were also carried out in whole cell extracts of strains harbouring a genomic *SMT3*-S-*eL40A* allele. As previously shown (Fernández-Pevida et al., 2012; Martín-Villanueva et al., 2019), no Ubi1-HA precursor but only mature eL40A-HA was detected in the *UBI1*-HA strains **(Figure 4, lanes 2 and 3)**. In contrast, although mature eL40A-HA was fairly well detected in the genomic *SMT3*-S-*eL40A*-HA *ubi2Δ* strain, some precursor protein could also be detected at the expected molecular mass, especially when the fusion Smt3-S-L40A protein variant is the sole cellular source of eL40 **(Figure 4, lanes 6 and 7)**. We conclude that replacement of the ubiquitin by a SUMO moiety followed by a linked serine at its C-terminus reduces the efficiency of the proteolytic processing of the precursor into SUMO and eL40A. Nevertheless, a clear increase in the total amount of produced mature eL40A-HA is observed in the cell extracts of the *SMT3*-S-*eL40S* strains.

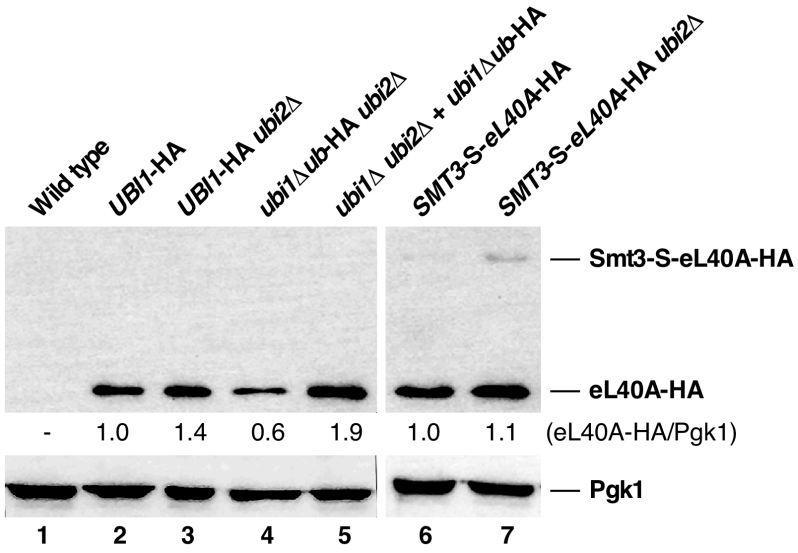


**FIGURE 4. Analysis of the eL40A-HA protein levels in the different mutants of this study.** Wild-type and the indicated strains expressing distinct C-terminally HA-tagged Ubi1 constructs from the genomic locus or from a centromeric plasmid, in a wild type *UBI2* or a *ubi2Δ* null mutant background, were grown in liquid YPD medium at 30 ºC. Total cell extracts were prepared and subjected to Western analysis using anti-HA and anti-Pgk1 (loading control) antibodies. The mature eL40A-HA and the Smt3-eL40A-HA precursor are indicated. The relative intensities of the specific bands from these western blots were quantified, and the ratios of the relative intensities between eL40A-HA and the corresponding Pgk1 signal were calculated. The ratios obtained for the *UBI1*-HA strain, which were arbitrarily set to 1.0, were used for normalisation.

## The genomic *ubi1Δub*-HA and *SMT3-S-eL40A*-HA mutations affect 60S r-subunit biogenesis and translation

As the genomic *ubi1Δub*-HA allele limits the production of eL40A protein in a *ubi2Δ* background, we wonder whether this is also accompanied by a 60S r-subunit shortage. Thus, we performed polysome profile analyses in the different *ubi1* mutants described in this study. We first examined the profiles of the control *UBI1*-HA *ubi2Δ* strain grown in YPD at 30 ºC. As shown in **Figure 5A**, this strain showed, as expected for the presence of the *ubi2Δ* allele (Fernández-Pevida et al., 2012), a very mild deficit in 60S r-subunits as evidence for the appearance of half-mer polysomes. In contrast, the analysis of the *ubi1Δub*-HA *ubi2Δ* strain reveals, in addition to the appearance of half-mer polysomes, a clear decrease in normal polysomes **(Figure 5B)**. These profiles resemble those obtained upon the depletion of eL40, including the nearly invariant free 60S/40S ratio found (Fernández-Pevida et al., 2012), therefore, confirming that the amount of eL40 is indeed limited in this strain. Consistently, amplification of the copy number of the *ubi1Δub* allele by positioning it in a *CEN* plasmid, lead to wild-type

polysome profile, as this overcomes the limitation in the eL40 accumulation **(Figure 4 and 5C)**. Altogether, these results indicate that the deletion of the ubiquitin moiety from a genomically expressed ubiquitin-free Ubi1ΔUb precursor, in the absence of eL40B, leads to a decrease production of eL40A and as a consequence of 60S r-subunits. Thus, we conclude that, as also occurring for the ubiquitin moiety of Ubi3 (Finley et al., 1989; Lacombe et al., 2009), the ubiquitin moiety of Ubi1 is important but not strictly required for ribosome synthesis.

We also assess the effects of the replacement of the ubiquitin by a SUMO moiety on ribosome biogenesis. As shown in **Figure 5D**, the *SMT3*-S-*eL40A*-HA *ubi2Δ* strain displayed a polysome profile showing an increase in the amount of free 60S r-subunits *vs* 40S r-subunits as well as half-mer polysomes. This profile is typical of mutants partially impaired in 60S to 40S r-subunit joining (e.g. (DeLabre et al., 2002; Eisinger et al., 1997; Fernández-Pevida et al., 2012)) that, strikingly, we have also observed for other *ubi1* mutants unable to efficiently remove the ubiquitin moiety of Ubi1 (Martín-Villanueva et al., 2019).

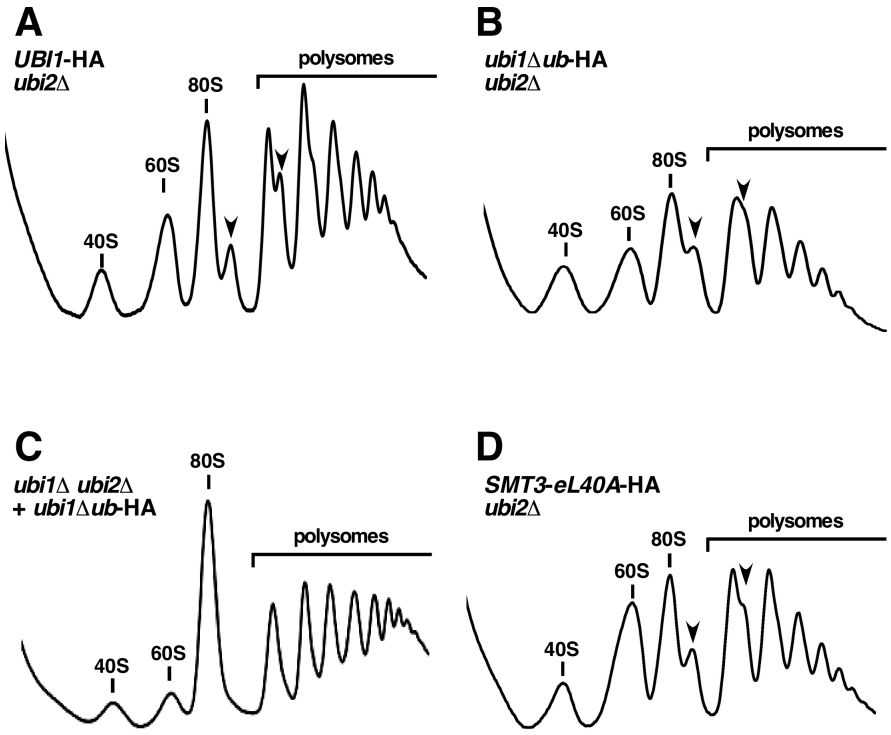


**FIGURE 5. The genomically integrated *ubi1Δub*-HA and *SMT3-eL40A* alleles lead to a deficit in 60S r-subunits.** Strains SMY256 (*UBI1*-HA *ubi2Δ*) **(A)**, SMY257 (*ubi1Δub*-HA *ubi2Δ*) **(B)**, SMY215 [YCplac111-ubi1Δub-HA] (*ubi1Δ ubi2Δ + ubi1Δub*-HA) **(C),** and SMY258 (SMT3-*eL40A*-HA *ubi2Δ*) **(D)** were grown in YPD medium at 30ºC to an $OD_{600}$ of about 0.8. Cell extracts were prepared and 10 $A_{260}$ units of each extract were resolved in 7–50% sucrose gradients. The $A_{245}$ was continuously measured. Sedimentation is from left to right. The peaks of free 40S and 60S r-subunits, 80S vacant ribosomes/monosomes and polysomes are indicated. Half-mer polysomes are labeled by arrows.

We next studied, in the different mutants, the distribution of their respective eL40A-HA r-protein variants in translating ribosomes by fractionation analysis. No apparent differences were found between the distribution of eL40-HA expressed either from the *ubi1Δub*-HA or the *UBI1*-HA alleles. In both cases, eL40A-HA is detected in 80S ribosome and polysome fractions as also is the 60S r-subunit control protein uL3. This result indicates that the ubiquitin moiety is not required for the assembly of eL40A protein into functional 60S r-subunits **(Figure 6)**. In contrast, when the *SMT3-S-eL40A*-HA *ubi2Δ* strain was studied, while mature eL40A-HA fractionated similarly as the 60S r-subunit control protein uL3, the non-cleaved Smt3-S-eL40A-HA mainly peaked in the 60S and to a lesser extend in the 80S fractions **(Figure 6)**. This

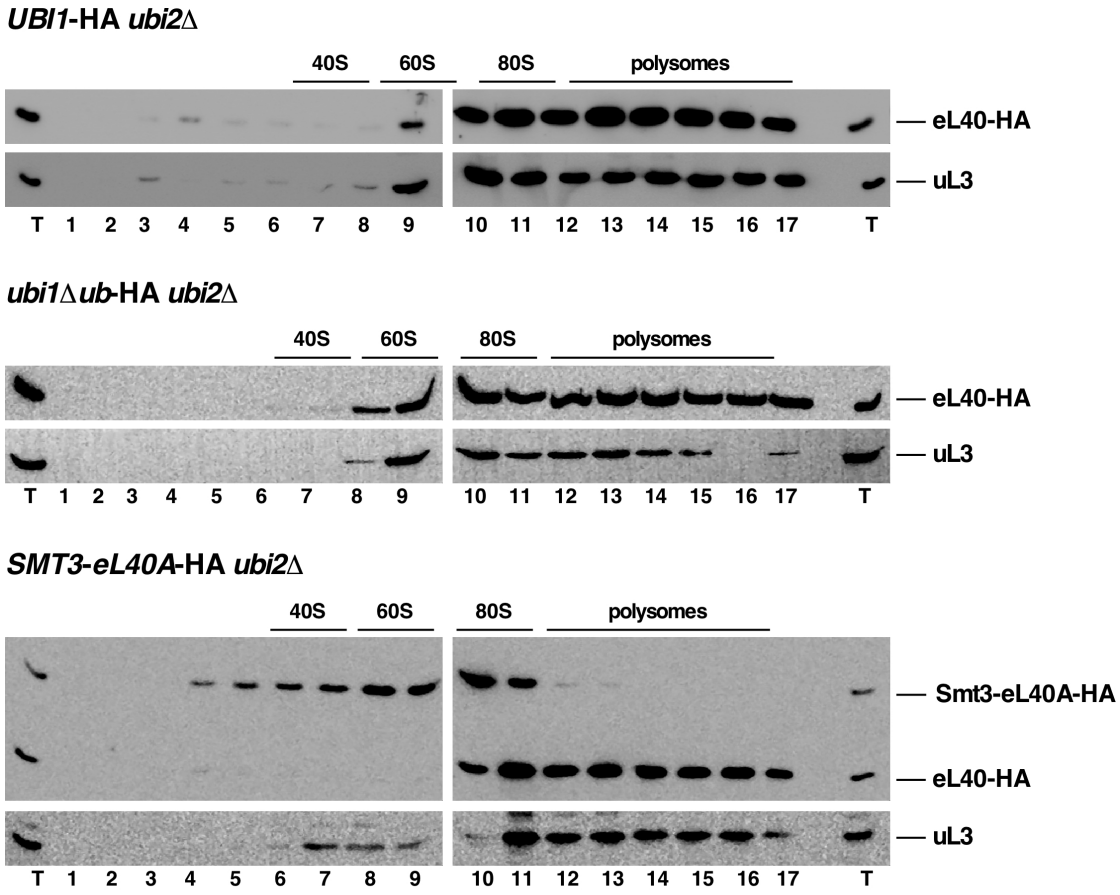


**FIGURE 6. Incorporation into translating ribosomes of the eL40A-HA protein derived of the Ubi1Δub-HA and Smt3-eL40A-HA precursors.** Strains SMY256 (*UBI1*-HA ubi2Δ), SMY257 (*ubi1Δub*-HA ubi2Δ) and SMY258 (*SMT3-eL40A*-HA ubi2Δ) were grown in YPD medium at 30 ºC to mid-log phase. Cell extracts were prepared and 10 $A_{260}$ units of each extract were resolved in 7–50% sucrose gradients. Fractions were collected from the gradients, then the proteins were extracted from each fraction, and equal volumes analyzed by western blotting using anti-HA and anti-uL3 antibodies. The position of free 40S and 60S r-subunits, 80S vacant ribosomes/monosomes and polysomes, obtained from the recorded $A_{245}$ profiles, are shown. T, total cell extract.

precursor protein is basically absent from the polysomal fraction. This result, which is similar to that we have previously observed for non-cleaved Ubi1 precursor variants (Martín-Villanueva et al., 2019), indicates that the Smt3-S-eL40A-HA precursor can assemble into pre-60S r-particles that are unable to engage in subunit joining and possible also in translation elongation. Strikingly, uL3 but not mature eL40A was identified in the 60S peak (see **Figure 6**, bottom panel, lanes 7-10); this result further supports the hypothesis that most of the 60S r-particles containing eL40A are efficiently recruited into polysomes while those containing Smt3-S-eL40A-HA are not and accumulate in this area of the gradient (see profile in **Figure 5D**).

**Expression *in trans* of free ubiquitin fails to rescue the deficiencies of the *ubi1Δub*-HA *ubi2Δ* and *SMT3-S-eL40A*-HA *ubi2Δ* mutants**

It could be reasoned that the mutants used in this study, *ubi1Δub*-HA *ubi2Δ* and *SMT3-S-eL40A*-HA *ubi2Δ*, may contain decreased levels of total cellular free ubiquitin since, in principle, this molecule could only be supply by the *UBI3* gene in actively growing mutant cells. Thus, the defects we observed in the above mutants might be rather due to an ubiquitin shortage. In this scenario, ectopic *in trans* expression of free ubiquitin would result in a suppression of the negative phenotypes of these mutants. To directly test this possibility, we transformed the different *ubi1* strains with a plasmid expressing the ubiquitin moiety to supplement the available amount of free ubiquitin or with an empty control plasmid. As shown in **Figure 7A**, the growth phenotype of the *UBI1*-HA *ubi2Δ, ubi1Δub*-HA *ubi2Δ* and *SMT3-S-eL40A*-HA *ubi2Δ* strains did not change when *in trans* expressing free ubiquitin from a plasmid compared to the control. In addition, we performed polysome profile analyses in the different *ubi1* mutants transformed with either an empty control plasmid or a plasmid expressing the ubiquitin moiety. As a result, the expression of free ubiquitin did not restore the 60S r-subunit shortage observed for the *ubi1Δub*-HA *ubi2Δ* and *SMT3-S-eL40A*-HA *ubi2Δ* mutants nor change the profiles obtained for the isogenic *UBI1*-HA *ubi2Δ* strain (**Figure 7B** and data not shown). Altogether, these results indicated that the contribution of ubiquitin to the synthesis and assembly of eL40 is exclusively exerted *in cis* not been able to perform it when expressed *in trans* as a free molecule.

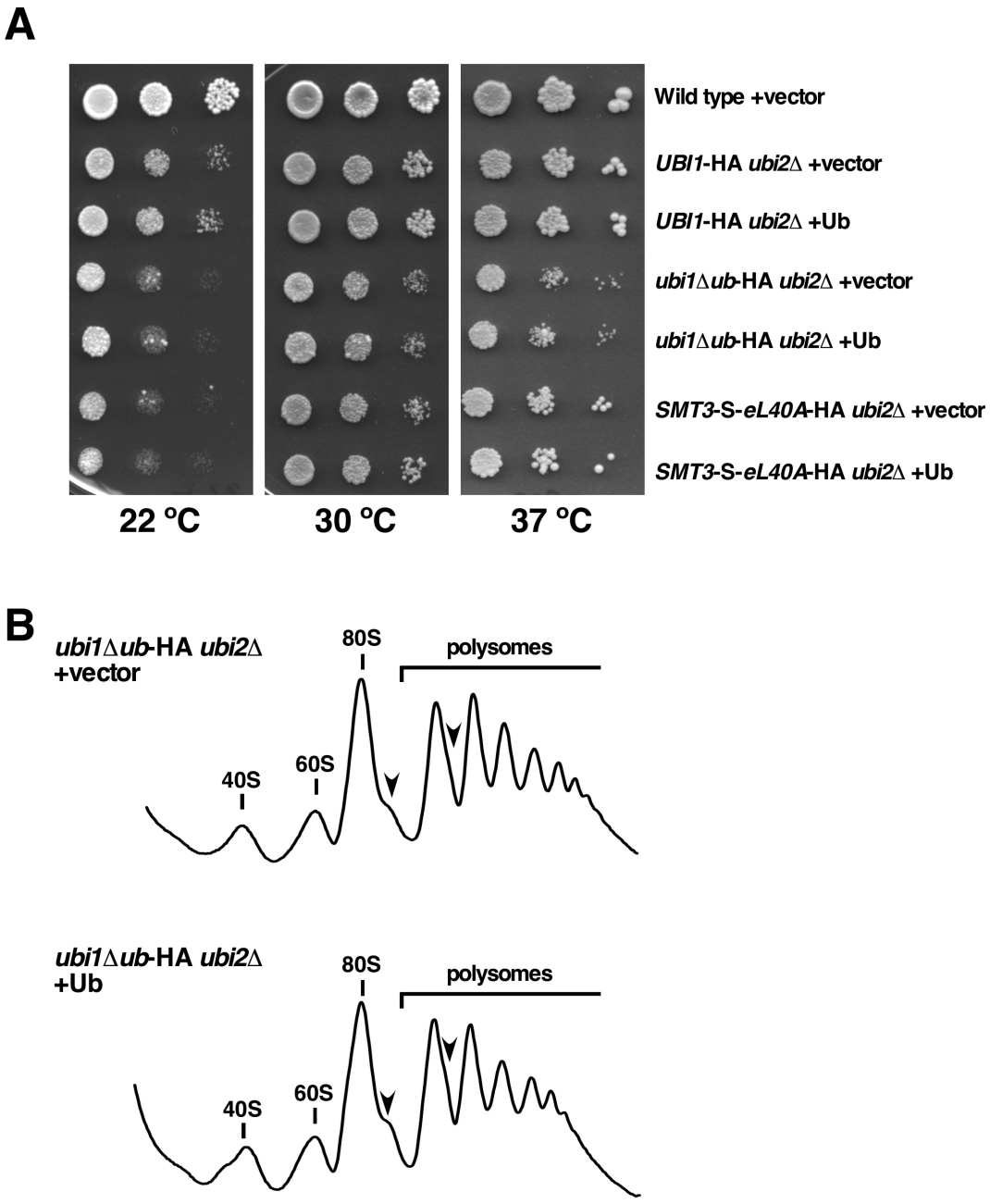


**FIGURE 7. Expression of free ubiquitin *in trans* does not restore the deficiencies conferred by neither the *ubi1Δub*-HA *ubi2Δ* nor the *SMT3-eL40A*-HA *ubi2Δ alleles*. (A)** Growth comparison of the strains W303-1A (Wild type), SMY256 (*UBI1*-HA *ubi2Δ*), SMY257 (*ubi1Δub*-HA *ubi2Δ*) and SMY258 (*SMT3-eL40A*-HA *ubi2Δ*) transformed with either an empty YCplac111 (vector) or YCplac111-Ub (Ub) plasmids. Transformants were selected on SD-Leu plates and then spotted in fivefold serial dilution steps onto SD-Leu plates, which were incubated for 4 days at 22 ºC and for 3 days at 30 ºC and 37 ºC. **(B)** Polysome profile analysis of *ubi1Δub*-HA *ubi2Δ* cells harboring an empty YCplac111 (vector) or YCplac111-Ub (Ub) plasmids. Cells were grown in SD-Leu at 30ºC to an $OD_{600}$ of about 0.8. Cell extracts were prepared and 10 $A_{260}$ units of each extract were resolved in 7–50% sucrose gradients. The $A_{245}$ was continuously measured. Sedimentation is from left to right. The peaks of free 40S and 60S r-subunits, 80S vacant ribosomes/monosomes and polysomes are indicated. Half-mer polysomes are labeled by arrows.

**Ubiquitin and SUMO modestly prevent eL40 or S31 protein aggregation**

It has been proposed that the N-terminal ubiquitin moiety of eL40 and eS31 acts as *cis*-acting molecular chaperones that facilitate the correct folding, and hence, the efficient synthesis and assembly of the respective r-proteins into pre-ribosomal particles (Finley et al., 1989). However, no experimental evidences for this hypothesis have ever been reported. Thus, to obtain experimental insight about this suspected role of ubiquitin, we monitored the levels of aggregated proteins in the different *ubi1* mutants used in this study. As a positive control for the protein aggregation assay, we included a strain lacking the Hsp70 chaperone SSB (a *ssb1Δ ssb2Δ* mutant), which have been described to cause pronounced aggregation of a variety of newly synthesized

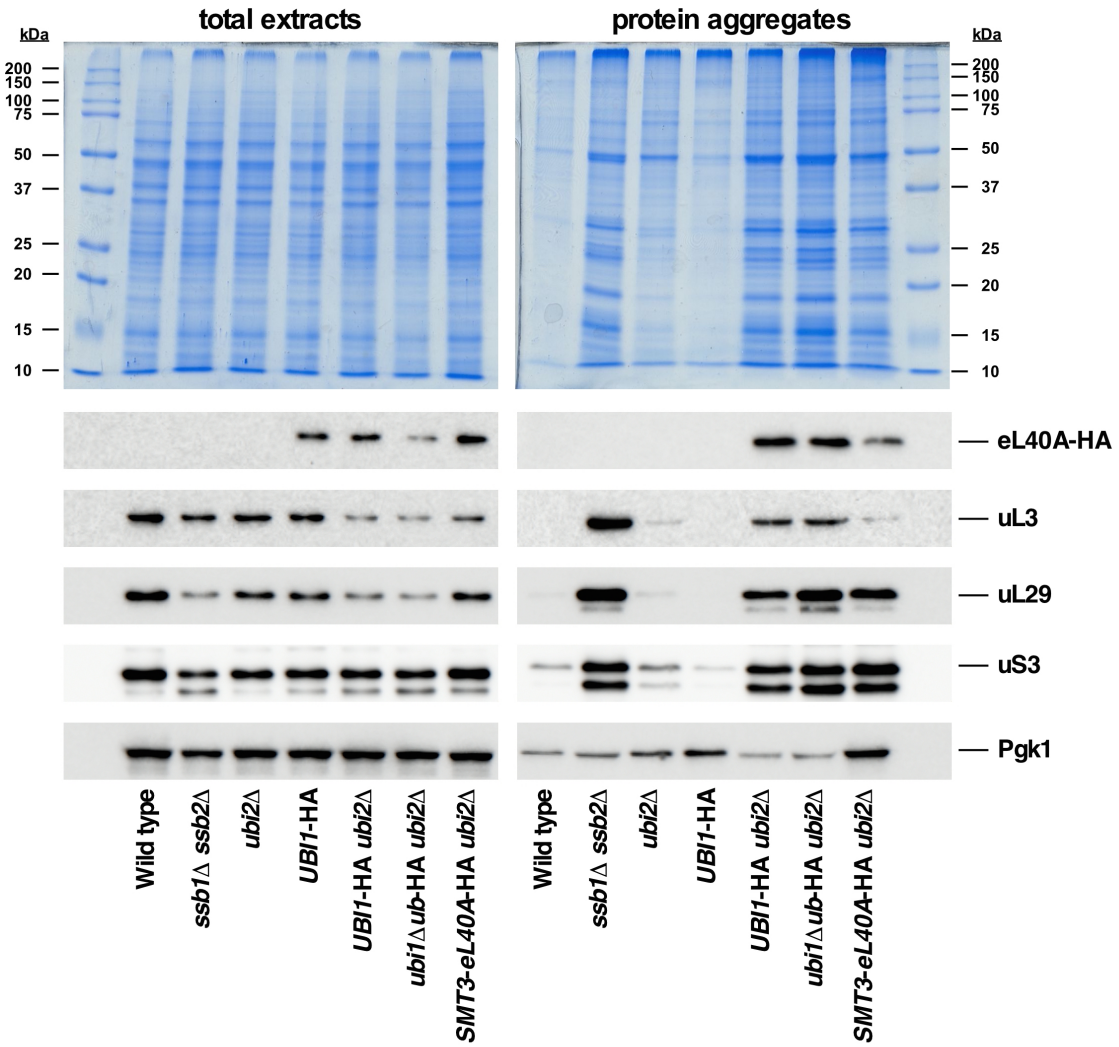


**FIGURE 8. Analysis of protein aggregation in *ubi1Δub*-HA and *SMT3-eL40A*-HA cells.** Strains W303-1A (Wild type), JDY532 (*ssb1Δ ssb2Δ*), JDY922 (*ubi2Δ*), SMY113 (*UBI1*-HA), SMY256 (*UBI1*-HA *ubi2Δ*), SMY257 (*ubi1Δub*-HA *ubi2Δ*), and SMY258 (SMT3-*eL40A*-HA *ubi2Δ*) were grown to logarithmic phase in YPD medium at 30 ºC. Then, total protein extracts and protein aggregates were prepared, separated by SDS-PAGE and visualized by Coomassie staining or subjected to western blot analysis using antibodies against the HA-tag and the uL3, uL29, uS3 and Pgk1 proteins.

proteins, especially r-proteins and factors involved in r-subunit biogenesis or translation (Koplin et al., 2010). As shown in **Figure 8**, substantial protein aggregation was found in strains expressing eL40A-HA as the sole cellular source of eL40 from either genomic *UBI1*-HA, *ubi1Δub*-HA or *SMT3-S-eL40A*-HA alleles, which could not be simply explained by the common presence of the *ubi2Δ* allele. Thus, the HA-tag seems to negatively interfere with protein aggregation, as also impact cell growth (see **Figure 2** and ref. (Martín-Villanueva et al., 2019)). Moreover, the global aggregation tendency was very similar in the three strains, albeit slightly more pronounced in *ubi1Δub*-HA cells **(Figure 8, upper panel)**. Western blotting against the HA-tag indicated that eL40A-HA is among the different aggregated proteins in extracts of the above strains, as also are other r-proteins such as uL3, uL29 or uS3 **(Figure 8, middle panels)**. Strikingly, the levels of eL40A-HA protein aggregates, although apparently did not increase when eL40A-HA is synthesized from the *ubi1Δub* allele, clearly diminished when it derived from the Smt3-S-eL40A-HA precursor. This result suggests a minor but positive role for SUMO as a molecular chaperone for proper folding, and thus, solubility of eL40 r-protein.

We did also analyse the levels of aggregated proteins in an *ubi3Δub*-HA strain and its isogenic *UBI3*-HA control. As shown in **Figure 9**, the aggregation analysis suggested less global accumulation of insoluble proteins in cells of these strains compared to the equivalent *UBI1*-HA *ubi2Δ* and *ubi1Δub*-HA *ubi2Δ* strains, especially for the couple *UBI3*-HA *versus UBI1*-HA *ubi2Δ*. Moreover, western blotting showed practically no aggregation of eS31-HA when produced from a wild-type Ubi3-HA precursor, but a significant aggregation of this r-protein when is produced from the ubiquitin-free Ubi3ΔUb precursor protein **(Figure 9, middle panels)**. Three other findings are remarkable to be mentioned: (i) first, aggregation samples containing either eL40A-HA or eS31-HA also include other r-proteins, such as the tested uL3, uL29 and uS3 (see **Figure 8** and **9, middle panels**). (ii) Second, aggregation of these r-proteins occurs not only in the control *ssb1Δ ssb2Δ* strain but also in strains defective in r-subunits or affected in ribosome biogenesis, such as the tested *ubi3Δ, rps12Δ, rpl39Δ* or *dob1-1* strains. This is consistent with the recent observation that imbalances in the synthesis of ribosomes lead to the rapid aggregation of newly synthesized r-

proteins and compromise essential cellular processes (Tye et al., 2019). (iii) Finally, in contrast to what have been previously reported (Koplin et al., 2010), we did find substantial amounts of eS31-HA among the different r-proteins present in the aggregates of *ssb1Δ ssb2Δ* cells. Thus, the ubiquitin moiety fused to eS31 seems that do not protect eS31-HA of aggregation in these circumstances, suggesting that this r-protein is also a client of the SSB chaperone system. Altogether, our observations suggest that, although the ubiquitin moiety fused to eS31 and eL40 has an important function for the optimal production of the respective r-proteins, its presence does not ensure the specific prevention of aggregation upon a cellular situation of loss of the SSB chaperon system or of a specific r-subunit shortage.

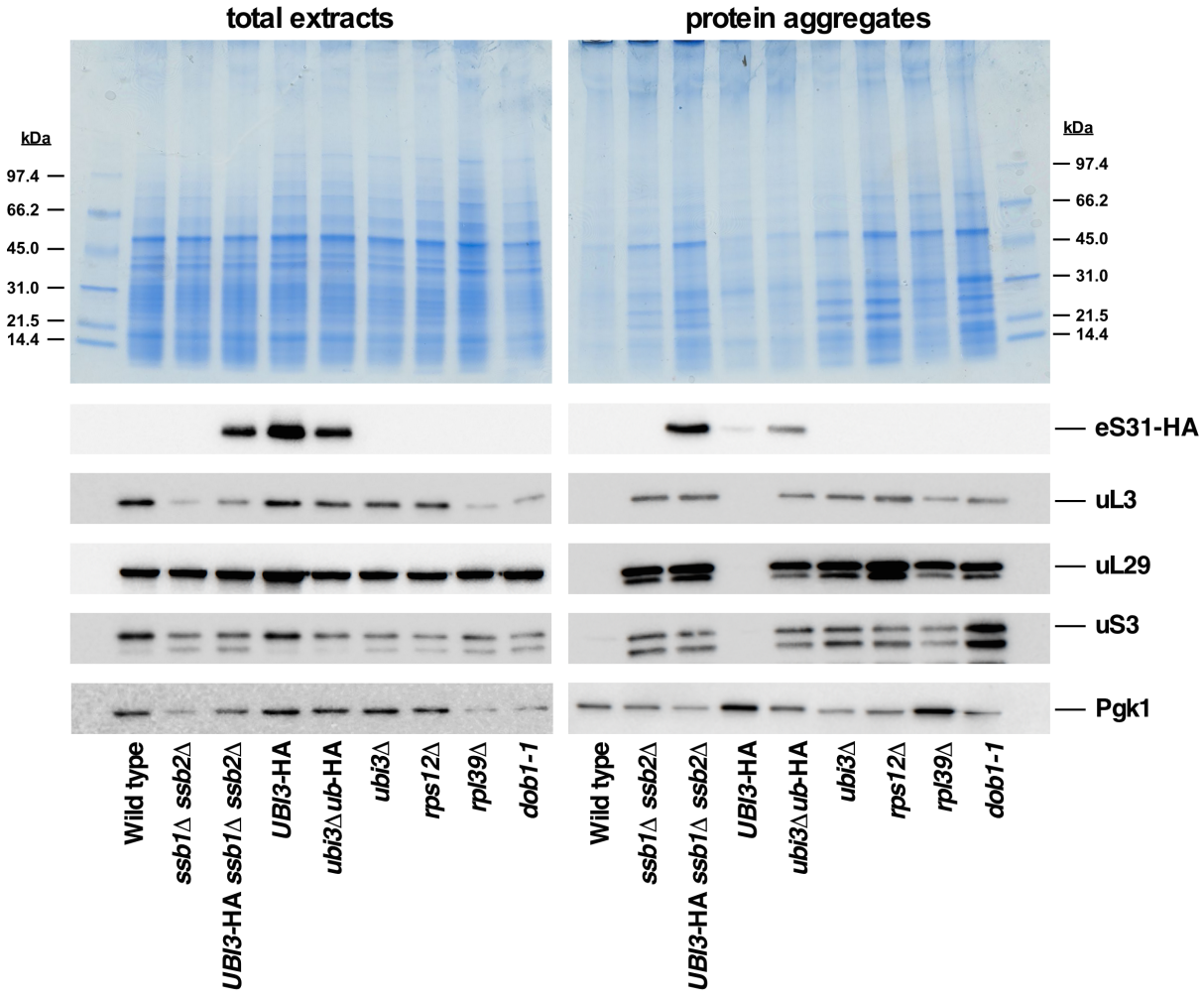


**FIGURE 9. Analysis of protein aggregation in cells from the *ubi3Δub*-HA strain, lacking ribosomal proteins or defective in ribosome biogenesis.** Strains W303-1A (Wild type), JDY532 (*ssb1Δ ssb2Δ*), SMY324 (*UBI3*-HA *ssb1Δ ssb2Δ*), TLY56.D3 (*UBI3*-HA), TLY61.A2 (*ubi3Δub*-HA), TLY14.3C (*ubi3Δ*), SMY315 (*rps12Δ*), ORY211 (*rpl39Δ*), and MS157-1A (*dob1-1*) were grown to logarithmic phase in YPD medium at 30 ºC. Total protein extracts or aggregated proteins were prepared from wild type cells and the indicated mutant strains and were separated by SDS-PAGE and stained with Coomassie (upper part) or subjected to western blot analysis (lower part) using anti-HA, anti-uL3, anti-uL29, anti-uS3 and anti-Pgk1 antibodies.

## DISCUSSION

Ubiquitin is an extremely conserved post-translational modifier present in all eukaryotes that is involved in various cellular processes (Clague and Urbé, 2010). In practically all eukaryotes where the organization of the genes encoding ubiquitin has been analyzed, a fusion of ubiquitin with r-protein eS31 (Ubi3 precursor) or eL40 (Ubi1 and Ubi2 precursors) is present (Archibald et al., 2003). As these particular combinations have been strictly maintained during evolution, it can be assumed that they might be beneficial for fitness of eukaryotes. While fusing a ubiquitin gene to a r-protein gene of each r-subunit could be an excellent manner to couple synthesis and degradation of proteins in eukaryotes, the explicit fusion to eS31 and eL40 goes beyond this possible strategy and suggest a specific function of ubiquitin over that of these r-proteins or *vice versa*. To understand this function, we have previously analyzed the consequences of impairing the ubiquitin removal within Ubi3 and Ubi1 precursors and we concluded that these precursors are likely co-translational cleaved, being their cleavage a pre-requisite for the correct assembly and function of the respective r-proteins (Lacombe et al., 2009; Martín-Villanueva et al., 2019). In human cells, whether processing of UBA52 and UBA80, the ubiquitin-eL40 and ubiquitin-eS31 human precursors, respectively, is co- or post-translational remains unanswered; still, it has recently been suggested that processing of UBA52 occurs post-translationally based on results obtained by a reticulocyte lysate-based translation system, which does not exactly rely on an *in vivo* situation (Grou et al., 2015). In any case, processing of UBA52 has also been shown to be critical for the function of eL40 in human cells (Kobayashi et al., 2016). Moreover, we and others have also experimentally addressed the effects of deleting the ubiquitin fused to Ubi3 and showed that a genomically integrated *ubi3Δub*-HA allele only supported a very sg phenotype (Finley et al., 1989; Lacombe et al., 2009). This was likely due to a 40S r-subunit shortage as the consequence of reduced expression levels of HA-tagged eS31 since increasing the gene dosage of this allele restored the wild-type situation (Finley et al., 1989; Lacombe et al., 2009). In this work, we have tackled the analysis of an equivalent genomic *ubi1Δub*-HA allele. As eL40 is encoded by two paralogous genes in yeast (Fernández-Pevida et al., 2012), we were forced to study this allele in a context of a *ubi2Δ*

background in order to achieve that the sole cellular source of eL40A-HA could come from the ubiquitin-free allele. As for a *ubi3Δub*-HA, the *ubi1Δub*-HA *ubi2Δ* cells showed a severe sg phenotype, reduced expression levels of eL40A-HA compared to those from an isogenic *UBI1*-HA strain **(Figures 2 and 4)**, and therefore, a 60S r-subunit shortage **(Figure 5)**. As for the *ubi3Δub* allele, increasing the dosage of the *ubi1Δub*-HA allele suppressed all above defects **(Figure 2 and 5)**. Thus, our experiments clearly show that the ubiquitin moiety of Ubi1, as it is also the case for that of Ubi3, is mainly required to facilitate the expression of the eL40 r-protein. The fact that expression in *trans* of free ubiquitin fails to restore the defects of *ubi1Δub*-HA *ubi2Δ* cells **(Figure 7)**, indicates that the role of ubiquitin is only exerted when in *cis* fused to eL40A. Moreover, we also concluded from this experiment that the defects associated to the *ubi1Δub*-HA *ubi2Δ* alleles were not due to a ubiquitin limitation; indeed, *ubi1Δ, ubi2Δ* and *ubi3Δ* cells have practically similar levels of ubiquitin than wild-type cells (Finley et al., 1989). Similarly, UBA52-deficient human cells exhibited normal levels of total ubiquitin and interestingly, the expression of eL40 from a ubiquitin-free *RPL40* allele is very poor and leads to very reduced levels of eL40 protein (Kobayashi et al., 2016).

How does *cis*-acting ubiquitin facilitate the expression of eS31 and eL40 r-proteins? This is a still unclear issue and some non-mutually exclusive possibilities, which also reconcile with the evolutionary conservation, can be envisaged: (**i**) It could be that ubiquitin assists assembly of eS31 and eL40 r-proteins. Thus, in the absence of ubiquitin, their assembly into the respective pre-ribosomal particles would be unproductive and therefore, the eS31 or eL40 unassembled r-protein fraction efficiently and rapidly degraded, as have been described is the general case for any r-protein that could not assemble properly (Lam et al., 2007; Maicas et al., 1988; Sung et al., 2016b; Warner et al., 1985). This possible ubiquitin role is questionable in yeast as the cleavage of the ubiquitin fusion precursors seems to occur co-translationally; although it still is conceptually possible that ubiquitin assists eL40 assembly since it occurs in the cytoplasm (Fernández-Pevida et al., 2012), is unlikely that ubiquitin targets or protect eS31 until its assembly site in the nucleolus (Fernández-Pevida et al., 2016; Sun et al., 2017). Still, in human cells, ubiquitin cleaved from UBA52 has been suggested to form a complex with eL40 for regulation of protein synthesis (Kobayashi

et al., 2016), however, this complex has not been shown to facilitate eL40 assembly. (**ii**) A more plausible scenario is that suggesting that ubiquitin has a *cis*-acting molecular chaperone role to facilitate translation and folding of eS31 and eL40. Only a properly folded r-protein could assemble while the misfolded fraction will aggregate and degrade. In agreement with this *cis*-acting role of ubiquitin, we showed that the genomic expression of ubiquitin-free eL40A was clearly reduced **(Figure 4)** and that the replacement of the ubiquitin moiety of Ubi1 by the ubiquitin-like protein SUMO (yeast Smt3), which is known to increase the efficient expression of fused proteins (Baker, 1996; Butt et al., 1989; Ecker et al., 1989; Marblestone et al., 2006), was able to partially suppress the *ubi1Δub*-HA *ubi2Δ* mutant, specially at high temperatures **(Figure 3)** and lead to better eL40A-HA protein yields **(Figure 4)**. The fact that the Smt3-S-eL40A-HA precursor is not efficiently processed **(Figure 4 and 6)** could be the reason for just a mildly suppression, as ubiquitin release from eL40 is required for cytoplasmic maturation and function of mature ribosomal subunits (Martín-Villanueva et al., 2019) (see also **Figure 6**). To further explore the role of ubiquitin as a chaperone of r-proteins eL40 and eS31, we have analyzed the aggregation status of different eL40 and eS31 protein variants. In general, most r-proteins have a high tendency to aggregate during or after their synthesis due to their particular characteristics, such as its extremely high isoelectric point and the presence of unstructured or intrinsically disordered extensions (Jäkel et al., 2002). These features have permitted the natural selection of proteins known as dedicated chaperones and escortins, which help import and/or assembly of individual r-proteins, thus impeding their degradation, inappropriate interaction with other cellular components and aggregation (Espinar-Marchena et al., 2017; Peña et al., 2017; Pillet et al., 2017). Additionally, r-proteins are among the major client proteins of the general ribosome-associated chaperones such as the nascent polypeptide-associated complex (NAC) and the Ssb-ribosome-associated complex (Ssb-RAC) (Koplin et al., 2010). It has been shown that the loss of NAC and Ssb-RAC complexes causes aggregation of most r-proteins from both r-subunits (Koplin et al., 2010) **(Figures 8 and 9)**. Although originally r-proteins eL40 and eS31 were not found among the species identified in the aggregation analysis of cells lacking NAC and Ssb-RAC, our results show that, at least, the ubiquitin moiety fused to eS31 does not prevent its specific aggregation in the absence of these chaperone

complexes **(Figure 9)**. Interestingly, the ubiquitin deletion from Ubi3 caused a mild enhancement of the aggregation levels of eS31. However, this enhancement is not only specific for eS31 but also for the rest of r-proteins tested (uL3, uL29 and uS3, see **Figure 9**). Indeed, we show herein that a defect in ribosome biogenesis (e.g. *ubi3Δ, rps12Δ, rpl39Δ* or *dob1-1* mutants) leads to a substantial increase on the amount of insoluble material detected in polyacrylamide gels, with aggregation of r-particles, similarly to that observed in cells lacking NAC and Ssb-RAC **(Figure 8 and 9)**. Very recently, Tye *et al.* demonstrated that an imbalance in the synthesis of r-proteins and rRNAs leads to the rapid aggregation of newly synthetized r-proteins (Tye et al., 2019). Thus, it is likely that the modest increase in the aggregation status detected in *ubi3Δub* cells could be attributable to the ribosome biogenesis defect caused by the *ubi3Δub* mutation, which impair 40S r-subunit synthesis (Lacombe et al., 2009). Similarly, the strain *UBI1*-HA *ubi2Δ* showed a substantial amount of insoluble material and aggregation of r-proteins, as both the *ubi2Δ* mutation and to the lesser extend the HA-tag of *UBI1* interfere with cell growth and ribosome biogenesis (Fernández-Pevida et al., 2012; Kruiswijk et al., 1978; Lacombe et al., 2009; Martín-Villanueva et al., 2019) **(Figure 2)**. Unfortunately, this basal status seems to be high enough to mask the possible additional negative effect caused by the *ubi1Δub* allele. In contrast, the fusion of Smt3 to eL40 seems to modestly ameliorate the aggregation levels of this r-protein. Altogether, these experiments, although not conclusive, strongly suggest that ubiquitin could be assisting *in cis* the folding of their respective fused r-proteins.

## MATERIALS AND METHODS



### Strains and microbiological methods

All yeast strains used in this study are listed in **Table 1** and are derived from the diploid W303 strain background (Thomas and Rothstein, 1989).

A two-step allele replacement method was used to replace genomic wild-type *UBI1* by *UBI1*-HA, *ubi1Δub*-HA or *SMT3-eL40*-HA alleles (Klockner et al., 2009). Briefly, SMY106, which is an *ubi1*::klURA3 (*URA3* gene from *Kluyveromyces lactis*) haploid null mutant strain, was co-transformed with 100 ng of empty YCplac111 vector and 1 µg of DNA fragments containing the *UBI1*-HA, *ubi1Δub*-HA, or *SMT3*-eL40-HA alleles excised by *Eco*RI/*Hin*dIII digestion from YCplac111-UBI1-HA, YCplac111-ubi1Δub-HA, or YCplac111-SMT3-eL40-HA, respectively. Transformants were selected onto SD-Leu plates. Then, several clones were replica-plated onto 5-FOA-containing plates to select for those that had lost the klURA3 marker because of a site-specific recombination event. Candidates were analysed by colony PCR and sequencing.

Strains SMY215 and SMY216 are generated by transforming the *UBI1/2* shuffle strain (TAY001) with YCplac111-ubi1Δub-HA or YCplac111-SMT3-eL40-HA plasmids; transformants were restreaked on 5-FOA-containing plates to counter-select against the presence of pHT4467Δ-UBI1.

Yeast cells were grown at the indicated temperatures either in YPD medium (1% yeast extract, 2% peptone and 2% glucose) or SD medium (synthetic dextrose; 0.15% yeast nitrogen base, 0.5% ammonium sulphate) supplemented with the appropriate amino acids and bases as nutritional requirements, and containing 2% glucose as carbon source. To prepare plates, 2% agar was added to the media before sterilization. Yeast genetic techniques and growth media have been previously described (Burke et al., 2000). Yeast cells were transformed by the lithium acetate method (Gietz et al., 1992). For tetrad dissection, a Singer MSM 400 micromanipulator was used. Standard molecular biology techniques were carried out according to the Sambrook

specifications (Sambrook et al., 1989). *Escherichia coli* DH5α was used for cloning and propagation of plasmids (Sambrook et al., 1989).



**Plasmids**

Plasmids used in this study are listed in **Table 2**. Cloned DNA fragments were generated by a fusion PCR strategy to include a single HA epitope at the C-terminal end of eL40A in wild-type and mutant versions of *UBI1*. All constructs were verified by DNA sequencing. Description of the oligonucleotides used for the PCRs and information on the construction of the different plasmids will be available upon request.

**Polysome analysis and sucrose gradient fractionation**

Cell extracts for polysome analysis were prepared and analysed as previously described (Foiani et al., 1991; Kressler et al., 1997). Ten $A_{260}$ units of each cell extract were loaded onto 7-50% sucrose gradients. These gradients were centrifuged at 39,000 rpm in a Beckman Coulter rotor SW41 for 2 h 45 min; the $A_{254}$ was continuously monitored using an ISCO UA-6 system. When needed, fractions of 0.5 ml were collected and proteins were precipitated from each fraction using trichloroacetic acid as previously described (de la Cruz et al., 1998a). The precipitated fractions were resuspended in 2X Laemmli loading buffer; an equal volume of each fraction was separated by SDS-PAGE and analysed by western blotting.

**Western blot analysis and antibodies**

Total yeast protein extracts were prepared by the alkaline lysis method of Yaffe and Schatz (Yaffe and Schatz, 1984), which immediately "freezes" the *in vivo* protein content, thus, preventing rapid protein turnover reactions. Proteins were separated by SDS-PAGE and analysed by western blotting according to standard procedures (Sambrook et al., 1989). The following primary antibodies were used: mouse monoclonal anti-HA 16B12 (Covance), anti-Pgk1 (Invitrogen) and anti-uL3 (gift from J.R. Warner) (Vilardell and Warner, 1997); rabbit polyclonal anti-uL29 (gift from M. Seedorf) (Frey et al., 2001) and anti-uS3 (gift from M. Seedorf) (Frey et al., 2001). Goat anti-mouse or anti-rabbit horseradish peroxidase-conjugated antibodies (Bio-Rad)

were used as secondary antibodies. Immune complexes were visualised using a chemiluminescence detection kit (Super-Signal West Pico, Pierce) and a ChemiDoc™ MP imaging system (Bio-Rad).



**Analysis of aggregated proteins**

Isolation of aggregated proteins was done from whole cell extracts as exactly described by Koplin *et at.* (Koplin et al., 2010) but following the sonication modifications described in Panasenko *et al.* (Panasenko and Collart, 2012). Samples of whole cell extracts and aggregated protein were resuspended in Laemmli sample buffer, separated by SDS-PAGE and analysed by colloidal blue Coomassie staining and western blotting.

**Table 1. Yeast strains used in this study.**

| Strain [(a)] | Relevant genotype | Source |
|---|---|---|
| W303-1A | *MAT***a** *ade2-1 his3-11,15 leu2-3,112 trp1-1 ura3-1* | (Thomas and Rothstein, 1989) |
| W303-1B | As W303-1A but *MAT*α | (Thomas and Rothstein, 1989) |
| TAY001 | *MAT***a** *ubi1*::*kanMX4* ubi2::kanMX4 *ade3*::kanMX4 [pHT4467Δ-UBI1] | (Martín-Villanueva et al., 2019) |
| SMY106 | *MAT***a** *ubi1*::klURA3 | This study |
| SMY113 | *MAT***a** *UBI1*-HA | This study |
| SMY256 | *MAT***a** *UBI1*-HA *ubi2*::kanMX4 | This study |
| SMY107 | *MAT***a** *ubi1Δub*-HA | This study |
| SMY257 | *MAT*α *ubi1Δub*-HA *ubi2*::kanMX4 | This study |
| SMY215 | *MAT***a** *ubi1*::kanMX4 *ubi2*::kanMX4 *ade3*::kanMX4 [YCplac111-ubi1Δub-HA] | This study |
| JDY922 | *MAT***a** *ubi2*::kanMX4 | (Fernández-Pevida et al., 2012) |
| SMY218 | *MAT*α *SMT3-eL40A*-HA | This study |
| SMY258 | *MAT*α SMT3-*eL40A*-HA *ubi2*::kanMX4 | This study |
| SMY216 | *MAT***a** *ubi1*::kanMX4 *ubi2*::kanMX4 *ade3*::kanMX4 [YCplac111-SMT3-eL40A-HA] | This study |
| JDY532 | *MAT***a** *ssb1*::HIS3MX6 *ssb2*::natNT2 | This study |
| SMY324 | *MAT***a** ssb1::HIS3MX6 ssb2::natNT2 UBI3-HA::kanMX4 | This study |
| TLY56.D3 | *MAT***a** *UBI3*-HA::kanMX4 | (Lacombe et al., 2009) |
| TLY61.A2 | *MAT***a** *ubi3Δub*-HA::kanMX4 | (Lacombe et al., 2009) |
| TLY14.3C | *MAT*α *ubi3*::HIS3MX6 | (Lacombe et al., 2009) |
| SMY315 | *MAT*α *rps12*::kanMX4 | This study |
| ORY211 | *MAT*α *rpl39*::natNT2 | This study |
| MS157-1A | *MAT*α *dob1-1* | (de la Cruz et al., 1998b) |

[(a)]Strains used in this study are isogenic with W303. To simplify, only the corresponding mating type of the W303 relevant genotype is provided.

**Table 2. Plasmids used in this study**

| Name (collection name) | Relevant information | Reference |
|---|---|---|
| pHT4467Δ-UBI1 | *CEN6* (instable), *URA3*, *ADE3*. Wild-type Ubi1; promoter and terminator of *UBI1* | (Martín-Villanueva et al., 2019) |
| YCplac111-UBI1-HA (pDK4131) | *CEN*, *LEU2*. C-terminally 1xHA-tagged eL40A; promoter and terminator of *UBI1* | (Martín-Villanueva et al., 2019) |
| YCplac111-ubi1Δub-HA (pDK4192) | *CEN*, *LEU2*. Allele *ubi1Δub*-HA (M-II); promoter and terminator of *UBI1* | This study |
| YCplac111-SMT3-eL40-HA (pDK4193) | *CEN*, *LEU2*. Allele *SMT3-eL40A*-HA (GG-S-II); promoter and terminator of *UBI1* | This study |
| YCplac111 | *CEN*, *LEU2* | (Gietz and Sugino, 1988) |
| YCplac111-Ub | *CEN*, *LEU2*. Ubiquitin | This study |

# CHAPTER 2

# Role of the beak ribosomal protein eS12 in ribosome biogenesis and function in *Saccharomyces cerevisiae*

## INTRODUCTION

In eukaryotes, ribosome biogenesis is a complex process that in addition to the ribosomal RNAs (rRNAs) and ribosomal proteins (r-proteins) required a plethora of RNA and protein *trans*-acting factors (Warner, 1999). Most of our current knowledge concerning this process comes from studies in the yeast *Saccharomyces cerevisiae*, where about 80 small nucleolar RNAs (snoRNAs) and about 300 protein *trans*-acting factors have been characterized (Woolford and Baserga, 2013). However, the precise functions of these factors, also known as ribosome assembly factors, it is only emerging in part due to the advances in the cryogenic electron microscopy (cryo-EM) characterization of distinct pre-ribosomal particles (for a review, see (Bassler and Hurt, 2018)). Different studies in yeast and humans indicate that r-proteins also play active roles in the process of ribosome assembly (for a review, see (de la Cruz et al., 2015)). Understanding the exact functions of r-proteins in ribosome assembly is a very pertinent issue as most of the human inherited diseases known as ribosomopathies are linked to ribosome defects caused by the loss-of-function mutations in r-protein genes (for reviews, see (Armistead and Triggs-Raine, 2014; Narla and Ebert, 2010; Teng et al., 2013)). The most common of these pathologies is Diamond-Blackfan anemia (DBA), an inherited and congenital disease linked to recessive mutations in r-protein genes of the 40S r-subunit such as *RPS19*, *RPS24*, *RPS17*, *RPS7*, *RPS10*, *RPS26* among others, in approximately 60% of the patients (e.g. (Narla and Ebert, 2010; Teng et al., 2013)).

The structure of small r-subunits is less complex than that of large ones. The 18S rRNA, and its equivalent prokaryotic 16S rRNA, can be divided into four, practically independent, folding domains, which upon the interaction of specific r-proteins form the typical morphological features of the 40S r-subunit (Rabl et al., 2011; Yusupova and Yusupov, 2014): the 5' domain of 18S rRNA forms the shoulder and the foot and, together with the 3' minor domain (helix H44), constitute the body of the 40S r-subunit; the central domain of 18S rRNA forms the platform and the 3' major domain forms the head. Protruding from the head, the region called beak is special in eukaryotes since has been transformed during evolution from the all-rRNA structure

(helix H33) found in prokaryotic ribosome to a protuberance of essentially the same structure but containing a reduced H33 and three eukaryotic-specific r-proteins (eS10, eS12 and eS31) **(Figure 1A)** (Rabl et al., 2011; Wilson and Doudna Cate, 2012).



The role during ribosome biogenesis of most, but not all, r-proteins from the 40S r-subunit have been studied by either specific studies or systematic analysis (e.g. (Ferreira-Cerca et al., 2005; Ferreira-Cerca et al., 2007; Ford et al., 1999; Jakovljevic et al., 2004; Lacombe et al., 2009; O'Donohue et al., 2010; Tabb et al., 2001)). These analyses reveal that 40S r-subunits assembly occurs co-transcriptionally and hierarchical in a 5'-to-3' direction with respect to rRNA; thus, r-proteins that bind to the body of the 40S r-subunits appears to bind early during transcription of the 35S precursor of rRNA (pre-rRNA) while those from the platform assemble slightly later but before those that form the head domain, which are the latest r-proteins binding in the nucleus to pre-40S r-particles. Few 40S r-proteins seem to assemble in the cytoplasm (see (Ferreira-Cerca et al., 2005; Ferreira-Cerca et al., 2007; O'Donohue et al., 2010)). Remarkably, the order in which r-proteins assemble to yeast and mammal 40S r-subunits seems to parallel the assembly of their bacterial counterparts *in vivo* and importantly *in vitro* (see (Davis and Williamson, 2017)); thus, the essential information for the assembly of small r-subunits seems to intrinsically reside in the biophysical properties of the interactions the r-proteins could perform with the 16S/18S rRNA (see (Sykes and Williamson, 2009)). Functional analyses have nicely demonstrated that, in general, the timing of action of different r-proteins from the 40S r-subunit correlates with their specific location within the subunits and, hence, with their specific course of assembly (Ferreira-Cerca et al., 2005; Ferreira-Cerca et al., 2007; O'Donohue et al., 2010). In this sense, loss-of-function of the r-proteins located in the body region of 40S r-subunits (as examples, eS6, eS8, eS24, uS4, uS17) strongly impairs processing of early pre-rRNAs (35S pre-rRNA in yeast, 47S pre-rRNA in human cells), whereas loss-of-function of r-proteins located in the head (as examples, eS31, uS2, uS3, uS5, uS10) impairs downstream maturation steps as the nucleo-cytoplasmic export of pre-40S r-particles and processing of late pre-rRNAs (20S pre-rRNA in yeast, 21S and 18S-E pre-rRNA in human cells) (de la Cruz et al., 2015; Ferreira-Cerca et al., 2005; Ferreira-Cerca et al., 2007; O'Donohue et al., 2010). Importantly, the recent publication of diverse

cryo-EM structures of yeast and human 90S and pre-40S r-particles is practically fully in agreement with this hierarchical assembly pathway of early *versus* late 40S r-proteins following 18S rRNA maturation in a 5'-to 3' direction (see (Bassler and Hurt, 2018; Chaker-Margot, 2018; Klinge and Woolford, 2019; Kressler et al., 2017) and references therein). However, surprisingly, the beak region of the head seems to be practically but not totally molded in the early 90S pre-ribosomal particles determined from cryo-EM studies; thus, the apical structure formed by eS12, eS31 and helix H33 is already shaped whereas its base, built in mature 40S r-subunits by eS10, is occupied by the *trans*-acting factor Enp1 in these particles (see e.g. (Sun et al., 2017)). The subsequent nuclear maturation of 90S into pre-40S r-particles comprises the release of most *trans*-acting factors with few exceptions such as Dim1, Enp1, and Pno1, and also the association of others factors, among them Tsr1, Nob1, Rio2 or Ltv1 (e.g. (Moriggi et al., 2015; Schäfer et al., 2006; Schäfer et al., 2003; Strunk et al., 2011)); this latter factor binds directly to Enp1 **(Figure 1B)** (Campbell and Karbstein, 2011; Heuer et al., 2017; Scaiola et al., 2018; Schäfer et al., 2006). The further release of Ltv1 and Enp1 from cytoplasmic pre-40S r-particles remodels the head region of 40S r-subunit to relocate the uS3 r-protein and then permit the assembly of eS10 and Asc1 (e.g. (Collins et al., 2018; Ghalei et al., 2016; Mitterer et al., 2016; Schäfer et al., 2006)).

We are interested in understanding the contribution of the r-proteins of the beak to ribosome biogenesis and function. We and others have previously shown that deletion of *UBI3*, the gene encoding eS31 as a fusion precursor protein with a single ubiquitin moiety, strongly impairs cytoplasmic 20S pre-rRNA processing in *S. cerevisiae* (Finley et al., 1989; Lacombe et al., 2009). Here, we have undertaken the functional characterization of the yeast r-protein eS12 in the biogenesis and function of ribosomes, which remained uncharacterized **(see Discussion)**. Our results indicate that eS12 is a quasi-essential protein for cell growth required for the normal accumulation of 40S r-subunits. Deletion of *RPS12* leads to a similar cytoplasmic accumulation of 20S pre-rRNA than the deletion of *UBI3*; this accumulation is not enhanced upon the simultaneous deletion of both genes. Moreover, we show a genetic interaction between the absence of either eS12 or eS31 and that of Ltv1 or Enp1, which is not apparently linked to the dynamics of incorporation or release of these *trans*-acting

factors to the pre-40S r-particles. Finally, we also show that the eS12-deprived ribosomes are more error-prone than wild-type ones.

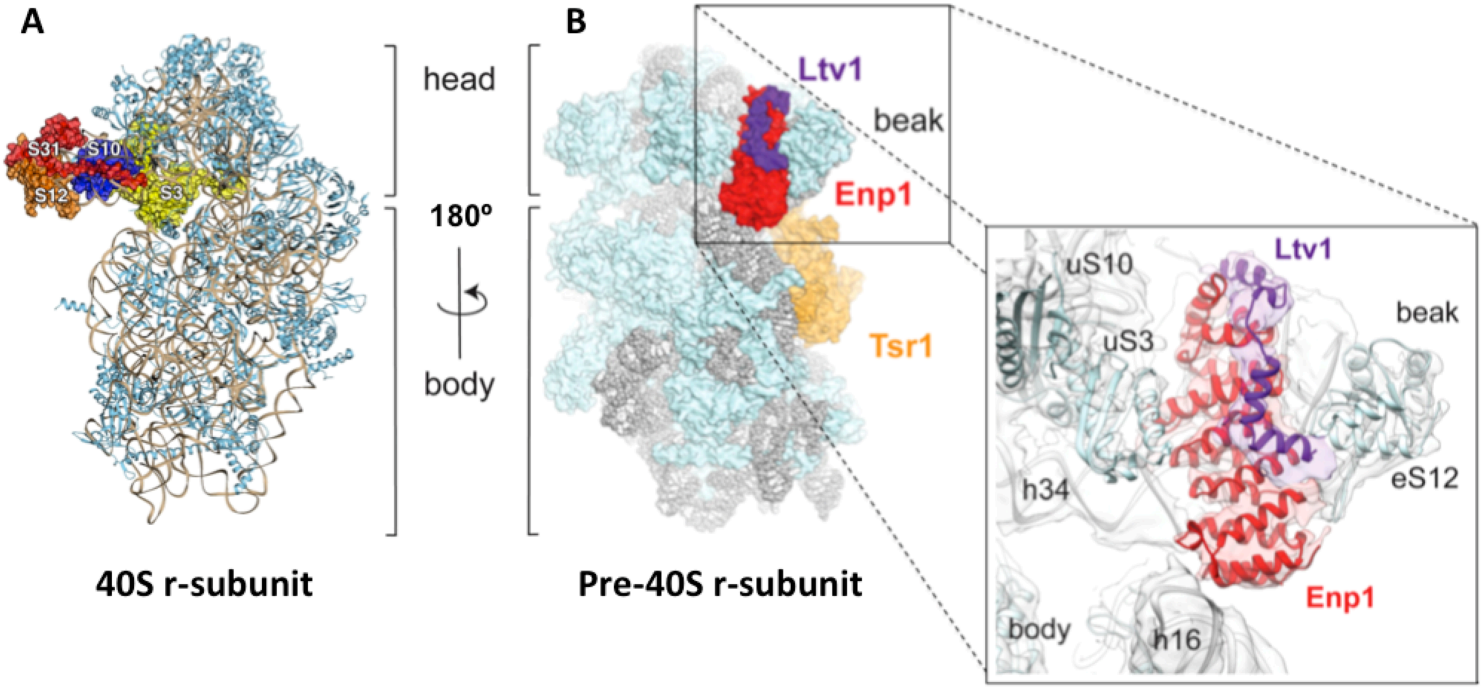


**FIGURE 1. Structure of mature and immature 40S r-subunit**. **(A)** Positions of r-proteins eS12 (orange), eS31 (red), eS10 (blue) in the beak domain and uS3 (yellow) in the base of the beak of the small r-subunit are shown. **(B)** Overview of back structure of the cytoplasmic pre-40S r-subunit. Positions of ribosome assembly factors Enp1 (red), Ltv1 (purple) and Tsr1 (orange) are shown. The rRNA is depicted in grey and r-proteins in light blue. Adapted from (Scaiola et al., 2018).

## RESULTS

### Loss of eS12 results in a severe growth defect

The r-protein eS12 is a eukaryotic-specific constituent of the 40S r-subunits (Lecompte et al., 2002). Unlike most yeast r-proteins (Warner, 1999), eS12 is encoded by a non-essential single gene (*RPS12, YOR369C*) (Giaever et al., 2002). This gene produces a small globular protein of ca. 16 kDa located on the beak of the 40S r-subunit, which interacts with the helix H33 of 18S rRNA and the also eukaryotic-specific r-proteins eS31 and eS10 **(Figure 1A)** (Rabl et al., 2011). The role of yeast r-proteins eS10 and eS31 in ribosome biogenesis has been previously studied (Fernández-Pevida et al., 2016; Ferreira-Cerca et al., 2005; Finley et al., 1989; Lacombe et al., 2009). Seemingly, the role of yeast eS12 in ribosome biogenesis has also been earlier explored, the authors concluding that it was not required for the formation of 40S r-subunits (Ferreira-Cerca et al., 2005). As we discuss below, this conclusion was unfortunately mistaken as, likely, the authors inadvertently use a non-appropriate strain.

To study the role of yeast eS12 in ribosome biogenesis and function, we first analysed the phenotypic consequences of deleting the *RPS12* gene. In contrast to the *rps12Δ* strain employed by Ferreira-Cerca *et al.*, which grew identically to the wild-type strain at 30 ºC on YPD plates (Ferreira-Cerca et al., 2005), the haploid *rps12Δ* strains we generated either in the W303 or the BY4741 background displayed a severe slow-growth (sg) defect at 30 ºC on YPD plates that was enhanced at 22 and 37 ºC **(Figure 2)**. Our results were, however, consistent with previous ones by Steffen *et al.*, who observed a quasi-lethal phenotype for haploid *rps12Δ* segregants upon sporulation of a heterozygous *RPS12/rps12Δ* diploid (Steffen et al., 2012). Thus, we conclude that Ferreira-Cerca *et al.* have likely analysed a spontaneous fast-growing bypass suppressor of the *rps12Δ* mutant.

The r-protein eS12 is a close neighbour of eS31 in the 40S r-subunit (Rabl et al., 2011). We and others have shown that a mutant lacking eS31 displayed a strong sg defect and a cold-sensitive (cs) phenotype (Finley et al., 1989; Lacombe et al., 2009).

To check whether the simultaneous absence of eS12 and eS31 have an enhanced growth defect, we constructed a double *rps12Δ ubi3Δ* strain in the W303 background. As shown in **Figure 2A**, this double mutant displayed growth defects very similar to that of the single *rps12Δ* one. Thus, the *rps12Δ* mutation seems to be epistatic to the *UBI3* gene.

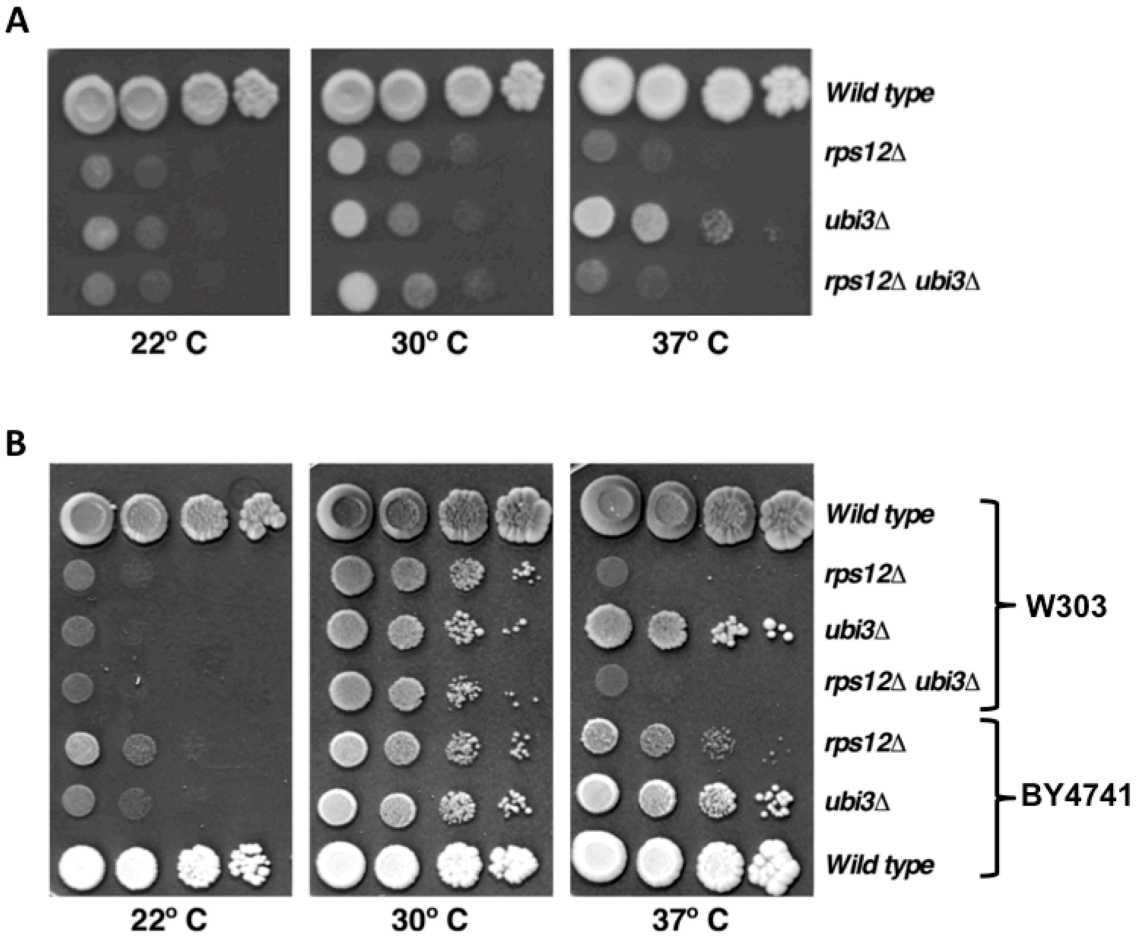


**FIGURE 2. Deletion of *RPS12* results in a slow growth phenotype**. **(A)** Growth analysis of the *rps12* null mutant in the W303 background. Cells of the strains W303-1A (*Wild type*), SMY315 (*rps12Δ*), TLY14.3C (*ubi3Δ*) and SMY372 (*rps12Δ ubi3Δ*) were spotted in 10-fold serial dilutions onto YPD plates and incubated at 22 ºC for 6 days and at 30 and 37 ºC for 3 days. **(B)** Growth comparison of the *rps12* null mutant in the W303 and BY4741 backgrounds. Cells of the strains BY4741 (*Wild type*), SMY227 (*rps12Δ*) and SMY231 (*ubi3Δ)* were spotted in 10-fold serial dilutions onto YPD plates and incubated at 22, 30 and 37 ºC for 5 days. The growth of these strains was compared to that of the isogeneic strains from the W303 background: W303-1A (*Wild type*), SMY315 (*rps12Δ*), TLY14.3C (*ubi3Δ*) and SMY372 (*rps12Δ ubi3Δ*), which were spotted in 10-fold serial dilutions onto the same plates.

**Loss of eS12 leads to a strong 40S r-subunit shortage**

To study the contribution of yeast eS12 to ribosome biogenesis, we first analysed polysome profiles from cell extracts of the *rps12* deletion mutant and compared it to those of isogenic *ubi3Δ* and wild-type strains. As shown in **Figure 3A**, polysome profile analysis of the *rps12Δ* mutant revealed a clear reduction in free 40S r-subunits and a huge increase in free 60S r-subunits; the polysomal content was also drastically reduced. The profile was similar to those of the single *ubi3Δ* and the double *ubi3Δ rps12Δ* isogenic mutants **(Figure 3A)**. Thus, the *rps12Δ* alone or in combination with the *ubi3Δ* mutation lead to a shortage of 40 S r-subunits. In agreement, quantification of total r-subunits by low-$Mg^{2+}$ sucrose gradients showed that deletion of either eS12 or eS31 leads to a ca. 55 % reduction of the 40S to 60S r-subunits compared to the wild-type control. This reduction was of about 70% for the double *rps12Δ ubi3Δ* mutant **(Figure 3B)**. We conclude that the absence of eS12 r-protein results in a severe deficiency in 40S r-subunits relative to 60S r-subunits, which is more pronounced when eS31 r-protein is simultaneously lacking.

**Deletion of *RPS12* impairs rRNA processing**

To determine whether the *rps12Δ* mutant was defective in the formation rather than the stability of 40S r-subunits, we examined the kinetics of rRNA production by pulse-chase analysis with the *rps12Δ* strain and its isogenic wild-type counterpart. Both strains were first transformed with an empty YCplac33 plasmid (*CEN*, *URA3*, **Table 2**) to make them prototrophic for uracil. Then, they were grown in liquid SD-Ura medium to mid-log phase at 30 ºC. The cells were pulse-labelled for 2 min with [5,6-$^{3}$H]uracil, then chased for 5, 15, 30 and 60 min with a large excess of non-radioactive uracil. Total RNA was extracted from each sample and analysed by agarose and acrylamide electrophoresis, followed by transfer to nylon membranes and exposition to tritium sensitive phosphor screens; results were revealed in a phosphor imaging system. As shown in **Figure 4A**, in wild-type cells, the early pre-rRNA precursors were converted rapidly into 27S and 20S species, which were further processed into mature 25S and 18S rRNA, respectively. After 15 min of chase, practically all label was in the mature rRNAs. Compared with the wild-type control, processing of 27S pre-rRNAs was delayed in the *rps12Δ* mutant since these precursors could be detected after the 30 min chase

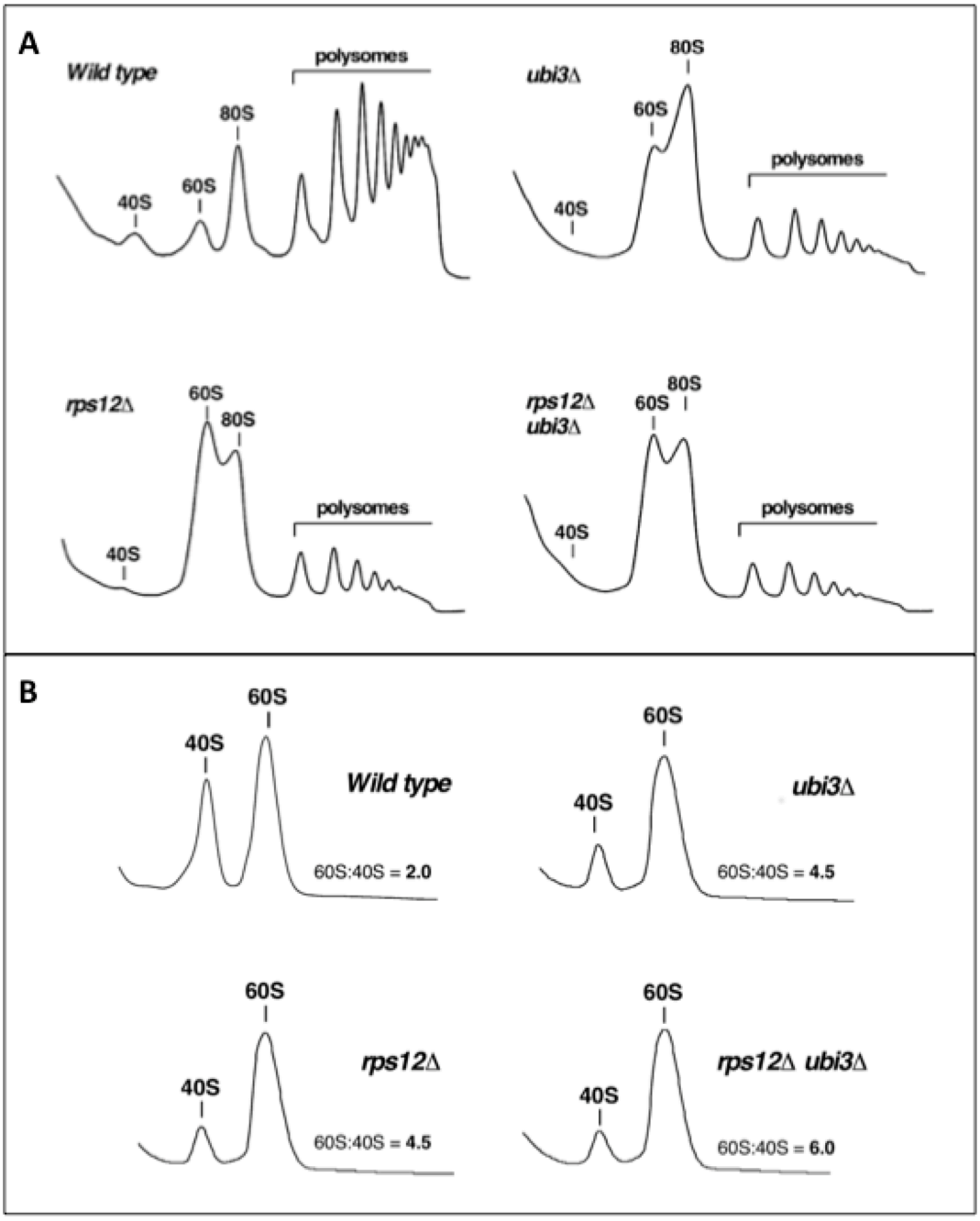


**FIGURE 3. Deletion of *RPS12* results in a deficit in 40S r-subunits. (A)** Polysome profile analysis of W303-1A (wild type), SMY315 (*rps12Δ*), TLY14.3C (*ubi3Δ*) and the double mutant strain SMY372 (*rps12Δ ubi3Δ*) strains. The peaks of free 40S and 60S r-subunits, 80S free couples/monosomes and polysomes are indicated. **(B)** Quantification of the 40S r-subunit relative to the 60S r-subunit abundance in the strains described above. Cell extracts were prepared under polysome run-off conditions, by the omission of cycloheximide, in a buffer lacking $MgCl_2$ to dissociate ribosomes in the 40S and 60S r-subunits. The peaks of total 40S and 60S r-subunits are indicated. The area under the curve was determined for individual peak, and the 60S/40S ratios was calculated for each profile; data are the average of three independent experiments; the relative standard deviation was less than 5% in each case. In both experiments, cells were grown in YPD medium at 30 ºC to an $OD_{600}$ of around 0.8. Ten $A_{260}$ units of each extract were resolved in 7-50% sucrose gradients. After centrifugation, changes in the $A_{254}$ value of each gradient were recorder by an on-line spectrophotometer. Sedimentation is from left to right.

time point; consistently, practically no labelled mature 25S rRNA was detected at early 5 min or 15 min chase time points **(Figure 4A)**. Similarly, a delayed conversion of 7S pre-rRNAs into mature 5.8S rRNAs was detected **(Figure 4B)**. More significant, synthesis of 18S rRNA was strongly inhibited since 20S pre-rRNA persisted even after the 60 min of chase.



To investigate in more detail the pre-rRNA processing defects occurring in the absence of eS12, we analysed the steady-state levels of pre- and mature rRNAs by northern hybridization in the *rps12Δ* mutant and compared them to those detected for a *ubi3Δ* and a double *rps12Δ ubi3Δ* strains. As shown in **Figure 5**, the single *rps12Δ* and *ubi3Δ* strains and the double *rps12Δ ubi3Δ* mutants led to practically identical pre-rRNA processing defects. Thus, none of these strains showed significant differences in the levels of 35S and 32S pre-rRNAs compared to the wild-type strain. However, some delay in the early pre-rRNA processing reactions might occur as an aberrant 21S pre-rRNA, which extends from site $A_1$ to $A_3$, slightly accumulated in the three mutant strains. Moreover, the 27S and 7S pre-rRNAs clearly decreased, however, levels of mature 25S and 5.8S rRNAs only slightly decreased. In agreement with the delayed conversion of 20S pre-rRNA to 18S rRNA seen in pulse chase analysis, steady-state levels of 20S pre-rRNA visibly accumulated in a similar manner in the three mutant strains **(Figure 5)**; as a consequence, levels of mature 18S rRNA significantly decreased. Altogether, our results indicate that the absence of eS12 leads to a general delay in pre-rRNA maturation that is much more pronounced for the 20S pre-rRNA conversion into mature 18S rRNA, which likely accounts for the deficit in 40S r-subunit detected in *rps12Δ* cells. These pre-RNA processing defects are quite similar to those observed in the *ubi3Δ* strain and only slightly enhanced by the *ubi3Δ* allele.

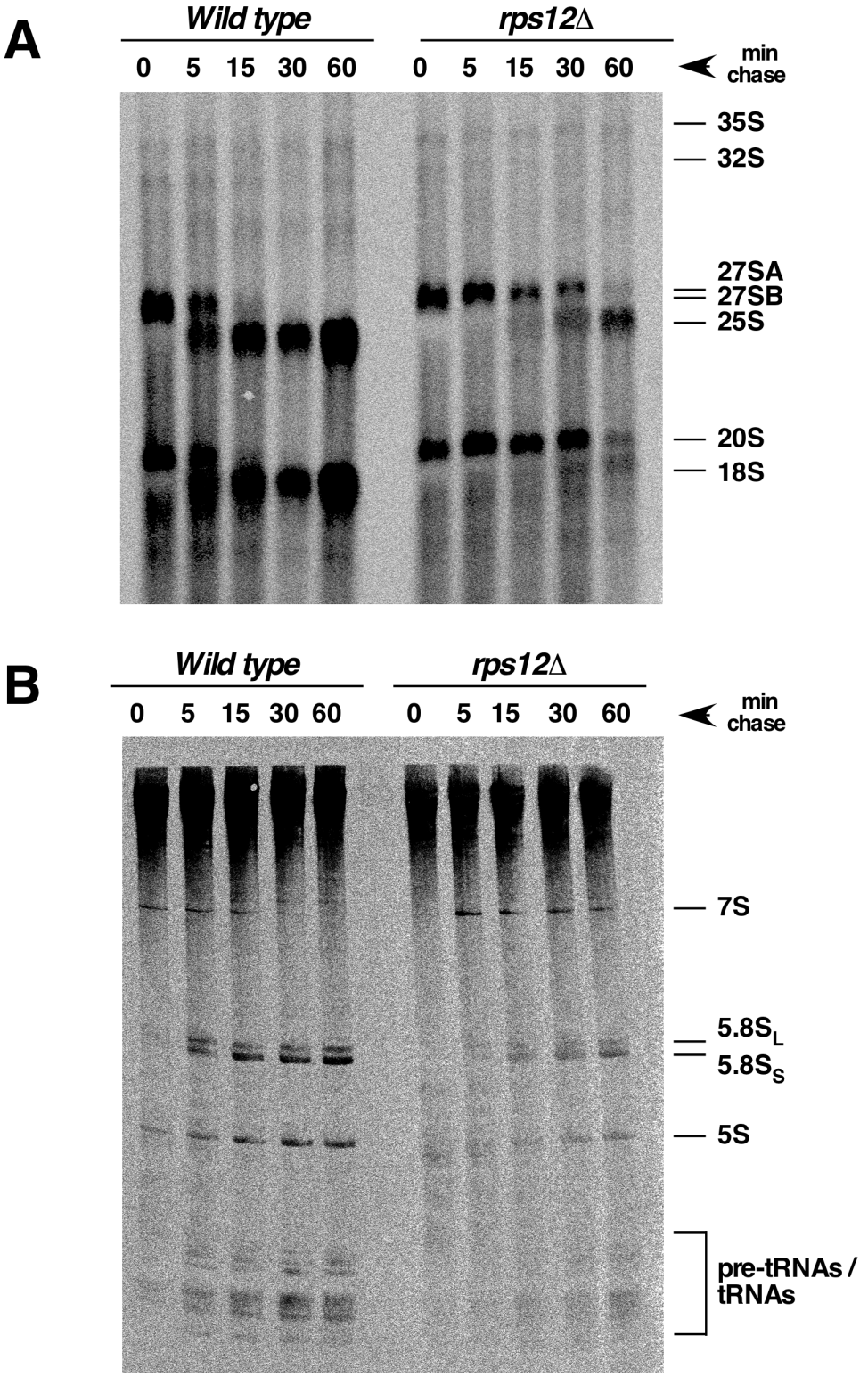


**FIGURE 4. Deletion of *RPS12* lead to delayed conversion of the 20S pre-rRNA to mature 18S rRNA.** The strains W303-1A (*Wild type*) and SMY315 (*rps12Δ*) were transformed with the YCplac33 plasmid and then grown in SD-Ura to an $OD_{600}$ of around 0.8 at 30 ºC. Cells were pulse-labelled for 2 min with [5,6-$^{3}$H]uracil and then chased for 5, 15, 30 and 60 min with an excess of unlabelled uracil. Total RNA was extracted and 3,000 cpm per sample were loaded and separated on **(A)** a 1.2% agarose-formaldehyde gel or **(B)** a 7% polyacrylamide-8 M urea gel, transferred to nylon membranes, exposed to a tritium sensitive phosphor screen and analyse by phosphorimager scanning. The position of the different pre-rRNAs and mature rRNAs are indicated.

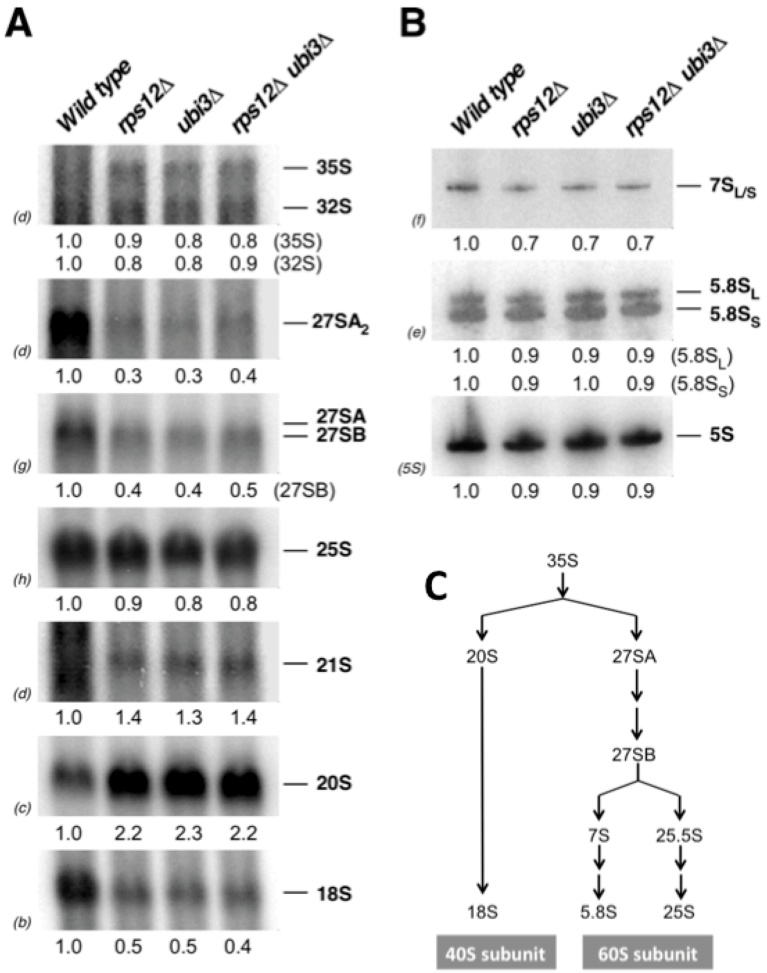


**FIGURE 5. Absence of eS12 leads to robust accumulation of 20S pre-rRNA and concomitant reduction in the steady-state levels of mature 18S rRNA.** The strains W303-1A (*Wild type*), SMY315 (*rps12Δ*), TLY14.3C (*ubi3Δ*) and SMY372 (*rps12Δ ubi3Δ*) were grown in YPD medium at 30 ºC to an $OD_{600}$ of around 0.8. Total RNA was extracted from each strain; equal amounts of RNA (5 µg) were analysed by northern blot. **(A)** Northern hybridisation of high-molecular-mass pre- and mature rRNAs, **(B)** Northern blot analysis of low-molecular-mass pre- and mature rRNAs. Signal intensities were measured by phosphorimager scanning (indicated below each panel) and normalised to those obtained for the wild-type, arbitrarily set to 1.0. Probes, between parentheses, are described in **Table 3**. **(C)** Main steps in pre-rRNA processing are shown.

## The *rps12Δ* deletion mutant accumulates the 20S pre-rRNA in the cytoplasm

Nuclear pre-40S r-particles are rapidly released through the nucleopore to the cytoplasm, where processing of 20S pre-rRNA to mature 18S rRNA occurs (Trapman and Planta, 1976; Udem and Warner, 1973). Therefore, a defect in 20S pre-rRNA processing might result from either reduced nuclear export of pre-40S r-particles or impaired cleavage of cytoplasmic 20S pre-rRNA. To assess this issue, we first analysed

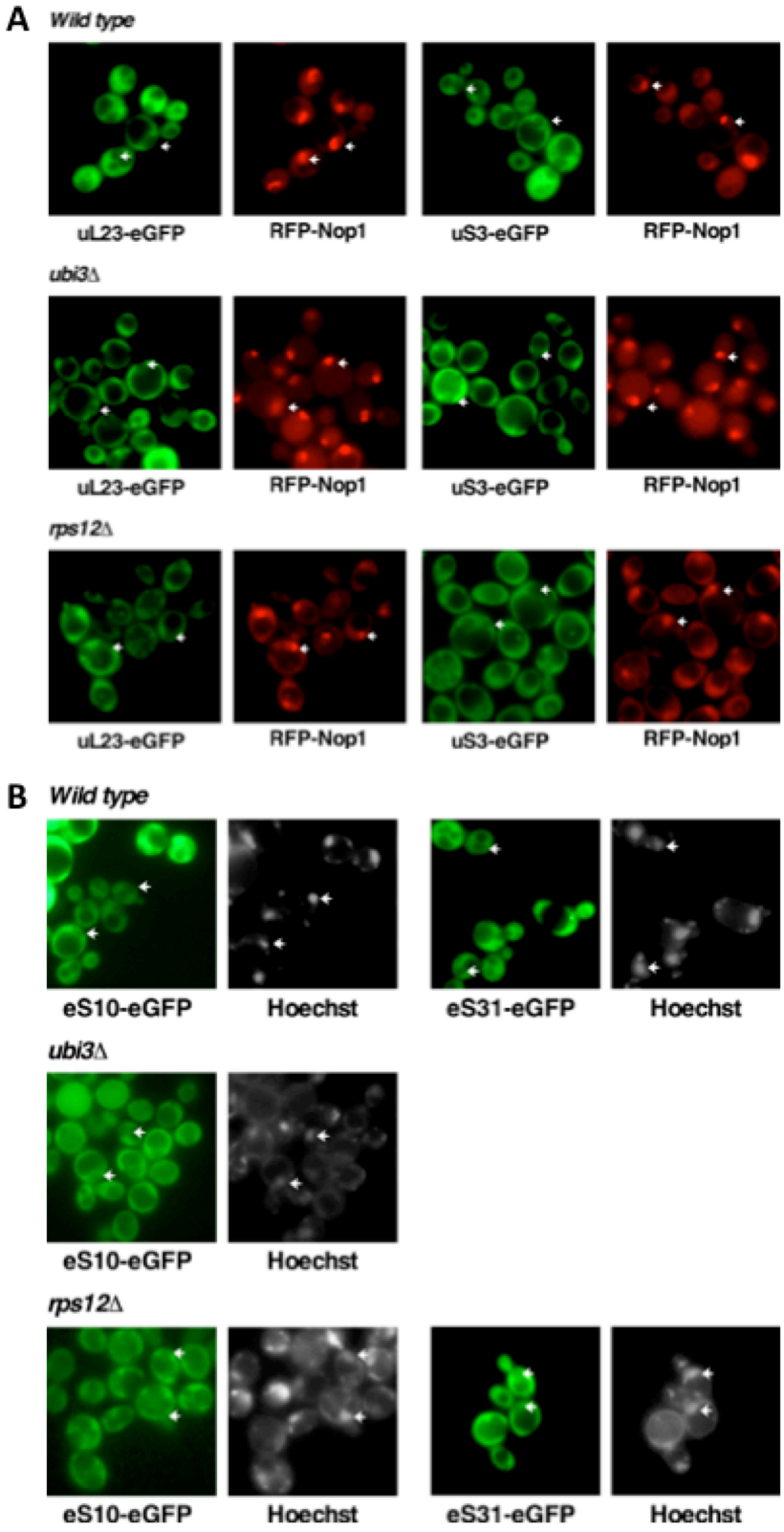


**FIGURE 6. The absence of eS12 does not impair export of nuclear pre-40S ribosomal particles. (A)** The strains W303-1A (*Wild type*), TLY14.3C (*ubi3Δ*) and SMY315 (*rps12Δ*) were transformed with plasmids expressing the nucleolar RFP-Nop1 reporter and either uL23-eGFP or uS3-GFP from their cognate promoters. Cells were exponentially grown in SD-Leu at 30 ºC and then the red and green fluorescent signals analysed by fluorescence microscopy. Arrows indicate the position of the nucleolus in selected cells. **(B)** The localisation of eS31 and eS10 r-proteins is not affected in *rps12Δ* cells. The strains indicated above were transformed with plasmids expressing GFP-tagged versions of eS10 and eS31 r-proteins. Cells were exponentially grown in SD-Leu at 30 ºC and then, the green fluorescent signal analysed by fluorescence microscopy. Hoechst staining reveals the nucleoplasm, whose position was indicated by arrows in selected cells.

the subcellular localization of a GFP-tagged version of uS3 r-protein, which assembles in the nucleus (Koch et al., 2012; Mitterer et al., 2016), in wild-type, *rps12Δ* and *ubi3Δ* cells. As shown in **Figure 6A**, both uS3-eGFP and the 60S r-subunit reporter uL23-eGFP, which also assembles in the nucleus (e.g. (Hurt et al., 1999)), were cytoplasmic in the wild-type and mutant *rps12Δ* and *ubi3Δ* strains. We also analysed the localisation of GFP-tagged versions of eS10 and eS31, which are close neighbour of eS12 at the beak (Rabl et al., 2011); eS31 has been shown to assemble in the nucle(ol)us (Fernández-Pevida et al., 2016; Sun et al., 2017) and eS10 has been suggested to predominantly assemble late in the cytoplasm (Collins et al., 2018; Strunk et al., 2011). As shown in **Figure 6B**, no nuclear accumulation of these two reporters could either be observed in the *rps12Δ* strain.

We also visualised the 20S pre-rRNA and its precursors (35S, 33S and 32S pre-rRNAs) by fluorescent in situ hybridisation (FISH) in the *rps12Δ* and *ubi3Δ* strain using a probe complementary to positions within the D-$A_2$ region of ITS1. As shown in **Figure 7**, as expected, a mainly nucleolar FISH signal was detected in wild-type cells given that 35S, 33S and 32S pre-rRNAs are nucleolar and cytoplasmic 20S pre-rRNA is rapidly processed to mature 18S rRNA in the cytoplasm. However, the FISH signal turned to be also abundant in the cytoplasm in the *rps12Δ* and *ubi3Δ* strains, thus, suggesting that 20S pre-rRNA is efficiently exported in these mutants. Altogether, these results reveal that pre-40S r-particles export from the nucleus is neither blocked in the *rps12Δ* or *ubi3Δ* mutant. Moreover, the increased levels of 20S pre-rRNA detected *rps12Δ* and *ubi3Δ* mutant cells are the result of an impairment of cytoplasmic 20S pre-rRNA processing.

**The accumulated 20S pre-rRNA is not efficiently incorporated into translating ribosomes in *rps12Δ* cells**

It has been previously reported that, in some mutants, pre-40S r-particles containing the 20S pre-rRNA could be efficiently incorporated into translating ribosomes (Lacombe et al., 2009) (García-Gómez et al., 2014; Pertschy et al., 2009). In contrast, in wild-type cells and most mutant that accumulate 20S pre-rRNA, pre-40S r-particles were only found to peak together with free 40S r-subunits or 80S ribosomes

(e.g. (Ghalei et al., 2017; Granneman et al., 2005; Jakovljevic et al., 2004; Soudet et al., 2010; Strunk et al., 2012)).

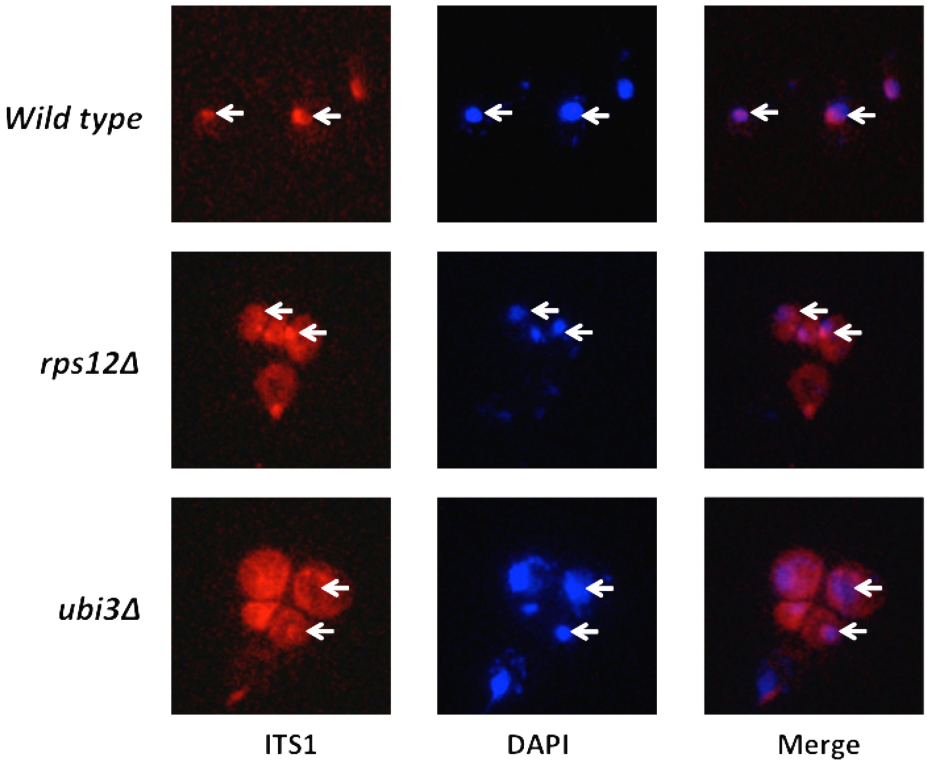


**FIGURE 7. The 20S pre-rRNA accumulates in the cytoplasm of *rps12Δ* and *ubi3Δ* cells.** The strains W303-1A (*Wild type*), TLY14.3C (*ubi3Δ*) and SMY315 (*rps12Δ*) were grown to mid-log phase in YPD medium at 30 ºC. Cells were fixed with formaldehyde, spheroblasted and subjected to FISH using a Cy3-labelled probe complementary to a sequence within the D-$A_2$ segment of ITS1, which hybridises to the 35S, 33S, 32S and 20S pre-rRNAs **(Table 3)**. DAPI staining visualises the nucleoplasm.

To examine whether pre-40S r-particles could engage in translation in *rps12*Δ mutant cells, we performed polysome gradients in the *rps12Δ* strain and subsequently analyse the distribution of 20S pre-rRNA in the different fractions of the gradients by northern blotting. The results were compared to those of an equivalent study done with wild-type and *ubi3Δ* cells. As expected, the bulk of 20S pre-rRNA co-migrated basically with the free 40S peak in wild-type cells **(Figure 8)**. However, in *rps12Δ* and *ubi3Δ* cells, 20S pre-rRNA was predominantly found in the 80S peak, its maximum shifted one fraction left to the maximum of 25S/18S in this peak **(Figure 8)**. Some portion of 20S pre-rRNA was also distributed in the polysomal fraction of the gradients in *rps12Δ* and *ubi3Δ* cells, as it accumulated at the similar low levels of 25S and 18S rRNAs in these fractions due to the fact that in these mutants there is a reduced content of polysomes **(see Figure 3A)**; indeed, graphs of the signal intensities of 20S

pre-rRNA and 25S and 18S mature rRNAs confirmed the similar distribution of these three rRNA species only in the gradients corresponding to *rps12Δ* and *ubi3Δ* cells, but not in those of isogenic wild-type cells **(Figure 8B)**. These data suggest that pre-40S r-particles lacking either eS12 or eS31 can assemble into 80S ribosomes but also inefficiently engage in translation.

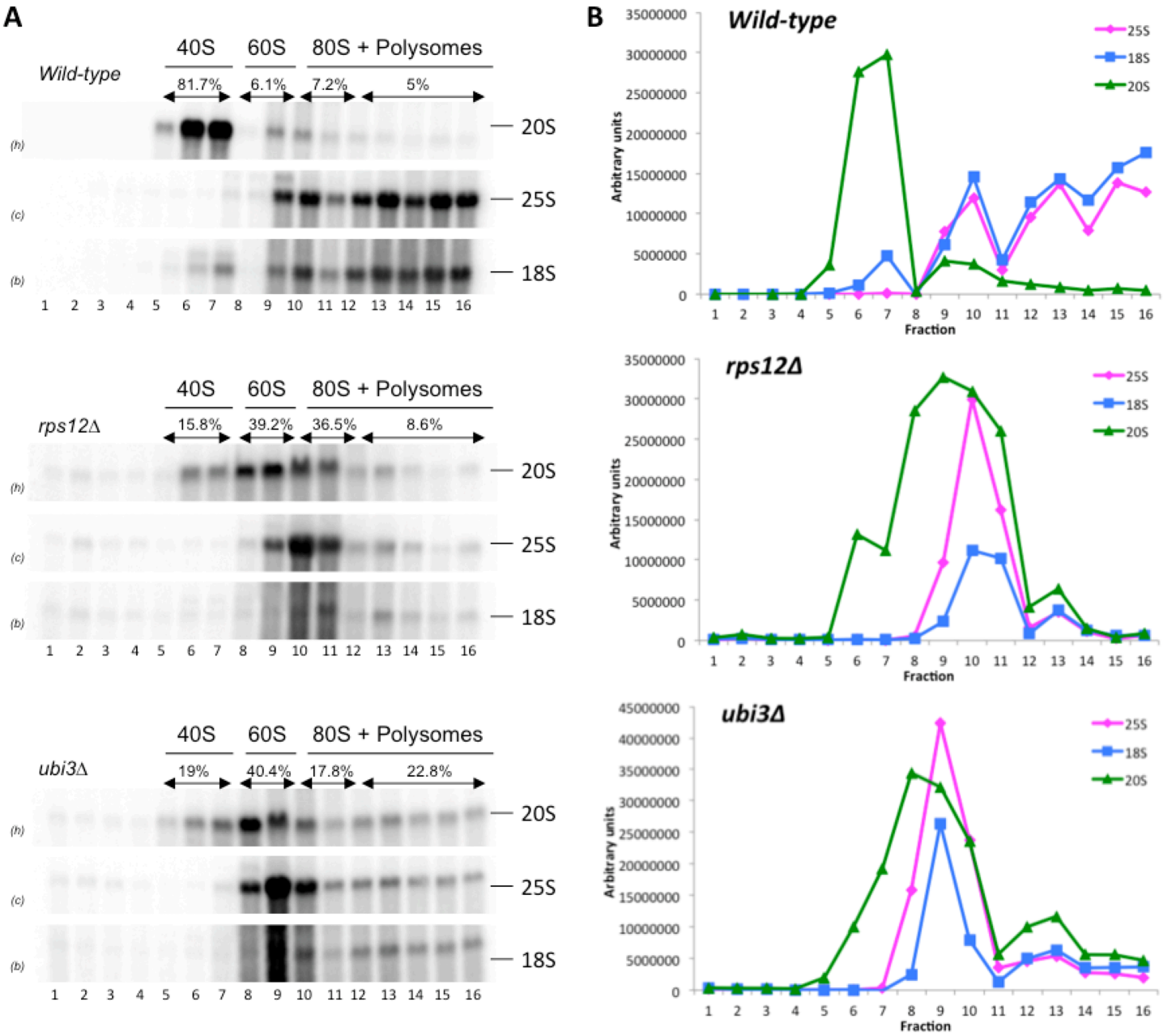


**FIGURE 8. The absence of either eS12 or eS31 alters the sedimentation behaviour of pre-ribosomal particles containing 20S pre-rRNA**. **(A)** The strains W303-1A (*Wild type*), TLY14.3C (*ubi3Δ*) and SMY315 (*rps12Δ*) were grown to mid-log phase in YPD medium at 30 ºC. Cell extracts were prepared and 10 $A_{260}$ units of each extract were resolved in 7-50% sucrose gradients and fractionated. RNA was extracted from each fraction and analysed by northern blotting using the indicated probes (between parentheses; see **Table 3**). The position of free 40S and 60S r-subunits, 80S ribosomes and polysomes are shown. Percentage of 20S pre-rRNA signal intensity in each case is represented. **(B)** The relative intensities of the hybridisation signals of the 20S pre-rRNA and mature 25S and 18S rRNAs were determined for each fraction by phosphorimager analysis and plotted as arbitrary units against the fraction number (20S pre-rRNA, triangles; 25S rRNA, squares; 18S rRNA, dots).

**Dynamics of the *trans*-acting factors Enp1 and Ltv1 during 40S r-subunit biogenesis in the *rps12Δ* and *ubi3Δ* mutants**

Cryo-EM analyses have shown that the *trans*-acting factors Enp1 and Ltv1 are present in cytoplasmic pre-40S r-particles at a position connecting the beak to the head structure **(see Figure 1B)** (Heuer et al., 2017; Johnson et al., 2017; Scaiola et al., 2018; Strunk et al., 2011). Moreover, the release of these two factors from cytoplasmic pre-40S particles upon their phosphorylation by the kinase Hrr25 (Schäfer et al., 2006) seems to induce a conformational rearrangement of the beak/head area, which allow the stable positioning of uS3 (Ghalei et al., 2016; Mitterer et al., 2016) and the efficient recruitment within the head of eS10, uS10, uS14 and RACK1 (Collins et al., 2018). Given that Enp1 associates to 90S pre-ribosomal particles, which apparently also contains eS12 and eS31 (Sun et al., 2017) while Ltv1 binds later to nucleoplasmic pre-40S r-particles (Moriggi et al., 2015; Schäfer et al., 2003; Seiser et al., 2006), we found particularly pertinent to examine both the functional relationship between eS12, eS31, Enp1 and Ltv1 and the dynamics of association/release of Enp1 and Ltv1 in the absence of eS12 and eS31.

We first evaluate whether the defects on growth caused by the absence of eS12 or eS31 could be enhanced by the absence of Ltv1 or the partial loss of function of Enp1. It has been reported that the *ltv1Δ* null allele leads to a sg phenotype for growth at 30 ºC **(see Figure 9A)** and significantly impairs 40S r-subunit synthesis due to defects in both 20S pre-rRNA maturation and export of pre-40S r-particles from the nucleus to the cytoplasm (Fassio et al., 2010; Pertschy et al., 2009; Seiser et al., 2006). In turn, the *enp1-1* mutation renders a temperature sensitive (ts) growth phenotype at 37 ºC, which is linked to a severe 40S r-subunit deficiency due to both the inhibition of pre-rRNA processing at the early $A_0$-$A_2$ cleavage sites and the block of nucleocytoplasmic 40S r-subunit export (Chen et al., 2003; Schäfer et al., 2003); however, at 30 ºC, the growth of *enp1-1* cells was apparently comparable to that of an isogenic wild-type strain **(see Figure 9B)**. As shown in **Figure 9A**, the *ltv1Δ* mutation confers synthetic lethality when combined with either the *rps12Δ* or the *ubi3Δ* alleles. Moreover, as shown in **Figure 9B**, the *enp1-1* mutant when combined with the *rps12Δ* allele or the *ubi3Δ* mutant were synthetically lethal or enhanced, respectively. These findings

strongly suggest an intimate functional interaction between the *trans*-acting factors Ltv1 and Enp1 and the r-proteins eS12 and eS31 during 40S r-subunit biogenesis.

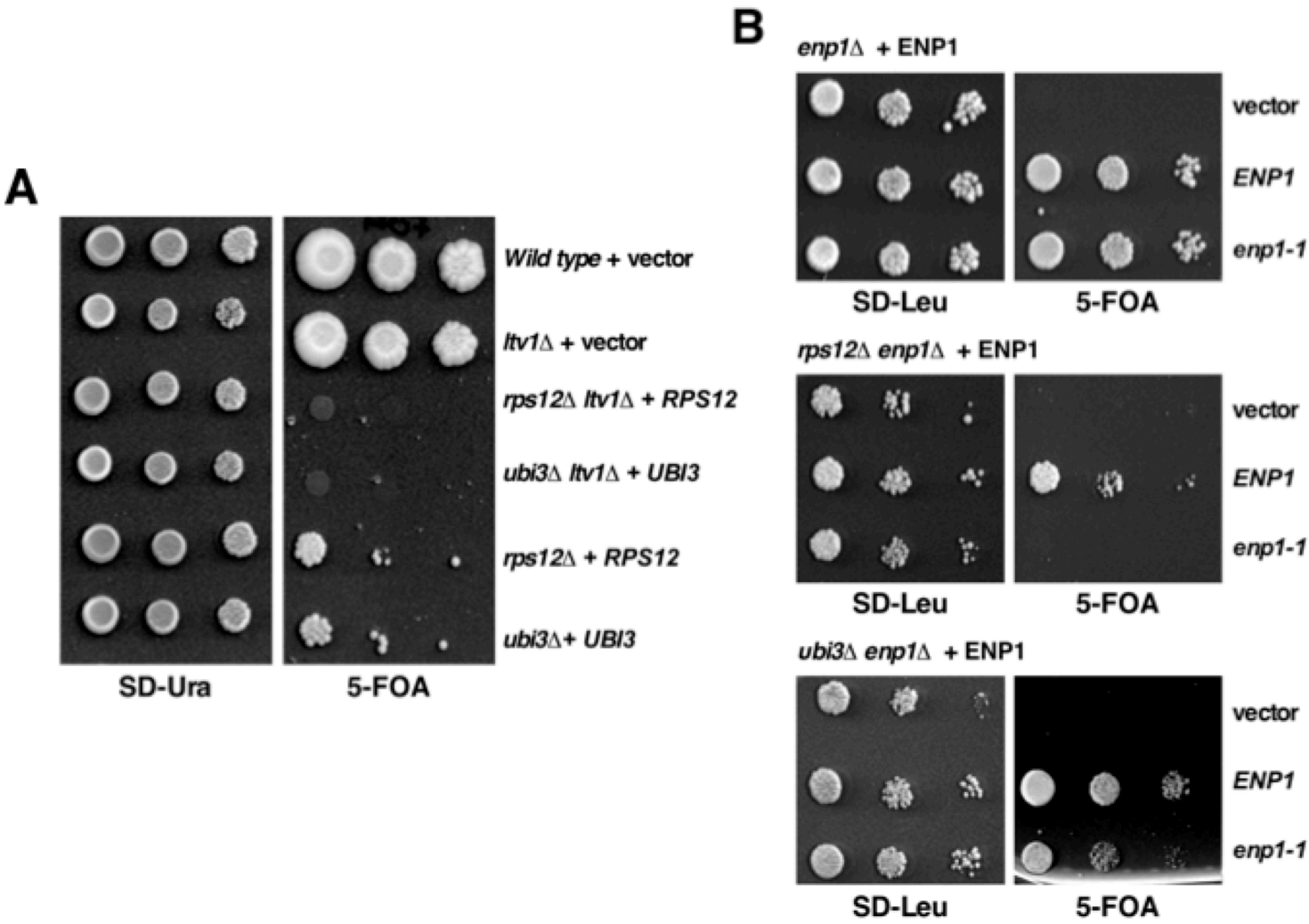


**FIGURE 9. Synthetic lethality or enhancement of the slow-growth phenotype of the *rps12Δ* and *ubi3Δ* mutants by the ltv1Δ and the enp1-1 alleles. (A)** The strains W303-1A (*Wild type*) and SMY307 (*ltv1Δ*), harbouring an empty YCplac33 plasmid (+ vector) and the strains SMY352 (*rps12Δ ltv1Δ*), SMY345 (*ubi3Δ ltv1Δ*), SMY315 (*rps12Δ*) and TLY14.3C (*ubi3Δ*) harbouring the *rps12* or *ubi3* null alleles complemented by a YCplac33-RPS12 (+ *RPS12*) or YCplac33-UBI3 (+ *UBI3*), respectively, were spotted in 10-fold serial dilutions onto SD-Ura and SD containing 5-FOA plates. Plates were incubated 3 and 10 days at 30 ºC, respectively. **(B)** Strains SMY310 (*enp1Δ*), SMY431 (*rps12Δ enp1Δ*) and SMY439 (*ubi3Δ enp1Δ*), which harbour the enp1 null allele complemented by a pRS316-ENP1 (+ *ENP1*) were transformed with an empty pRS415 vector (vector) or pRS315 plasmids that carry either the wild-type *ENP1* (*ENP1*) or the mutant *enp1-1* (*enp1-1*) allele. Then, cells were spotted in 10-fold serial dilution steps onto SD-Leu or SD containing 5-FOA plates. Plates were incubated 3 and 5 days at 30 ºC, respectively.

Second, we studied whether the dynamics of association or release of Enp1 and Ltv1 from pre-ribosomal particles changed in the absence of either eS12 or eS31. To do so, we analyzed the localization of GFP-tagged reporters of Enp1 and Ltv1, expressed from genomic loci, in the *rps12Δ* and *ubi3Δ* mutants and compared to that in an isogenic wild-type control. Consistent with previous reports, we found that while Enp1-GFP has a nucleolar steady-state localization in wild-type cells (**Figure 10;** see (Chen et al., 2003; Moriggi et al., 2015; Schäfer et al., 2003)) Ltv1-GFP had a cytoplasmic localization (**Figure 10;** see (Mitterer et al., 2016; Moriggi et al., 2015; Seiser et al., 2006)). We also made use of a Ltv1ΔNES-GFP reporter, which localized to the nucleus of *RPS12 UBI3* cells **(Figure 10)**, in agreement with previous findings (Merwin et al., 2014; Mitterer et al., 2016). As clearly also shown in **Figure 10**, absence of eS12 or eS31 did not apparently modify the subcellular localization of Enp1 or Ltv1.

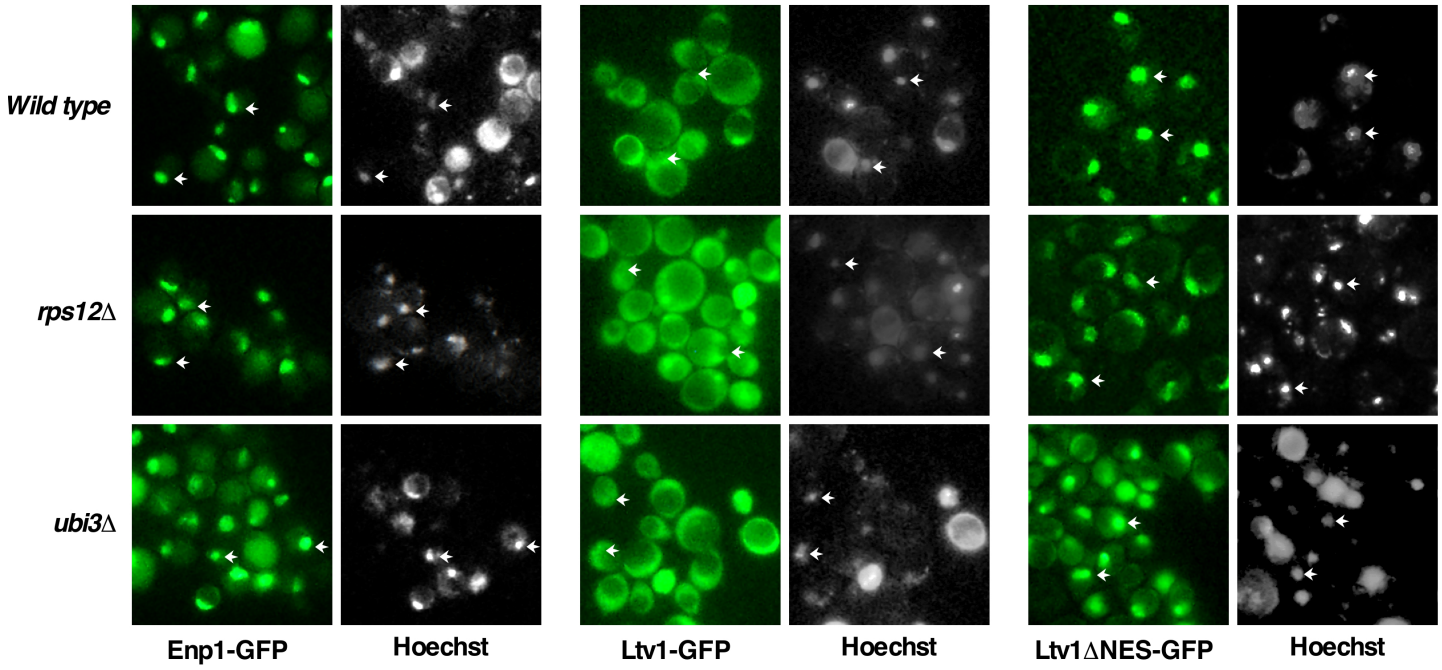


**FIGURE 10. Subcellular distribution of Enp1 and Ltv1 in *rps12Δ* and *ubi3Δ* mutants.** The localisation of wild-type Enp1-GFP, wild-type Ltv1-GFP or mutant Ltv1ΔNES-GFP was examined in wild-type, and *rps12Δ* or ubi3Δ mutants. Strains YGM96 (*ENP1-GFP*), YGM131 (*LTV1-GFP*), YGM138 (*LTV1ΔNES-GFP*), SMY443 (*rps12Δ ENP1-GFP*), SMY447 (*rps12Δ LTV1-GFP*), SMY452 (*rps12Δ LTV1ΔNES-GFP*), SMY456 (*ubi3Δ ENP1-GFP*), SMY459 (*ubi3Δ LTV1-GFP*) and SMY466 (*ubi3Δ LTV1ΔNES-GFP*) were grown in YPD medium at 30 ºC. Then the green fluorescent signal was analysed by fluorescence microscopy. Nuclei were revealed by staining DNA with Hoechst. Arrows indicate the position of the nuclei in selected cells.

To further explore the dynamics of Ltv1 in mutants lacking eS12 or eS31, we made use of *ltv1* mutants harbouring substitution of different conserved serines within the protein to alanine. These mutants were *ltv1*[S336,339>A] and *ltv1*[S336,S339,S342>A] which showed a negative effect in growth and *ltv1*[S336,S339,S342,S344,S345,S346>A] (thereafter *ltv1*[S6>A]) that showed wild-type growth **(Figure 11)**. It has been shown that at least the Ltv1 residues S336, S339 and S342 are phosphorylated by the kinase Hrr25, causing the Ltv1 release from pre-40S r-particles (Ghalei et al., 2016; Mitterer et al., 2016). Consistently, the Ltv1[S336,S339,S342>A] protein remains trapped within pre-40S r-particles (Ghalei et al., 2016; Mitterer et al., 2016). In contrast, the Ltv1[S6>A] has been shown to bind with less affinity to pre-40S r-particles, thereby allowing spontaneous dissociation of the phosphomutant protein (Mitterer et al., 2016). Strikingly, when we combined the *ltv1*[S336,339>A] and *ltv1*[S336,S339,S342>A] mutants with the *rps12Δ* or *ubi3Δ* null

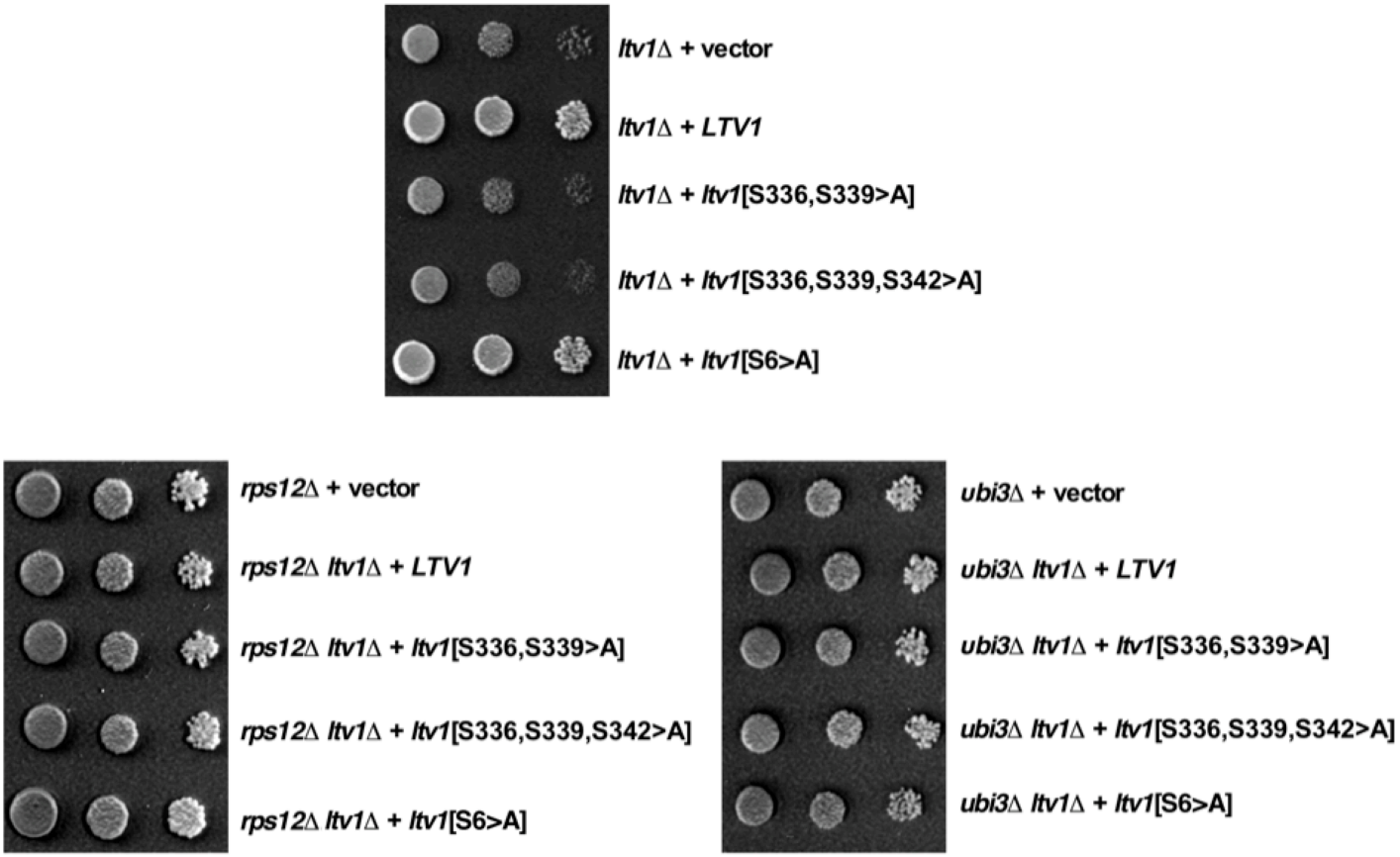


**FIGURE 11. The *rps12Δ* and *ubi3Δ* alleles suppresses the growth defect linked to the expression of the *ltv1*[S336,S339>A] and *ltv1*[S336,S339,S342>A] phosphomutants.** The indicated ltv1 phosphomutants were expressed from the YCplac111 plasmid in the strains SMY307 (*ltv1Δ*), SMY315 (*rps12Δ*), SMY353 (*rps12Δ ltv1Δ*), TLY14.3C (*ubi3Δ*) and SMY345 (*ubi3Δ ltv1Δ*), whch lack Ltv1, eS12, eS12 and Ltv1, eS31, and eS31 and Ltv1, respectively. Growth was examined in SD-Leu plates, which were incubated 3-4 days at 30 ºC.

alleles, a clear suppression of their sg phenotypes was observed **(Figure 11)**. Altogether, these results indicate a functional interaction between the trans-acting factors Enp1 and Ltv1 and the r-proteins eS12 and eS31 in the process of 40S r-subunit biogenesis. Although the dynamics of association and release of these *trans*-acting factors does not substantially change in the absence of the beak r-proteins, our results suggest that the *rps12Δ* and *ubi3Δ* mutations weaken the interaction of Ltv1 with pre-40S r-subunits.

**The absence of eS12 or eS31 induces an increase in translational misincorporation**

It has been previously shown numerous examples of mutations in yeast r-proteins and translation factors causing a reduction in the accuracy of translation (e.g. (Alksne et al., 1993; Anthony and Liebman, 1995; Cui et al., 1998; Dresios et al., 2000; Salas-Marco and Bedwell, 2005; Synetos et al., 1996; Wawiorka et al., 2017)). To assess whether the ribosome lacking either eS12 or eS31 are defective in the accuracy of translation, we first compared the efficiency of stop-codon recognition in isogenic wild type and *rps12Δ* and *ubi3Δ* mutant cells. To do so, we made use of a tandem *Renilla* and firefly luciferase plasmidic reporter system (Salas-Marco and Bedwell, 2005). In this system, the two types of luciferase genes are separated by an in-frame linker sequence in the control plasmid, resulting in the synthesis of both enzymes as a single polypeptide chain; in the readthrough reporter, there is a single in-frame stop codon **(Figure 12A)**; in this reporter, the activity of firefly luciferase, encoded by the distal open reading frame (ORF), results from translation beyond the stop-codon as the result of a readthrough event; the activity of *Renilla* luciferase, encoded by the proximal ORF, serves as an internal control for mRNA abundance and efficiency of translation initiation as both luciferase enzymes initiate translation from the same start codon (for details, see (Keeling et al., 2004; Salas-Marco and Bedwell, 2005)). As shown in **Figure 12B**, no significant differences were observed in the stop-codon suppression when the *rps12Δ* and *ubi3Δ* strains were compared to the isogenic counterpart. We also made use of an equivalent misincorporation reporter system; this system uses a control plasmid identical to the above described; on the other hand, in the misincorporation reporter by introducing a near-cognate missense mutation at a certain codon, the His residue at position 245 (codon CAC) of the firefly luciferase,

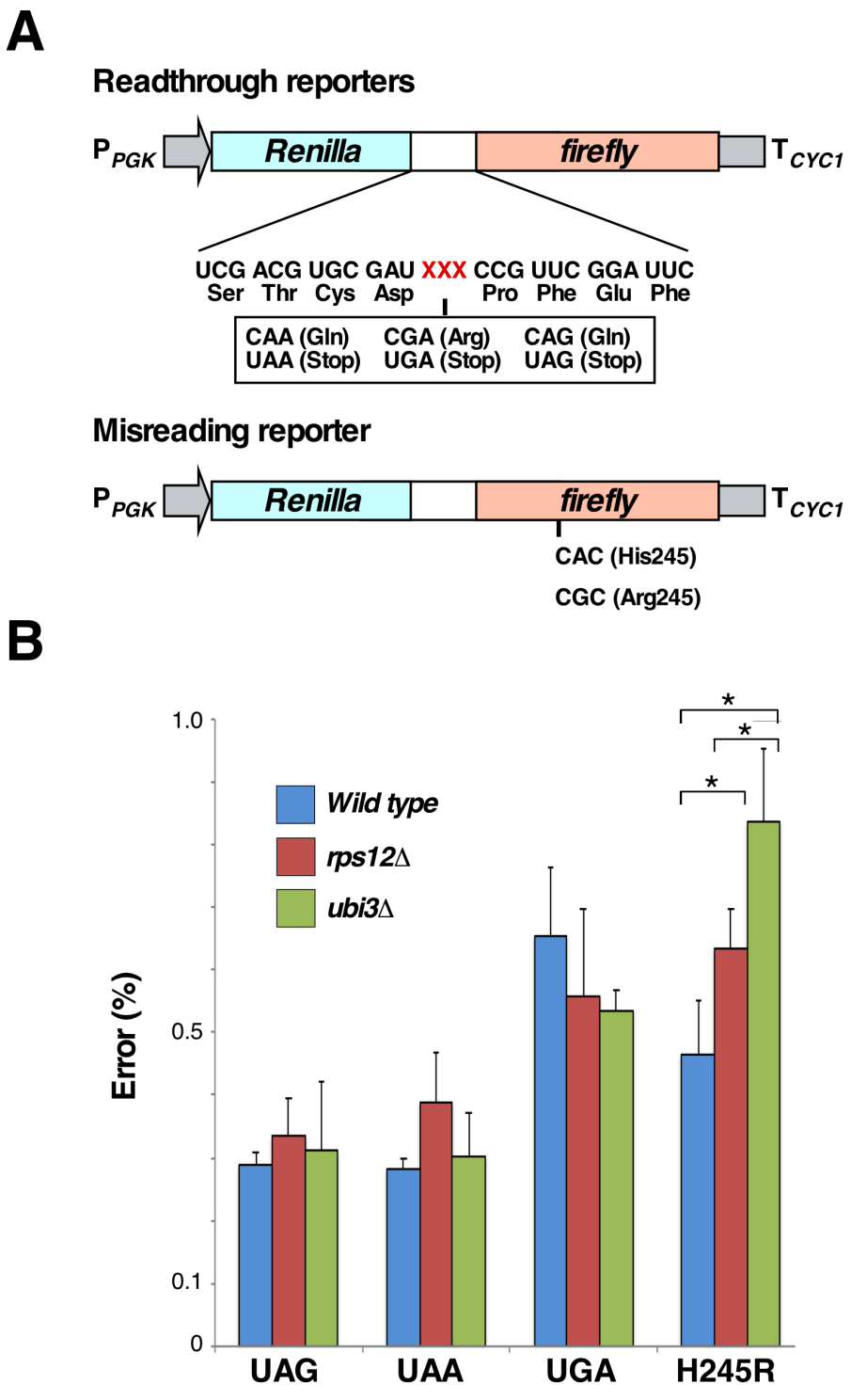


**FIGURE 12. Effects of *RPS12* or *UBI3* deletion on readthrough and misreading during translation.** **(A)** Scheme of the dual luciferase readthrough and misincorporation reporter systems. **(B)** Measurement of the readthrough and misincorporation frequencies in yeast strains lacking eS12 or eS31. Strains W303-1A (*Wild type*), TLY14.3C (*ubi3Δ*) and SMY315 (*rps12Δ*) were transformed with plasmids pDB720 or pDB721 (UAG stop codon), pDB722 or pDB723 (UAA stop codon), pDB690 or pDB691 (UGA stop codon) to measure readthrough or with pDB688 and pDB868 to measure misreading (Arg245(GGC) to His245(CAC)). Transformants were grown in SD-Ura to mid-log phase at 30 ºC and then *Renilla* and firefly luciferase activity was measured. Assays were done in quadruplicate, and the data were expressed as the mean ± the standard deviation. The percentage of readthrough in each strain was expressed as the firefly/*Renilla* luciferase activity (nonsense) divided by the firefly/*Renilla* luciferase activity (sense) multiplied by 100. The percentage of misreading was expressed as the firefly (H245R)/*Renilla* luciferase activity divided by the firefly (wild type)/*Renilla* luciferase activity multiplied by 100. For further details see (Keeling et al., 2004; Salas-Marco and Bedwell, 2005). Significance levels were determined by Student's *t* test (*, p<0.05).

which play an important role in its enzymatic activity, has been substituted by an Arg residue (codon CGC) resulting on a protein with only residual enzymatic activity (Salas-Marco and Bedwell, 2005); thus, the activity of firefly luciferase results from a misreading event that allow misincorporation of a non-deleterious amino acid (normally His *via* a His-tRNA(GUG)$^{His}$) at the mutated CGC codon (Salas-Marco and Bedwell, 2005). Interestingly, as also shown in **Figure 12B**, a significant increase in misreading was found following *RPS12* deletion, which was even higher upon *UBI3* deletion. These results suggest that eS12 and eS31 are involved in the fidelity of translation elongation, thus ribosome lacking either eS12 or eS31 are error-prone leading to an increase in the misreading rate.

## DISCUSSION

In last years, the knowledge about the contribution of r-proteins to ribosome biogenesis has increased significantly (de la Cruz et al., 2015). However, some r-proteins remain uncharacterized yet. In this work, we have addressed the role of the eukaryotic specific r-protein eS12 in yeast 40S r-subunit biogenesis and function. The r-protein eS12 is located on the beak of the small r-subunit, closed to eukaryotic specific r-proteins eS10 and eS31. With this study, we provide the first report dissecting the contribution of the r-proteins of the beak to ribosome biogenesis.

Analysis of the *rps12* null mutant shows that, contrary to most r-proteins in yeast, eS12 is not an essential r-protein, albeit absence of eS12 strongly impairs cell growth at all tested temperatures in different genetic backgrounds **(Figure 2)**. Similar results have been reported by (Steffen et al., 2012). The absence of nonessential r-proteins reduces cell growth rates to different extents, being almost dispensable for growth in some cases (Steffen et al., 2012).

Relative to the wild type, deletion of *RPS12* causes a strong 40S r-subunit shortage **(Figure 3)**. Analysis of pre-rRNA processing by northern blotting and pulse-chase labelling analysis clearly indicates that the 40S r-subunit deficit exhibited by the rps12 mutant is due to a strong inhibition of processing of the 20S pre-rRNA, which leads to reduced formation of mature 18S rRNA. The delay in 20S pre-rRNA processing of *rps12Δ* cells results from reduced cleavage of cytoplasmic 20S pre-rRNA at site D since 20S pre-rRNA was accumulated in the cytoplasm and export of pre-40S particles was not impaired, as we did not observe nuclear accumulation of the SSU reporters in *rps12Δ* cells **(Figures 6 and 7)**. In a similar way, it has been described that human eS12 is required in the conversion of 18S-E to 18S, homologous to the 20S pre-rRNA to 18S rRNA yeast processing (O'Donohue et al., 2010). Moreover, pre-rRNA processing at site $A_2$ seems to be slightly delayed as suggested by the decrease of 27S pre-rRNA and the appearance of the aberrant 21S pre-rRNA upon depletion of yeast eS12 **(Figures 4 and 5)**.

The effects of the *RPS12* deletion are very similar to those shown and previously

reported for the depletion of its neighbour r-protein eS31. The r-protein eS31 is also a quasi-essential protein located on the beak of the small r-subunit. Absence of eS31 causes a strong 40S r-subunit shortage due to delayed pre-rRNA cleavage at sites $A_2$ and cytoplasmic maturation of 20S pre-rRNA at site D, similarly to the absence of eS12 **(Figures 3 and 5)** (Finley et al., 1989; Lacombe et al., 2009). We have shown that simultaneous deletion of both genes did not enhance these phenotypes.

Similar defects in pre-rRNA processing have been reported for different r-protein mutants, especially for those r-proteins located on the head of the small r-subunit (Ferreira-Cerca et al., 2005; Ferreira-Cerca et al., 2007). However, it is not clear how might r-proteins located on the beak affect the conversion of 20S pre-rRNA to mature 18S rRNA. Due its positions, it seems unlikely that eS12 or eS31 directly catalyses cleavage of 20S pre-rRNA in yeast ribosomes. Two explanations are possible. First, these r-proteins could be important to establish the conformation of the 3' end of 20S pre-rRNA required for efficient cleavage at site D indirectly through general effects on 40S r-subunit structure. Analysis of the structure of small ribosomal subunits suggests a general effect in subunit structure since eS12 neither eS31 are not close enough to interact with sequences in ITS1. Second, it is also possible that eS12 and eS31 were necessary to recruit or position nucleases or other cofactors, such as Nob1, required for cleavage of 20S pre-rRNA. Further experiments are required to check if such cofactors are present in pre-ribosomal particles in absence of eS12 or eS31 to address the precise effect both r-proteins in pre-rRNA processing.

On the other hand, pre-40S r-particles containing the 20S pre-rRNA present in *rps12Δ* mutant cells are not competent for translation elongation since the 20S pre-rRNA accumulated in these cells was only found to associate with 40S r-subunits and 80S ribosomes, but not with translating ribosomes **(Figure 8)**. However, we cannot exclude the possibility that subunits containing the 20S pre-rRNA are at least partially active in protein synthesis because small amounts of this precursor co-sedimented with polysomes. By contrast, 20S pre-rRNA-containing 40S r-subunits could engage in translation upon depletion of eS31. Although pre-40S r-particles are not found in polysomes in wild-type cells or in most mutants that accumulate cytoplasmic 20S pre-rRNA (e.g.(Ford et al., 1999; Jakovljevic et al., 2004; Strunk et al., 2012)), presence of

20S pre-rRNA in ribosome-polysome fractions is also observed when the N-terminal ubiquitin moiety of eS31 was deleted, or when some r-proteins or ribosome biogenesis factors were depleted (e.g. (García-Gómez et al., 2014; Lacombe et al., 2009)).

Probably, qualitative differences between 40S r-subunits containing 20S pre-rRNA in r-particles lacking eS12 or eS31 could be found. Moreover, it seems that these 40S r-subunits containing the 20S pre-rRNA present in *rps12Δ* and *ubi3Δ* cells were altered in such a way that they affect the correct function of the translation machinery since both strains are defective in translation elongation **(Figure 12).** In this sense, we had previously reported that the truncation of the N-terminal extension of eS31, which reaches the A-site of the 40S r-subunit, affects the fidelity of translation (Fernández-Pevida et al., 2016).

Finally, we have also analysed the connection between eS12, eS31 and ribosomal biogenesis factors Enp1 and Ltv1 to further unravel how eS12 and eS31 contribute to the biogenesis of 40S r-subunits. These factors are assembled close eS12 and eS31 and both are important for beak formation (Scaiola et al., 2018). The *trans*-acting factor Enp1 is already present in 90S pre-ribosomes, whereas Ltv1 binds directly to Enp1 later in pre-40S r-particles (Schäfer et al., 2003). In the cytoplasm, both factors forms a complex that is phosphorylation-dependent released to permit the final remodelling of the head region of 40S r-subunits (Collins et al., 2018). Moreover, mutations related with both factors lead to defects in ribosome biogenesis that resembled those seen in strains genetically depleted of r-proteins eS12 and eS31 (Chen et al., 2003; Seiser et al., 2006). Thus, *trans*-acting factors Enp1 and Ltv1 could be somehow link with eS12 or eS31. In agreement with this hypothesis, we have found genetic interaction between the absence of either eS12 or eS31 and Ltv1 or Enp1 **(Figure 9)**. However, this interaction it seems not to be related with the incorporation or release of these factors into pre-40S r-particles, since we had not found significant changes in the subcellular localization of these *trans*-acting factors upon eS12 or eS31 depletion **(Figure 10)**. On the other hand, r-protein eS12 apparently is not required to eS31 assembly as suggest the cytoplasmic signal of eS31-GFP in *rps12Δ* cells **(Figure 6)**. Clearly, future experiments are required in order to understand the relation between eS12 and eS31 and *trans*-acting factors.

In conclusion, our data clearly indicate that formation of the beak is a pre-requisite for the efficient maturation of 40S r-subunits and its proper function. However, some aspects as the timing of eS12 assembly remain unexplored. Some analyses suggest that r-proteins that form the head domain of the 40S r-subunits are the latest r-proteins assembled during ribosome biogenesis (e.g. (Ferreira-Cerca et al., 2007; O'Donohue et al., 2010)). In this sense, r-proteins located in the head are important for downstream maturation steps as the nucleo-cytoplasmic export of pre-40S r-particles and processing of late pre-rRNAs (de la Cruz et al., 2015; Ferreira-Cerca et al., 2007; O'Donohue et al., 2010). In agreement, a predominantly late nucle(ol)ar assembly of eS31 has been suggested (Fernández-Pevida et al., 2016). Taking into account the defects in pre-rRNA processing in *rps12Δ* cells, we could assumed that stable assembly of eS12 occurs at a relatively late stage during ribosome biogenesis. Surprisingly, in recent cryo-EM studies the beak structure of the head region seems to be practically molded in the early 90S pre-ribosomal particles (Sun et al., 2017). In that sense, we cannot rule out the possibility of an early association in pre-ribosomal particles of r-proteins eS12 and eS31 in an immature conformation considering that the head domain region is reorganized before 20S pre-rRNA cleavage, 40S r-proteins interact particularly weakly with 90S pre-ribosomal particles, and a conformational change of the N-terminus of eS31 has been described in human pre-40S r-particles (Ameismeier et al., 2018; Schäfer et al., 2006). Thus, further experiments are required to address the precise timing of eS12 assembly into pre-ribosomal particles.

## MATERIALS AND METHODS

### Strains and microbiological methods

All yeast strains used in this work are listed in **Table 1**. Unless otherwise indicated, experiments were conducted in the W303 genetic background. Strains SMY227 and SMY231 are meiotic *rps12Δ* and *ubi3Δ* null segregants of strains Y21666 and Y24116 (Euroscarf), respectively. Strain SMY315 was generated by PCR-based gene disruption of the *RPS12* gene in the diploid W303 strain. To this end, we used genomic DNA of the SMY227 strain, which harbours a genomic *rps12*::kanMX4 allele, as a template and the oligonucleotide pair EcoRI_S12up and S12_check_down (see **Table 3**). Transformants were selected on YPD plates containing 200 µg/ml G418, some candidates were chosen and the correctness of the integration verified by PCR. Positive heterozygous candidates were transformed with the YCplac33-RPS12 plasmid, then sporulated, and tetrads were dissected. SMY315 was selected as a representative *rps12Δ* null haploid mutant.

To generate SMY372, TLY14.3C was crossed to SMY315 [YCplac33-RPS12]; the resulting diploid was sporulated, and tetrads were dissected. Spore clones from different tetratypes were obtained and restreaked on 5-FOA-containing plates. Other strains, listed in **Table 1**, harbouring combinations of different alleles were obtained by a similar approach.

Growth and handling of yeast and yeast media were done following established procedures (Kaiser et al., 1994). Strains were grown at the indicated temperatures either in rich YPD medium (1% yeast extract, 2% peptone and 2% glucose) or synthetic minimal medium (0.15% yeast nitrogen base, 0.5% ammonium sulphate) supplemented with the appropriate amino acids and bases as nutritional requirements, and containing 2% glucose (SD) as carbon source. To prepare plates, 2% agar was added to the media before sterilization. Yeast cells were transformed by a lithium acetate method (Gietz et al., 1992). Tetrads were dissected with a MSM200 micromanipulator (Singer Instruments, UK). *Escherichia coli* strain DH5α was used for

cloning and propagation of plasmids. All recombinant DNA techniques were done according to established procedures (Sambrook et al., 1989).



**Plasmids**

Plasmids used in this work are listed in **Table 2**. To generate YCplac33-RPS12, a PCR was performing using yeast genomic DNA as template and the oligonucleotides BamHI_S12up and S12_SacIdown (**Table 3**), placed plus-minus 1 kb upstream and downstream from the start-stop codon of the *RPS12* ORF. The ca. 2.4 kb PCR product was restricted with *Bam*HI and *Sac*I and cloned into YCplac33, which was also digested with the same enzymes. The rest of plasmids have been reported elsewhere (see **Table 2**).

**Sucrose gradient centrifugation**

Polysome and ribosomal subunit analyses were performed as previously described (Kressler et al., 1997). Ten $A_{260}$ of total cell extract were load onto 7-50% sucrose gradients. These gradients were centrifuged at 39,000 rpm in a Beckman Coulter rotor SW41 for 2 h 45 min (for polysome profile analyses) or for 4 h 30 min (for ribosomal subunit analyses); then, the $A_{254}$ was continuously monitor using an ISCO UA-6 system.

When required, fractions of 0.5 ml were collected from the gradient. RNA was extracted from each fraction and an equal volume of RNA from individual fractions was subjected to northern analyses (see below) as previously described (de la Cruz et al., 1998a).

**RNA extractions and northern hybridization analyses**

Total RNA was extracted from samples corresponding to 10 $OD_{600}$ units of exponentially grown cells by the acid-phenol method (Ausubel et al., 1994). Equal amounts of total RNA were loaded on 1.2% agarose-6% formaldehyde or on 7% polyacrylamide-8M urea gels as previously described (Venema et al., 1998). Specific antisense-oligonucleotides (**Table 3**) were used to detect specific pre- and mature rRNAs. Oligonucleotides were 5'-end labelled with [$\gamma$-$^{32}$P]ATP (6000 Ci/mmol; Perkin

Elmer) as previously described (Venema et al., 1998). Phosphorimager analysis was performed with a Typhoon™ FLA-9000 imaging system (GE Healthcare) and signals intensities were quantified using the GelQuant.NET software (biochemlabsolutions.com).



**Pulse-chase labelling of pre-RNA**

For [5,6-$^{3}$H]uracil pulse-chase labelling analysis, strains W303-1A and SMY315 were first transformed with an empty YCplac33 plasmid to make them prototrophic for uracil. Transformants were grown in 50 ml of liquid SD-Ura medium to mid-log phase at 30 ºC. Then, the cells were concentrated in 1 ml of SD-Ura medium and pulse-labelled using 100 µCi of [5,6-$^{3}$H]uracil (45 to 50 Ci/mmol; Perkin Elmer) per 40 $OD_{600}$ units of yeast cells as exactly described in Kressler *et al.* (Kressler et al., 1998). Cells were chased for 5, 15, 30 and 60 min after diluting 200 µl aliquots of pulse-labelled cells in 4 ml of SD medium containing an excess (1 mg/ml) of non-radioactive uracil. Total RNA was extracted by the acid-phenol method as above.

Uracil incorporation was measured by scintillation counting and 3000 cpm per RNA sample was loaded and resolved on 1.2% agarose–6% formaldehyde and 7% polyacrylamide-8M urea gels. RNA was then transferred to Hybond-N nylon membranes (GE Healthcare), crosslinked to the membranes, and exposed to a tritium screen (BAS-IP TR2040E; GE Healthcare). Visualization was performed with a Typhoon™ FLA-9000 imaging system (GE Healthcare).

**Detection of fluorescent proteins by microscopy**

To test pre-ribosomal particle export, the appropriate strains were transformed with pRS315-RPL25-eGFP-NOP1-mRFP, pRS315-RPS3-eGFP-NOP1-mRFP (gifts from J. Bassler and E. Hurt), YCplac111-RPS10-yEGFP or YCplac111-UBI3-yEGFP plasmids (see **Table 2**). Transformants were grown in selective SD medium. Cells were washed and resuspended in PBS buffer (140 mM NaCl, 8 mM $Na_2HPO_4$, 1.5 mM $KH_2PO_4$, 2.75 mM KCl, pH 7.3) before their microscopy inspection. When required, Hoechst was used to stain nuclear DNA. Cells were examined with an Olympus BX61 fluorescence

microscope equipped with a digital camera; images were analysed using the CellSens software (Olympus).



To study the subcellular location of GFP-tagged Enp1, Ltv1 and Ltv1ΔNES, the appropriate strains (see **Table 1**) were grown in YPD medium. Hoechst was used to stain DNA in the nucleus. Fluorescently labelled cells were inspected as described above.

**Fluorescence *in situ* hybridization microscopy**

To examine the localization of the 20S pre-rRNA, fluorescence *in situ* hybridisation (FISH) was performed in spheroblasted cells fixed with formaldehyde, as previously described (Grosshans et al., 2000; Rodríguez-Galán et al., 2015). A Cy3-labelled ITS1-specific probe (see **Table 3**) was used. Cells were also stained with DAPI (4,6-diamidino-2-phenylindole) to visualize DNA. Cells were examined by fluorescence microscopy as described above.

**Quantification of translation accuracy.**

To measure the efficiency of translation termination and of amino acid misincorporation, the strains W303-1A, SMY315 and TLY14.3C were transformed with the different dual-luciferase reporter plasmids generously provided by D. Bedwell (see **Table 2**). Luciferase activities were measured as previously described (Salas-Marco and Bedwell, 2005) using the Dual-Glo® Luciferase Assay System (Promega). Cells from each strain were grown in liquid SD-Ura medium to mid-log phase at 30ºC and firefly and *Renilla* luciferase luminescence levels were measured at room temperature with a CLARIOstar 1.20 microplate reader (BMG Labtech, Germany) adjusts to readtype endpoint and default settings. Assays were done in quadruplicate and the data were expressed as the mean ± the standard deviation. Error rates for each strain were calculated as the percentage of the firefly/*Renilla* luciferase activity (mutant plasmid) divided by the firefly/*Renilla* luciferase activity (wild-type plasmid).

**Table 1. Yeast strains**

| Strain | Relevant genotype | Source |
|---|---|---|
| BY4741 | *MAT***a** *his3Δ1 leu2Δ0 met15Δ0 ura3Δ0* | Euroscarf |
| Y21666 | *MAT**a**/MAT*α *his3Δ1/his3Δ1 leu2Δ0/leu2Δ0 met15Δ0/MET15 LYS2/lys2Δ0 ura3Δ0/ura3Δ0 RPS12/rps12::*kanMX4 | Euroscarf |
| Y24116 | *MAT**a**/MAT*α *his3Δ1/his3Δ1 leu2Δ0/leu2Δ0 met15Δ0/MET15 LYS2/lys2Δ0 ura3Δ0/ura3Δ0 UBI3/ubi3::*kanMX4 | Euroscarf |
| SMY227 | As BY4741 but *rps12*::kanMX4 | This work |
| SMY231 | As BY4741 but *ubi3*::kanMX4 | This work |
| W303-1A | *MAT***a** *ade2-1 his3-11,15 leu2-3,112 trp1-1 ura3-1* | (Thomas and Rothstein, 1989) |
| W303-1B | As W303-1A but *MAT*α | (Thomas and Rothstein, 1989) |
| SMY315 | As W303-1B but *rps12*::kanMX4 | This work |
| TLY14.3C | As W303-1A but *ubi3*::HIS3MX6 | (Lacombe et al., 2009) |
| SMY372 | As W303-1B but *rps12*::kanMX4 *ubi3*::HIS3MX6 | This work |
| YGM96 | As W303-1A but *ENP1*-GFP::HIS3MX6 | (Moriggi et al., 2015) |
| YGM131 | As W303-1A but *LTV1*-GFP::natNT2 *ade3*::kanMX4 | D. Kressler's lab |
| YGM138 | As W303-1A but *LTV1ΔNES*-GFP::natNT2 *ade3*::kanMX4 | D. Kressler's lab |
| SMY443 | As W303-1A but *rps12*::kanMX4 *ENP1*-GFP::HIS3MX6 | This work |
| SMY447 | As W303-1A but *rps12*::kanMX4 *LTV1*-GFP::natNT2 | This work |
| SMY452 | As W303-1A but *rps12*::kanMX4 *LTV1ΔNES*-GFP::natNT2 | This work |
| SMY456 | As W303-1A but *ubi3*::HIS3MX6 *ENP1*-GFP::HIS3MX6 | This work |
| SMY459 | As W303-1A but *ubi3*::HIS3MX6 *LTV1*-GFP::natNT2 | This work |
| SMY466 | As W303-1A but *ubi3*::HIS3MX6 *LTV1ΔNES*-GFP::natNT2 | This work |
| SMY307 | As W303-1A but *ltv1*::hphNT1 | B. Pertschy's lab |
| SMY353 | As W303-1A but *rps12*::kanMX4 *ltv1*::HIS3MX6 [YCplac33-RPS12] | This work |
| SMY345 | As W303-1A but *ubi3*::HIS3MX6 *ltv1*::hphNT1 [YCplac33-UBI3] | This work |
| SMY310 | As BY4742 but *enp1*::kanMX4 [pRS316-ENP1] | E. Hurt's lab |
| SMY431 | As BY4741 but *rps12*::kanMX4 *enp1*::kanMX4 [pRS316-ENP1] | This work |
| SMY439 | As BY4741 but *ubi3*::HIS3MX6 *enp1*::kanMX4 [pRS316-ENP1] | This work |

**Table 2. Plasmids used in this work**

| Name (collection name) | Relevant information | Reference |
|---|---|---|
| YCplac33 | *CEN*, *URA3* | (Gietz and Sugino, 1988) |
| YCplac111 | *CEN*, *LEU2* | (Gietz and Sugino, 1988) |
| YCplac33-RPS12 | eS12; *CEN*, *URA3* | This work |
| YCplac33-UBI3 | Ubi3; *CEN*, *URA3* | (Lacombe et al., 2009) |
| pRS315-RPL25-eGFP-NOP1-mRFP | uL23-eGFP, Nop1-mRFP; *CEN*, *LEU2* | (Ulbrich et al., 2009) |
| pRS315- RPS3-eGFP-NOP1-mRFP | uS3-eGFP, Nop1-mRFP; *CEN*, *LEU2* | (Ulbrich et al., 2009) |
| YCplac111-UBI3-yEGFP (pDK4516) | Ubi3-yEGFP; *CEN*, *LEU2* | (Fernández-Pevida et al., 2016) |
| YCplac111-RPS10A-yEGFP | *RPS10A*-yEGFP; *CEN*, *LEU2* | (Fernández-Pevida et al., 2016) |
| YEplac195-lucCAAA (pDB688) | *Renilla* and Firefly construct containing a CAC codon control (H245), 2µ, *URA3*. | (Salas-Marco and Bedwell, 2005) |
| YEplac195-lucCAAA H245 CGC (pDB868) | *Renilla* and Firefly construct containing a CGC codon (H245R), 2µ, *URA3*. | (Salas-Marco and Bedwell, 2005) |
| YEplac195-lucCAAC (pDB722) | *Renilla* and Firefly construct containing a CAA codon control, 2µ, *URA3*. | (Keeling et al., 2004) |
| YEplac195-lucUAAC (pDB723) | *Renilla* and Firefly construct containing a UAA stop codon, 2µ, *URA3*. | (Keeling et al., 2004) |
| YEplac195-lucCGAC (pDB690) | *Renilla* and Firefly construct containing a CGA codon control, 2µ, *URA3*. | (Keeling et al., 2004) |
| YEplac195-lucUGAC (pDB691) | *Renilla* and Firefly construct containing a UGA stop codon, 2µ, *URA3*. | (Keeling et al., 2004) |
| YEplac195-lucCAGC (pDB721) | *Renilla* and Firefly construct containing a CAG codon control, 2µ, *URA3*. | (Keeling et al., 2004) |
| YEplac195-lucUAGC (pDB720) | *Renilla* and Firefly construct containing a UAG stop codon, 2µ, *URA3*. | (Keeling et al., 2004) |
| YCplac111-LTV1 | Ltv1; *CEN*, *LEU2* | (Mitterer et al., 2016) |
| YCplac111-ltv1-S336/S339>A | Ltv1[S336A S339A]; *CEN*, *LEU2* | (Mitterer et al., 2016) |
| YCplac111-ltv1-S336/S339/S342>A | Ltv1[S336A S339A S342A]; *CEN*, *LEU2* | (Mitterer et al., 2016) |
| YCplac111-ltv1-S6>A | Ltv1[S336A S339A S342A S344A S345A S346A]; *CEN*, *LEU2* | (Mitterer et al., 2016) |
| pRS316-ENP1 | Enp1; *CEN*, *URA3* | (Chen et al., 2003) |
| pRS315 | *CEN*, *LEU2* | (Sikorski and Hieter, 1989) |

| | | |
|---|---|---|
| pRS315-ENP1 | Enp1, *CEN*, *LEU2* | E. Hurt's lab |
| pRS315-enp1-1 | Enp1[W242G, V415A], *CEN*, *LEU2* | E. Hurt's lab |

**Table 3. Oligonucleotides used in this study**

| Name | 5'-3' Sequence |
|---|---|
| EcoRI_S12up | GCAAACTTTCAAGCAAACTTAC |
| S12_check_down | AAGTGAGGATGAAGAGAATC |
| BamHI_S12up | GGATCCGGAGTATGTTCCTAGGGAAAG |
| S12_SacIdown | GAGCTCCGTTCATTTCTGAGAGAGTGGAG |
| Probe b (18S) | CATGGCTTAATCTTTGAGAC |
| Probe c (3-D/$A_2$) | GACTCTCCATCTCTTGTCTTCTTG |
| Probe d ($A_2$/$A_3$) | TGTTACCTCTGGGCCC |
| Probe e (5.8S) | TTTCGCTGCGTTCTTCATC |
| Probe f (E/$C_2$) | GGCCAGCAATTTCAAGTTA |
| Probe g ($C_1$/$C_2$) | GAACATTGTTCGCCTAGA |
| Probe h (25S) | CTCCGCTTATTGATATGC |
| Probe 5S | GGTCACCCACTACACTACTCGG |
| Probe ITS1 (FISH) | Cy3-ATGCTCTTGCCAAAACAAAAAAATCCATTTTCAAAATTATTAAATTTCTT |

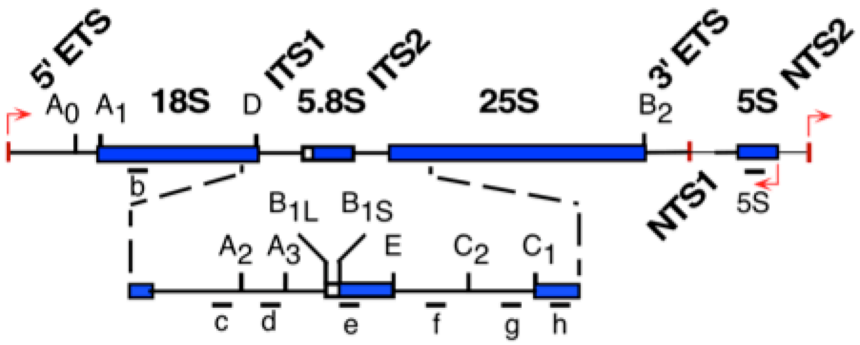


Structure of an rDNA repeat unit. The mature rRNA species are shown as bars and the spacers as lines. The transcription start sites are highlighted by red arrows. The processing sites and the location of the hybridization probes are shown.

# 5. GENERAL DISCUSSION

Ribosome biosynthesis is an important cellular process which requires the participation of r-proteins and more than 200 non-ribosomal *trans*-acting factors in yeast (Woolford and Baserga, 2013). Dysregulation of ribosome biogenesis has deep consequences since ribosomes play key roles in cell growth and proliferation (Teng et al., 2013). Indeed, mutations in r-proteins or ribosome assembly factors are linked to a group of diverse rare human diseases known as ribosomopathies (Teng et al., 2013). Thus, increasing our knowledge about ribosome biogenesis is not only pertinent for academic purposes but also for health reasons. Specifically, the group where this Thesis Work has been performed is interested in understanding the role of r-proteins in ribosome biosynthesis. Although the role of most r-proteins in the biogenesis of each r-subunit has been addressed, there are still a subgroup of ribosomal proteins, mostly non-essential ones, that still require characterization (de la Cruz et al., 2015).

In this Thesis Work, we have studied the role of the eukaryotic specific r-proteins eL40, eS31 and eS12 in ribosome biogenesis and function of the yeast *S. cerevisiae*.

In **Chapter 1**, we have addressed the role of the ubiquitin moiety fused to the eL40 r-protein in ribosome synthesis. Interestingly, both eL40 and eS31 are synthesized as precursors fused to an ubiquitin molecule. In yeast, eL40 is encoded by the paralogous *UBI1* and *UBI2* genes whereas eS31 is encoded by the *UBI3* gene. These genes are the main source of ubiquitin in exponentially growing cells. Understanding the role of the ubiquitin fused to ribosomal proteins becomes relevant as these proteins are practically invariably eS31 and eL40 along the evolution, so an intentional choice for the selection of these two r-proteins can be inferred. We have previously reported that the ubiquitin moiety fused to r-proteins eL40 and eS31 is likely co-translationally cleaved (Lacombe et al., 2009; Martín-Villanueva et al., 2019). Moreover, this cleavage is necessary for the function of eL40 and eS31, and hence, for function of 60S and 40S r-subunits, respectively (Lacombe et al., 2009; Martín-Villanueva et al., 2019). On the other hand, it has been proposed that the ubiquitin moiety contribute to the synthesis of eS31 and consequently, its assembly into 40S r-subunits (Lacombe et al., 2009). In this work, we have deleted the ubiquitin moiety

from the Ubi1 precursor and studied the consequences of the absence of the cis-acting ubiquitin moiety of Ubi1 in the expression and assembly of eL40 in 60S r-subunits.



As for Ubi3, genomic expression of a ubiquitin-free eL40A protein (*ubi1Δub* allele) as the sole source of eL40 leads to reduced eL40A protein levels and, as a consequence, this *ubi1Δub* strain showed also a slow-growth phenotype and a deficit of 60S r-subunits. Both defects are fully suppressed by an increased dosage of the *ubi1Δub* allele and partially by the replacement of ubiquitin by the ubiquitin-like SUMO protein (yeast Smt3), which increase the solubility and expression of fused proteins (Marblestone et al., 2006). Our results clearly show that the ubiquitin fusion facilitates the expression of eL40 r-protein since the ubiquitin moiety of Ubi1 was only required when its expression is driven from a single-copy allele. In agreement with this hypothesis, it has been proposed a chaperone role for the *cis*-acting ubiquitin moiety facilitating the correct folding and the efficient synthesis of eS31 (Finley et al., 1989; Lacombe et al., 2009). Using aggregation assays, we could report the first experimental evidence for this hypothesis, suggesting enhanced aggregation of eS31 when expressed from a ubiquitin-free precursor and reduced aggregation of eL40A when expressed from a Smt3-S-eL40A-HA precursor. We can conclude that the *cis*-acting ubiquitin moiety within Ubi1 and Ubi3 facilitates the efficient synthesis of eL40 and eS31 r-proteins, respectively, being not directly required to eL40 and eS31 assembly into its respective r-subunits **(see Discussion, chapter 1)**. The necessity of a co-chaperone for eL40 and eS31 seems plausible given that, in general, r-proteins are especially prone to aggregate due to presence of intrinsically disordered extensions and its high isoelectric point (Jäkel et al., 2002). For these reasons, some r-proteins interact specifically to dedicated chaperones to prevent their aggregation (Pillet et al., 2017). Interestingly, eukaryotic eS31 contains a highly basic long N-terminal extension, so it is putative prone to aggregate (Fernández-Pevida et al., 2016). Despite eS31 is probably assembled in the nucleus, no specific importins neither dedicated chaperones of eS31 have been found yet. Strikingly, the N-terminal extension of eS31, as well as its ubiquitin moiety, is absent in the eS31 archaeal orthologue, which could suggest that the ubiquitin might be important to stabilize the long extension of eS31. Although evolution had not led to specific chaperones for eS31 neither eL40, the

general ribosome-associated chaperones NAC/Ssb-RAC may not be enough to ensure the proper folding of these r-proteins. Thus, an additional strategy such as fusing ubiquitin to eS31 and eL40 could help these r-proteins to acquire its correct conformation.



In conclusion, the use of amenable tools on yeast biochemistry and genetics is allowing us to unveil the biological role of ubiquitin fused to r-proteins eL40 and eS31. Our findings provide evidence of how ubiquitin could contribute to the expression of r-proteins eL40 and eS31, their further assembly into pre-ribosomal particles and their function. With the exception of the protozoan parasite *Giardia lamblia*, there is so far no evidence of a naturally occurring non-cleaved form of ubiquitin fused to eS31 or eL40 as constituent of mature ribosomes (Catic et al., 2007), thus proteolytic cleavage of the ubiquitin moiety of the precursors seems to be a general requirement for the ribosomal functionality of these two r-proteins. Instead, ubiquitin may act as a *in vivo* molecular chaperone for efficient synthesis of eL40 and eS31, a function that, although partially, could artificially fulfil the yeast ubiquitin-like Smt3 protein. In support to this cellular function, ubiquitin fused to eS31 has evolutionarily diverged into ubiquitin-like proteins in some organisms such as *Caenorhabditis elegans* or *C. briggsae* (Jones and Candido, 1993). However, some aspects remain opened yet. Why are eL40 and eS31 the sole r-proteins fused to ubiquitin? It could serve to maintain the stoichiometry of 60S and 40S r-subunits? Once the ubiquitin is cleaved, it remains non-covalently attached to eL40 and eS31? Could be Ubi1/2 the source of ubiquitin for the cytoplasm and Ubi3 for the nucleus? Future experiments are required in order to understand exactly when and how the cleavage of ubiquitin precursors takes place and hence, to better clarify how r-proteins eL40 and eS31 contribute to ribosome biogenesis.

In this sense, although some functional aspects of r-protein eS31 has been previously studied (Ferreira-Cerca et al., 2005; Ferreira-Cerca et al., 2007; Finley et al., 1987; Lacombe et al., 2009), in **Chapter 2** we have analysed in more details the role of this protein in ribosome biogenesis and function, in the context of the beak region of 40S r-subunit. To this end, we have generated and analysed mutants lacking the r-proteins eS12 and eS31, alone or in combination. Both proteins are located on the

beak of the small r-subunit, a eukaryotic-specific structure that has been transformed from the helix H33 found in prokaryotic ribosomes. Our analysis is the first report in which eS12 has been characterized and hence, the first study about the contribution of the r-proteins of the beak to ribosome biogenesis and function.



Herewith, we have analysed the consequences for ribosome biogenesis of the deletion of *RPS12* and *UBI3* genes, which codes for the *quasi*-essential proteins eS12 and eS31, respectively. Interestingly, deletion of any of these genes results in very similar severe defects in ribosome biogenesis: a strong deficit in 40S r-subunit and an impairment of cytoplasmic 20S pre-rRNA processing at site D. Moreover, pre-40S r-particles containing the 20S pre-rRNA in *rps12Δ* and *ubi3Δ* cells can assemble into 80S ribosomes but inefficiently engage in translation. On the other hand, ribosomes lacking eS12 or eS31 are slightly defective in translation accuracy. The important role of eS12 and eS31 in ribosome biogenesis is also inferred by the evidence that a genetic interaction between the absence of either eS12 or eS31 and that the ribosomal *trans*-acting factors Ltv1 or Enp1 has been found. Furthermore, deletion of *RPS12* or *UBI3* leads to similar levels of r-protein aggregation **(see Figure 9, chapter 1).**

Considering the above results, we conclude that r-proteins eS12 and eS31 display similar roles in ribosome biogenesis and hence, the beak domain is important for 40S r-subunit maturation and function. This work opens new research lines to study some aspects that remain undiscovered yet regarding the role of these proteins. For example, further experiments are required to understand when and how eS12 is assembled into pre-ribosomal particles, to determine whether the assembly of eS12 depends on some r-proteins like eS31 and to better define the connection between eS12 and eS31 and the *trans*-acting factors Ltv1 and Enp1.

In summary, the studies carried out in this Thesis Work represents a modest but relevant contribution to our knowledge about the function of r-proteins in ribosome assembly. As we mentioned above, ribosomopathies are linked to ribosome defects caused by mutations in r-protein genes, so understanding the exact functions of r-proteins during ribosome assembly is a very pertinent issue. Moreover, one of these

pathologies, the Diamond-Blackfan anemia, has been linked with mutations in r-proteins especially of the small r-subunit (Narla and Ebert, 2010). Interestingly, mutations in human eS31 and eS10, neighbours to eS12, seem to be related with the Diamond-Blackfan anemia (Doherty et al., 2010; Gazda et al., 2008). Thus, our progress in understanding the role of eS12 and eS31 in ribosome biogenesis can help us to clarify the underlying physiopathological mechanisms of these diseases.

# 6. CONCLUSIONS

1. The N-terminal ubiquitin moiety fused to r-protein eS31 and eL40 is required for the efficient production of eS31 and eL40, respectively.
2. The ubiquitin moiety of Ubi1 is not strictly needed for the assembly of eL40 into pre-60S r-particles.
3. The ubiquitin-like protein SUMO could artificially replace the ubiquitin moiety of Ubi1, which increases the expression and solubility of eL40A.
4. Ribosomal proteins of the beak eS12 and eS31 are *quasi*-essential proteins required for cell growth and synthesis of 40S r-subunits.
5. Ribosomal proteins eS12 and eS31 are necessary for efficient cytoplasmic 20S pre-rRNA processing but are dispensable for pre-40S r-particles export from the nucleus.
6. Both ribosomal proteins of the beak are required for translation accuracy.

# 6. BIBLIOGRAPHY

Albanèse, V., Yam, A.Y., Baughman, J., Parnot, C., and Frydman, J. (2006). Systems analyses reveal two chaperone networks with distinct functions in eukaryotic cells. Cell *124*, 75-88.

Alksne, L.E., Anthony, R.A., Liebman, S.W., and Warner, J.R. (1993). An accuracy center in the ribosome conserved over 2 billion years. Proc. Natl. Acad. Sci. USA *90*, 9538-9541.

Ameismeier, M., Cheng, J., Berninghausen, O., and Beckmann, R. (2018). Visualizing late states of human 40S ribosomal subunit maturation. Nature *558*, 249-253.

Amerik, A.Y., and Hochstrasser, M. (2004). Mechanism and function of deubiquitinating enzymes. Biochim. Biophys. Acta *1695*, 189-207.

Anthony, R.A., and Liebman, S.W. (1995). Alterations in ribosomal protein RPS28 can diversely affect translational accuracy in *Saccharomyces cerevisiae*. Genetics *140*, 1247-1258.

Archibald, J.M., Teh, E.M., and Keeling, P.J. (2003). Novel ubiquitin fusion proteins: ribosomal protein P1 and actin. J. Mol. Biol. *328*, 771-778.

Armistead, J., and Triggs-Raine, B. (2014). Diverse diseases from a ubiquitous process: the ribosomopathy paradox. FEBS Lett. *588*, 1491-1500.

Ausubel, F.M., Brent, R., Kingston, R.E., Moore, D.D., Seidman, J.G., Smith, J.A., and Struhl, K. (1994). *Saccharomyces cerevisiae*. In Current Protocols in Molecular Biology (New York, N. Y.: John Wiley & Sons, Inc.), pp. 13.10.11-13.14.17.

Baker, R.T. (1996). Protein expression using ubiquitin fusion and cleavage. Curr. Opin. Biotechnol. *7*, 541-546.

Baker, R.T., and Board, P.G. (1987). The human ubiquitin gene family: structure of a gene and pseudogenes from the Ub B subfamily. Nucleic Acids Res. *15*, 443-463.

Barandun, J., Chaker-Margot, M., Hunziker, M., Molloy, K.R., Chait, B.T., and Klinge, S. (2017). The complete structure of the small-subunit processome. Nat Struct Mol Biol *24*, 944-953.

Barandun, J., Hunziker, M., and Klinge, S. (2018). Assembly and structure of the SSU processome-a nucleolar precursor of the small ribosomal subunit. Curr. Opin. Struct. Biol. *49*, 85-93.

Barrio-García, C., Thoms, M., Flemming, D., Kater, L., Berninghausen, O., Bassler, J., Beckmann, R., and Hurt, E. (2015). Architecture of the Rix1-Rea1 checkpoint machinery during pre-60S-ribosome remodeling. Nat. Struct. Mol. Biol. *23*, 37-44.

Bassler, J., and Hurt, E. (2018). Eukaryotic Ribosome Assembly. Annu. Rev. Biochem.

Ben-Shem, A., Garreau de Loubresse, N., Melnikov, S., Jenner, L., Yusupova, G., and Yusupov, M. (2011). The structure of the eukaryotic ribosome at 3.0 Å resolution. Science *334*, 1524-1529.

Ben-Shem, A., Jenner, L., Yusupova, G., and Yusupov, M. (2010). Crystal structure of the eukaryotic ribosome. Science *330*, 1203-1209.

Braten, O., Livneh, I., Ziv, T., Admon, A., Kehat, I., Caspi, L.H., Gonen, H., Bercovich, B., Godzik, A., Jahandideh, S.*, et al.* (2016). Numerous proteins with unique characteristics are degraded by the 26S proteasome following monoubiquitination. Proc Natl Acad Sci U S A *113*, E4639-4647.

Burke, D., Dawson, D., and Stearns, T. (2000). Methods in Yeast Genetics: a Cold Spring Harbor Laboratory Course Manual (Cold Spring Harbor, N. Y.: Cold Spring Harbor Laboratory Press).

Butt, T.R., Jonnalagadda, S., Monia, B.P., Sternberg, E.J., Marsh, J.A., Stadel, J.M., Ecker, D.J., and Crooke, S.T. (1989). Ubiquitin fusion augments the yield of cloned gene products in Escherichia coli. Proc. Natl. Acad. Sci. USA *86*, 2540-2544.

Callis, J., Carpenter, T., Sun, C.W., and Vierstra, R.D. (1995). Structure and evolution of genes encoding polyubiquitin and ubiquitin-like proteins in Arabidopsis thaliana ecotype Columbia. Genetics *139*, 921-939.

Calviño, F.R., Kharde, S., Ori, A., Hendricks, A., Wild, K., Kressler, D., Bange, G., Hurt, E., Beck, M., and Sinning, I. (2015). Symportin 1 chaperones 5S RNP assembly during ribosome biogenesis by occupying an essential rRNA-binding site. Nat. Commun. *6*, 6510.

Campbell, M.G., and Karbstein, K. (2011). Protein-protein interactions within late pre-40S ribosomes. PLoS One *6*, e16194.

Cappadocia, L., and Lima, C.D. (2018). Ubiquitin-like Protein Conjugation: Structures, Chemistry, and Mechanism. Chem Rev *118*, 889-918.

Catic, A., and Ploegh, H.L. (2005). Ubiquitin--conserved protein or selfish gene? Trends Biochem Sci *30*, 600-604.

Catic, A., Sun, Z.Y., Ratner, D.M., Misaghi, S., Spooner, E., Samuelson, J., Wagner, G., and Ploegh, H.L. (2007). Sequence and structure evolved separately in a ribosomal ubiquitin variant. EMBO J. *26*, 3474-3483.

Chaillou, T. (2019). Ribosome specialization and its potential role in the control of protein translation and skeletal muscle size. J Appl Physiol (1985).

Chaker-Margot, M. (2018). Assembly of the small ribosomal subunit in yeast: mechanism and regulation. RNA *24*, 881-891.

Chaker-Margot, M., Barandun, J., Hunziker, M., and Klinge, S. (2016). Architecture of the yeast small subunit processome. Science *355*.

Chen, W., Bucaria, J., Band, D.A., Sutton, A., and Sternglanz, R. (2003). Enp1, a yeast protein associateed with U3 and U14 snoRNAs, is required for pre-rRNA processing and 40S subunit synthesis. Nucleic Acids Res. *31*, 690-699.

Cheng, L., Watt, R., and Piper, P.W. (1994). Polyubiquitin gene expression contributes to oxidative stress resistance in respiratory yeast (*Saccharomyces cerevisiae*). Mol. Gen. Genet. *243*, 358-362.

Chu, S., Archer, R.H., Zengel, J.M., and Lindahl, L. (1994). The RNA of RNase MRP is required for normal processing of ribosomal RNA. Proc. Natl. Acad. Sci. USA *91*, 659-663.

Ciganda, M., and Williams, N. (2011). Eukaryotic 5S rRNA biogenesis. Wiley Interdiscip Rev RNA *2*, 523-533.

Clague, M.J., and Urbé, S. (2010). Ubiquitin: same molecule, different degradation pathways. Cell *143*, 682-685.

Collins, J.C., Ghalei, H., Doherty, J.R., Huang, H., Culver, R.N., and Karbstein, K. (2018). Ribosome biogenesis factor Ltv1 chaperones the assembly of the small subunit head. J Cell Biol *217*, 4141-4154.

Cui, Y., Dinman, J.D., Kinzy, T.G., and Peltz, S.W. (1998). The Mof2/Sui1 protein is a general monitor of translational accuracy. Mol. Cell. Biol. *18*, 1506-1516.

Davis, J.H., and Williamson, J.R. (2017). Structure and dynamics of bacterial ribosome biogenesis. Philos. Trans. R. Soc. Lond. B. Biol. Sci. *372*.

de la Cruz, J., Gómez-Herreros, F., Rodríguez-Galán, O., Begley, V., Muñoz-Centeno, M.C., and Chávez, S. (2018). Feedback regulation of ribosome assembly. Curr. Genet. *64*, 393-404.

de la Cruz, J., Karbstein, K., and Woolford, J.L., Jr. (2015). Functions of ribosomal proteins in assembly of eukaryotic ribosomes *in vivo*. Annu. Rev. Biochem. *84*, 93-129.

de la Cruz, J., Kressler, D., Rojo, M., Tollervey, D., and Linder, P. (1998a). Spb4p, an essential putative RNA helicase, is required for a late step in the assembly of 60S ribosomal subunits in *Saccharomyces cerevisiae*. RNA *4*, 1268-1281.

de la Cruz, J., Kressler, D., Tollervey, D., and Linder, P. (1998b). Dob1p (Mtr4p) is a putative ATP-dependent RNA helicase required for the 3' end formation of 5.8S rRNA in *Saccharomyces cerevisiae*. EMBO J. *17*, 1128-1140.

Deisenroth, C., and Zhang, Y. (2010). Ribosome biogenesis surveillance: probing the ribosomal protein-Mdm2-p53 pathway. Oncogene *29*, 4253-4260.

DeLabre, M.L., Kessl, J., Karamanou, S., and Trumpower, B.L. (2002). *RPL29* codes for a non-essential protein of the 60S ribosomal subunit in *Saccharomyces cerevisiae* and exhibits synthetic lethality with mutations in genes for proteins required for subunit coupling. Biochim. Biophys. Acta *1574*, 255-261.

Doherty, L., Sheen, M.R., Vlachos, A., Choesmel, V., O'Donohue, M.F., Clinton, C., Schneider, H.E., Sieff, C.A., Newburger, P.E., Ball, S.E.*, et al.* (2010). Ribosomal protein genes RPS10 and RPS26 are commonly mutated in Diamond-Blackfan anemia. Am. J. Hum. Genet. *86*, 222-228.

Dresios, J., Derkatch, I.L., Liebman, S.W., and Synetos, D. (2000). Yeast ribosomal protein L24 affects the kinetics of protein synthesis and ribosomal protein L39 improves translational accuracy, while mutants lacking both remain viable. Biochemistry *39*, 7236-7244.

Ecker, D.J., Stadel, J.M., Butt, T.R., Marsh, J.A., Monia, B.P., Powers, D.A., Gorman, J.A., Clark, P.E., Warren, F., Shatzman, A.*, et al.* (1989). Increasing gene expression in yeast by fusion to ubiquitin. J. Biol. Chem. *264*, 7715-7719.

Eisinger, D.P., Dick, F.A., Denke, E., and Trumpower, B.L. (1997). *SQT1*, which encodes an essential WD domain protein of *Saccharomyces cerevisiae*, suppresses dominant-negative mutations of the ribosomal protein gene *QSR1*. Mol. Cell. Biol. *17*, 5146-5155.

Eppens, N.A., Rensen, S., Granneman, S., Raué, H.A., and Venema, J. (1999). The roles of Rrp5p in the synthesis of yeast 18S and 5.8S rRNA can be functionally and physically separated. RNA *5*, 779-793.

Espinar-Marchena, F.J., Babiano, R., and de la Cruz, J. (2017). Placeholder factors in ribosome biogenesis: please, pave my way. Microbial Cell *4*, 144-168.

Faber, A.W., Vos, H.R., Vos, J.C., and Raué, H.A. (2006). 5'-end formation of yeast $5.8S_L$ rRNA is an endonucleolytic event. Biochem. Biophys. Res. Commun. *345*, 796-802.

Fassio, C.A., Schofield, B.J., Seiser, R.M., Johnson, A.W., and Lycan, D.E. (2010). Dominant mutations in the late 40S biogenesis factor Ltv1 affect cytoplasmic maturation of the small ribosomal subunit in *Saccharomyces cerevisiae*. Genetics *185*, 199-209.

Fatica, A., Oeffinger, M., Dlakic, M., and Tollervey, D. (2003). Nob1p is required for cleavage of the 3' end of 18S rRNA. Mol. Cell. Biol. *23*, 1798-1807.

Fennell, L.M., Rahighi, S., and Ikeda, F. (2018). Linear ubiquitin chain-binding domains. FEBS J *285*, 2746-2761.

Fernández-Pevida, A., Kressler, D., and de la Cruz, J. (2015). Processing of preribosomal RNA in *Saccharomyces cerevisiae*. Wiley Interdiscip. Rev. RNA *6*, 191-209.

Fernández-Pevida, A., Martín-Villanueva, S., Murat, G., Lacombe, T., Kressler, D., and de la Cruz, J. (2016). The eukaryote-specific N-terminal extension of ribosomal protein S31 contributes to the assembly and function of 40S ribosomal subunits. Nucleic Acids Res. *44*, 7777-7791.

Fernández-Pevida, A., Rodríguez-Galán, O., Díaz-Quintana, A., Kressler, D., and de la Cruz, J. (2012). Yeast ribosomal protein L40 assembles late into precursor 60S ribosomes and is required for their cytoplasmic maturation. J. Biol. Chem. *287*, 38390-38407.

Ferreira-Cerca, S., Pöll, G., Gleizes, P.E., Tschochner, H., and Milkereit, P. (2005). Roles of eukaryotic ribosomal proteins in maturation and transport of pre-18S rRNA and ribosome function. Mol. Cell *20*, 263-275.

Ferreira-Cerca, S., Pöll, G., Kuhn, H., Neueder, A., Jakob, S., Tschochner, H., and Milkereit, P. (2007). Analysis of the *in vivo* assembly pathway of eukaryotic 40S ribosomal proteins. Mol. Cell *28*, 446-457.

Ferreira-Cerca, S., Sagar, V., Schafer, T., Diop, M., Wesseling, A.M., Lu, H., Chai, E., Hurt, E., and LaRonde-LeBlanc, N. (2012). ATPase-dependent role of the atypical kinase Rio2 on the evolving pre-40S ribosomal subunit. Nat Struct Mol Biol *19*, 1316-1323.

Finley, D., Bartel, B., and Varshavsky, A. (1989). The tails of ubiquitin precursors are ribosomal proteins whose fusion to ubiquitin facilitates ribosome biogenesis. Nature *338*, 394-401.

Finley, D., Özkaynak, E., and Varshavsky, A. (1987). The yeast polyubiquitin gene is essential for resistance to high temperatures, starvation, and other stresses. Cell *48*, 1035-1046.

Finley, D., Ulrich, H.D., Sommer, T., and Kaiser, P. (2012). The ubiquitin-proteasome system of Saccharomyces cerevisiae. Genetics *192*, 319-360.

Foiani, M., Cigan, A.M., Paddon, C.J., Harashima, S., and Hinnebusch, A.G. (1991). GCD2, a translational repressor of the *GCN4* gene, has a general function in the initiation of protein synthesis in *Saccharomyces cerevisiae*. Mol. Cell. Biol. *11*, 3203-3216.

Ford, C.L., Randal-Whitis, L., and Ellis, S.R. (1999). Yeast proteins related to the p40/laminin receptor precursor are required for 20S ribosomal RNA processing and the maturation of 40S ribosomal subunits. Cancer Res. *59*, 704-710.

Fraser, J., Luu, H.A., Neculcea, J., Thomas, D.Y., and Storms, R.K. (1991). Ubiquitin gene expression: response to environmental changes. Curr. Genet. *20*, 17-23.

Frey, S., Pool, M., and Seedorf, M. (2001). Scp160p, an RNA-binding, polysome-associated protein, localizes to the endoplasmic reticulum of *Saccharomyces cerevisiae* in a microtubule-dependent manner. J. Biol. Chem. *276*, 15905-15912.

Fromm, L., Falk, S., Flemming, D., Schuller, J.M., Thoms, M., Conti, E., and Hurt, E. (2017). Reconstitution of the complete pathway of ITS2 processing at the pre-ribosome. Nat Commun *8*, 1787.

García-Gómez, J.J., Fernández-Pevida, A., Lebaron, S., Rosado, I.V., Tollervey, D., Kressler, D., and de la Cruz, J. (2014). Final Pre-40S Maturation Depends on the Functional Integrity of the 60S Subunit Ribosomal Protein L3. PLoS Genet. *10*, e1004205.

Gasse, L., Flemming, D., and Hurt, E. (2015). Coordinated Ribosomal ITS2 RNA Processing by the Las1 Complex Integrating Endonuclease, Polynucleotide Kinase, and Exonuclease Activities. Mol Cell *60*, 808-815.

Gatti, M., Pinato, S., Maiolica, A., Rocchio, F., Prato, M.G., Aebersold, R., and Penengo, L. (2015). RNF168 promotes noncanonical K27 ubiquitination to signal DNA damage. Cell Rep *10*, 226-238.

Gazda, H.T., Sheen, M.R., Vlachos, A., Choesmel, V., O'Donohue, M.F., Schneider, H., Darras, N., Hasman, C., Sieff, C.A., Newburger, P.E.*, et al.* (2008). Ribosomal protein L5 and L11 mutations are associated with cleft palate and abnormal thumbs in Diamond-Blackfan anemia patients. Am. J. Hum. Genet. *83*, 769-780.

Gemayel, R., Yang, Y., Dzialo, M.C., Kominek, J., Vowinckel, J., Saels, V., Van Huffel, L., van der Zande, E., Ralser, M., Steensels, J.*, et al.* (2017). Variable repeats in the eukaryotic polyubiquitin gene ubi4 modulate proteostasis and stress survival. Nat Commun *8*, 397.

Genuth, N.R., and Barna, M. (2018). The Discovery of Ribosome Heterogeneity and Its Implications for Gene Regulation and Organismal Life. Mol Cell *71*, 364-374.

Ghalei, H., Schaub, F.X., Doherty, J.R., Noguchi, Y., Roush, W.R., Cleveland, J.L., Stroupe, M.E., and Karbstein, K. (2016). Hrr25/CK1δ-directed release of Ltv1 from pre-40S ribosomes is necessary for ribosome assembly and cell growth. J. Cell Biol. *208*, 745-759.

Ghalei, H., Trepreau, J., Collins, J.C., Bhaskaran, H., Strunk, B.S., and Karbstein, K. (2017). The ATPase Fap7 Tests the Ability to Carry Out Translocation-like Conformational Changes and Releases Dim1 during 40S Ribosome Maturation. Mol. Cell *67*, 990-1000.e1003.

Giaever, G., Chu, A.M., Ni, L., Connelly, C., Riles, L., Veronneau, S., Dow, S., Lucau-Danila, A., Anderson, K., Andre, B.*, et al.* (2002). Functional profiling of the *Saccharomyces cerevisiae* genome. Nature *418*, 387-391.

Gietz, D., St. Jean, A., Woods, R.A., and Schiestl, R.H. (1992). Improved method for high efficiency transformation of intact yeast cells. Nucleic Acids Res. *20*, 1425.

Gietz, R.D., and Sugino, A. (1988). New yeast-*Escherichia coli* shuttle vectors constructed with *in vitro* mutagenized yeast genes lacking six-base pair restriction sites. Gene *74*, 527-534.

Goldstein, G., Scheid, M., Hammerling, U., Schlesinger, D.H., Niall, H.D., and Boyse, E.A. (1975). Isolation of a polypeptide that has lymphocyte-differentiating properties and is probably represented universally in living cells. Proc Natl Acad Sci U S A *72*, 11-15.

Graciet, E., Hu, R.G., Piatkov, K., Rhee, J.H., Schwarz, E.M., and Varshavsky, A. (2006). Aminoacyl-transferases and the N-end rule pathway of prokaryotic/eukaryotic specificity in a human pathogen. Proc. Natl. Acad. Sci. U. S. A. *103*, 3078-3083.

Granneman, S., Nandineni, M.R., and Baserga, S.J. (2005). The putative NTPase Fap7 mediates cytoplasmic 20S pre-rRNA processing through a direct interaction with Rps14. Mol. Cell. Biol. *25*, 10352-10364.

Granneman, S., Petfalski, E., and Tollervey, D. (2011). A cluster of ribosome synthesis factors regulate pre-rRNA folding and 5.8S rRNA maturation by the Rat1 exonuclease. EMBO J. *30*, 4006-4019.

Greber, B.J., Gerhardy, S., Leitner, A., Leibundgut, M., Salem, M., Boehringer, D., Leulliot, N., Aebersold, R., Panse, V.G., and Ban, N. (2016). Insertion of the biogenesis factor Rei1 probes the ribosomal tunnel during 60S maturation. Cell *164*, 91-102.

Grosshans, H., Hurt, E., and Simos, G. (2000). An aminoacylation-dependent nuclear tRNA export pathway in yeast. Genes Dev. *14*, 830-840.

Grou, C.P., Pinto, M.P., Mendes, A.V., Domingues, P., and Azevedo, J.E. (2015). The *de novo* synthesis of ubiquitin: identification of deubiquitinases acting on ubiquitin precursors. Sci. Rep. *5*, 12836.

Grousl, T., Ivanov, P., Frydlova, I., Vasicova, P., Janda, F., Vojtova, J., Malinska, K., Malcova, I., Novakova, L., Janoskova, D*., et al.* (2009). Robust heat shock induces eIF2alpha-phosphorylation-independent assembly of stress granules containing eIF3 and 40S ribosomal subunits in budding yeast, Saccharomyces cerevisiae. J. Cell Sci. *122*, 2078-2088.

Heuer, A., Thomson, E., Schmidt, C., Berninghausen, O., Becker, T., Hurt, E., and Beckmann, R. (2017). Cryo-EM structure of a late pre-40S ribosomal subunit from Saccharomyces cerevisiae. Elife *6*.

Hierlmeier, T., Merl, J., Sauert, M., Perez-Fernandez, J., Schultz, P., Bruckmann, A., Hamperl, S., Ohmayer, U., Rachel, R., Jacob, A.*, et al.* (2012). Rrp5p, Noc1p and Noc2p form a protein module which is part of early large ribosomal subunit precursors in S. cerevisiae. Nucleic Acids Res. *41*, 1191-1210.

Hochstrasser, M. (2000). Evolution and function of ubiquitin-like protein-conjugation systems. Nat. Cell Biol. *2*, E153-157.

Hughes, J.M.X., and Ares, M., Jr. (1991). Depletion of U3 small nucleolar RNA inhibits cleavage in the 5' external transcribed spacer of yeast pre-ribosomal RNA and impairs formation of 18S ribosomal RNA. EMBO J. *10*, 4231-4239.

Hunziker, M., Barandun, J., Petfalski, E., Tan, D., Delan-Forino, C., Molloy, K.R., Kim, K.H., Dunn-Davies, H., Shi, Y., Chaker-Margot, M.*, et al.* (2016). UtpA and UtpB chaperone nascent pre-ribosomal RNA and U3 snoRNA to initiate eukaryotic ribosome assembly. Nat. Commun. *7*, 12090.

Hurt, E., Hannus, S., Schmelzl, B., Lau, D., Tollervey, D., and Simos, G. (1999). A novel *in vivo* assay reveals inhibition of ribosomal nuclear export in Ran-cycle and nucleoporin mutants. J. Cell Biol. *144*, 389-401.

Ichimura, Y., Kirisako, T., Takao, T., Satomi, Y., Shimonishi, Y., Ishihara, N., Mizushima, N., Tanida, I., Kominami, E., Ohsumi, M.*, et al.* (2000). A ubiquitin-like system mediates protein lipidation. Nature *408*, 488-492.

Ide, S., Miyazaki, T., Maki, H., and Kobayashi, T. (2010). Abundance of ribosomal RNA gene copies maintains genome integrity. Science *327*, 693-696.

Iyer, L.M., Burroughs, A.M., and Aravind, L. (2006). The prokaryotic antecedents of the ubiquitin-signaling system and the early evolution of ubiquitin-like beta-grasp domains. Genome Biol. *7*, R60.

Jäkel, S., Mingot, J.M., Schwarzmaier, P., Hartmann, E., and Görlich, D. (2002). Importins fulfil a dual function as nuclear import receptors and cytoplasmic chaperones for exposed basic domains. EMBO J. *21*, 377-386.

Jakovljevic, J., de Mayolo, P.A., Miles, T.D., Nguyen, T.M., Léger-Silvestre, I., Gas, N., and Woolford, J.L., Jr. (2004). The carboxy-terminal extension of yeast ribosomal protein S14 is necessary for maturation of 43S preribosomes. Mol. Cell *14*, 331-342.



Ji, C.H., and Kwon, Y.T. (2017). Crosstalk and Interplay between the Ubiquitin-Proteasome System and Autophagy. Mol Cells *40*, 441-449.

Johnson, E.S. (2004). Protein modification by SUMO. Annu. Rev. Biochem. *73*, 355-382.

Johnson, M.C., Ghalei, H., Doxtader, K.A., Karbstein, K., and Stroupe, M.E. (2017). Structural heterogeneity in pre-40S ribosomes. Structure *25*, 329-340.

Jones, D., and Candido, E.P. (1993). Novel ubiquitin-like ribosomal protein fusion genes from the nematodes Caenorhabditis elegans and Caenorhabditis briggsae. J Biol Chem *268*, 19545-19551.

Joret, C., Capeyrou, R., Belhabich-Baumas, K., Plisson-Chastang, C., Ghandour, R., Humbert, O., Fribourg, S., Leulliot, N., Lebaron, S., Henras, A.K*., et al.* (2018). The Npa1p complex chaperones the assembly of the earliest eukaryotic large ribosomal subunit precursor. PLoS Genet. *14*, e1007597.

Kaiser, C., Michaelis, S., and Mitchell, A. (1994). Methods in yeast genetics: a Cold Spring Harbor Laboratory Course Manual (Cold Spring Harbor, N. Y.: Cold Spring Harbor Laboratory Press).

Kappel, L., Loibl, M., Zisser, G., Klein, I., Fruhmann, G., Gruber, C., Unterweger, S., Rechberger, G., Pertschy, B., and Bergler, H. (2012). Rlp24 activates the AAA-ATPase Drg1 to initiate cytoplasmic pre-60S maturation. J. Cell Biol. *199*, 771-782.

Kater, L., Thoms, M., Barrio-García, C., Cheng, J., Ismail, S., Ahmed, Y.L., Bange, G., Kressler, D., Berninghausen, O., Sinning, I.*, et al.* (2017). Visualizing the assembly pathway of nucleolar pre-60S ribosomes. Cell *171*, 1599-1610 e1514.

Keeling, K.M., Lanier, J., Du, M., Salas-Marco, J., Gao, L., Kaenjak-Angeletti, A., and Bedwell, D.M. (2004). Leaky termination at premature stop codons antagonizes nonsense-mediated mRNA decay in S. cerevisiae. RNA *10*, 691-703.

Kellis, M., Birren, B.W., and Lander, E.S. (2004). Proof and evolutionary analysis of ancient genome duplication in the yeast Saccharomyces cerevisiae. Nature *428*, 617-624.

Klinge, S., Voigts-Hoffmann, F., Leibundgut, M., Arpagaus, S., and Ban, N. (2011). Crystal structure of the eukaryotic 60S ribosomal subunit in complex with initiation factor 6. Science *334*, 941-948.

Klinge, S., Voigts-Hoffmann, F., Leibundgut, M., and Ban, N. (2012). Atomic structures of the eukaryotic ribosome. Trends Biochem. Sci. *37*, 189-198.

Klinge, S., and Woolford, J.L., Jr. (2019). Ribosome assembly coming into focus. Nat Rev Mol Cell Biol *20*, 116-131.

Klockner, C., Schneider, M., Lutz, S., Jani, D., Kressler, D., Stewart, M., Hurt, E., and Kohler, A. (2009). Mutational uncoupling of the role of Sus1 in nuclear pore complex targeting of an mRNA export complex and histone H2B deubiquitination. J. Biol. Chem. *284*, 12049-12056.

Kobayashi, M., Oshima, S., Maeyashiki, C., Nibe, Y., Otsubo, K., Matsuzawa, Y., Nemoto, Y., Nagaishi, T., Okamoto, R., Tsuchiya, K.*, et al.* (2016). The ubiquitin hybrid gene UBA52 regulates ubiquitination of ribosome and sustains embryonic development. Sci. Rep. *6*, 36780.

Koch, B., Mitterer, V., Niederhauser, J., Stanborough, T., Murat, G., Rechberger, G., Bergler, H., Kressler, D., and Pertschy, B. (2012). Yar1 protects the ribosomal protein Rps3 from aggregation. J. Biol. Chem. *287*, 21806-21815.

Koplin, A., Preissler, S., Ilina, Y., Koch, M., Scior, A., Erhardt, M., and Deuerling, E. (2010). A dual function for chaperones SSB-RAC and the NAC nascent polypeptide-associated complex on ribosomes. J. Cell Biol. *189*, 57-68.

Kornprobst, M., Turk, M., Kellner, N., Cheng, J., Flemming, D., Kos-Braun, I., Kos, M., Thoms, M., Berninghausen, O., Beckmann, R*., et al.* (2016). Architecture of the 90S Pre-ribosome: A Structural View on the Birth of the Eukaryotic Ribosome. Cell *166*, 380-393.

Koš, M., and Tollervey, D. (2010). Yeast pre-rRNA processing and modification occur cotranscriptionally. Mol. Cell *37*, 809-820.

Kos-Braun, I.C., Jung, I., and Koš, M. (2016). Tor1 and CK2 kinases control a switch between alternative ribosome biogenesis pathways in a growth-dependent manner. PLoS Biol. *15*, e2000245.

Kraft, C., Deplazes, A., Sohrmann, M., and Peter, M. (2008). Mature ribosomes are selectively degraded upon starvation by an autophagy pathway requiring the Ubp3p/Bre5p ubiquitin protease. Nat. Cell Biol. *10*, 602-610.

Krebber, H., Wostmann, C., and Bakker-Grunwald, T. (1994). Evidence for the existence of a single ubiquitin gene in Giardia lamblia. FEBS Lett *343*, 234-236.

Kressler, D., Bange, G., Ogawa, Y., Stjepanovic, G., Bradatsch, B., Pratte, D., Amlacher, S., Strauss, D., Yoneda, Y., Katahira, J*., et al.* (2012). Synchronizing nuclear import of ribosomal proteins with ribosome assembly. Science *338*, 666-671.

Kressler, D., de la Cruz, J., Rojo, M., and Linder, P. (1997). Fal1p is an essential DEAD-box protein involved in 40S-ribosomal-subunit biogenesis in *Saccharomyces cerevisiae*. Mol. Cell. Biol. *17*, 7283-7294.

Kressler, D., de la Cruz, J., Rojo, M., and Linder, P. (1998). Dbp6p is an essential putative ATP-dependent RNA helicase required for 60S-ribosomal-subunit assembly in *Saccharomyces cerevisiae*. Mol. Cell. Biol. *18*, 1855-1865.

Kressler, D., Hurt, E., and Bassler, J. (2010). Driving ribosome assembly. Biochim. Biophys. Acta *1803*, 673-683.

Kressler, D., Hurt, E., and Bassler, J. (2017). A puzzle of life: crafting ribosomal subunits. Trends Biochem. Sci. *42*, 640-654.

Kruiswijk, T., Planta, R.J., and Krop, J.M. (1978). The course of the assembly of ribosomal subunits in yeast. Biochim. Biophys. Acta *517*, 378-389.

Kwon, Y.T., and Ciechanover, A. (2017). The Ubiquitin Code in the Ubiquitin-Proteasome System and Autophagy. Trends Biochem. Sci. *42*, 873-886.

Lacombe, T., García-Gómez, J.J., de la Cruz, J., Roser, D., Hurt, E., Linder, P., and Kressler, D. (2009). Linear ubiquitin fusion to Rps31 and its subsequent cleavage are required for the efficient production and functional integrity of 40S ribosomal subunits. Mol. Microbiol. *72*, 69-84.

Lam, Y.W., Lamond, A.I., Mann, M., and Andersen, J.S. (2007). Analysis of nucleolar protein dynamics reveals the nuclear degradation of ribosomal proteins. Curr. Biol. *17*, 749-760.

Lebaron, S., Schneider, C., van Nues, R.W., Swiatkowska, A., Walsh, D., Bottcher, B., Granneman, S., Watkins, N.J., and Tollervey, D. (2012). Proofreading of pre-40S ribosome maturation by a translation initiation factor and 60S subunits. Nat. Struct. Mol. Biol. *19*, 744-753.

Lecompte, O., Ripp, R., Thierry, J.C., Moras, D., and Poch, O. (2002). Comparative analysis of ribosomal proteins in complete genomes: an example of reductive evolution at the domain scale. Nucleic Acids Res. *30*, 5382-5390.

Lee, C.D., Sun, H.C., Hu, S.M., Chiu, C.F., Homhuan, A., Liang, S.M., Leng, C.H., and Wang, T.F. (2008). An improved SUMO fusion protein system for effective production of native proteins. Protein Sci. *17*, 1241-1248.



Leidig, C., Bange, G., Kopp, J., Amlacher, S., Aravind, A., Wickles, S., Witte, G., Hurt, E., Beckmann, R., and Sinning, I. (2013). Structural characterization of a eukaryotic chaperone--the ribosome-associated complex. Nat Struct Mol Biol *20*, 23-28.

Leidig, C., Thoms, M., Holdermann, I., Bradatsch, B., Berninghausen, O., Bange, G., Sinning, I., Hurt, E., and Beckmann, R. (2014). 60S ribosome biogenesis requires rotation of the 5S ribonucleoprotein particle. Nat. Commun. *5*, 3491.

Loibl, M., Klein, I., Prattes, M., Schmidt, C., Kappel, L., Zisser, G., Gungl, A., Krieger, E., Pertschy, B., and Bergler, H. (2014). The drug diazaborine blocks ribosome biogenesis by inhibiting the AAA-ATPase Drg1. J. Biol. Chem. *289*, 3913-3922.

Ma, C., Wu, S., Li, N., Chen, Y., Yan, K., Li, Z., Zheng, L., Lei, J., Woolford, J.L., Jr., and Gao, N. (2017). Structural snapshot of cytoplasmic pre-60S ribosomal particles bound by Nmd3, Lsg1, Tif6 and Reh1. Nat. Struct. Mol. Biol. *24*, 214-220.

MacDiarmid, C.W., Taggart, J., Jeong, J., Kerdsomboon, K., and Eide, D.J. (2016). Activation of the Yeast UBI4 Polyubiquitin Gene by Zap1 Transcription Factor via an Intragenic Promoter Is Critical for Zinc-deficient Growth. J. Biol. Chem. *291*, 18880-18896.

Maicas, E., Pluthero, F.G., and Friesen, J.D. (1988). The accumulation of three yeast ribosomal proteins under conditions of excess mRNA is determined primarily by fast protein decay. Mol. Cell. Biol. *8*, 169-175.

Marblestone, J.G., Edavettal, S.C., Lim, Y., Lim, P., Zuo, X., and Butt, T.R. (2006). Comparison of SUMO fusion technology with traditional gene fusion systems: enhanced expression and solubility with SUMO. Protein Sci. *15*, 182-189.

Martín-Villanueva, S., Fernández-Pevida, A., Fernández-Fernández, J., Kressler, D., and de la Cruz, J. (2019). Ubiquitin release from eL40 is required for cytoplasmic maturation and function of 60S ribosomal subunits in *Saccharomyces cerevisiae*. FEBS J.

Matsuo, Y., Granneman, S., Thoms, M., Manikas, R.G., Tollervey, D., and Hurt, E. (2014). Coupled GTPase and remodelling ATPase activities form a checkpoint for ribosome export. Nature *505*, 112-116.

Mazumder, B., Sampath, P., Seshadri, V., Maitra, R.K., DiCorleto, P.E., and Fox, P.L. (2003). Regulated release of L13a from the 60S ribosomal subunit as a mechanism of transcript-specific translational control. Cell *115*, 187-198.

McCaughan, U.M., Jayachandran, U., Shchepachev, V., Chen, Z.A., Rappsilber, J., Tollervey, D., and Cook, A.G. (2016). Pre-40S ribosome biogenesis factor Tsr1 is an inactive structural mimic of translational GTPases. Nat. Commun. *7*, 11789.

Melnikov, S., Ben-Shem, A., Garreau de Loubresse, N., Jenner, L., Yusupova, G., and Yusupov, M. (2012). One core, two shells: bacterial and eukaryotic ribosomes. Nat. Struct. Mol. Biol. *19*, 560-567.

Melnikov, S., Manakongtreecheep, K., and Soll, D. (2018). Revising the Structural Diversity of Ribosomal Proteins Across the Three Domains of Life. Mol Biol Evol *35*, 1588-1598.

Merwin, J.R., Bogar, L.B., Poggi, S.B., Fitch, R.M., Johnson, A.W., and Lycan, D.E. (2014). Genetic analysis of the ribosome biogenesis factor Ltv1 of *Saccharomyces cerevisiae*. Genetics *198*, 1071-1085.

Mevissen, T.E.T., and Komander, D. (2017). Mechanisms of Deubiquitinase Specificity and Regulation. Annu Rev Biochem *86*, 159-192.

Miles, T.D., Jakovljevic, J., Horsey, E.W., Harnpicharnchai, P., Tang, L., and Woolford, J.L., Jr. (2005). Ytm1, Nop7, and Erb1 form a complex necessary for maturation of yeast 66S preribosomes. Mol. Cell. Biol. *25*, 10419-10432.

Mitterer, V., Murat, G., Rety, S., Blaud, M., Delbos, L., Stanborough, T., Bergler, H., Leulliot, N., Kressler, D., and Pertschy, B. (2016). Sequential domain assembly of ribosomal protein S3 drives 40S subunit maturation. Nat. Commun. *7*, 10336.

Moriggi, G., Nieto, B., and Dosil, M. (2015). Rrp12 and the Exportin Crm1 participate in late assembly events in the nucleolus during 40S ribosomal subunit biogenesis. PLoS Genet. *10*, e1004836.

Muller, S., Hoege, C., Pyrowolakis, G., and Jentsch, S. (2001). SUMO, ubiquitin's mysterious cousin. Nat. Rev. Mol. Cell. Biol. *2*, 202-210.

Narla, A., and Ebert, B.L. (2010). Ribosomopathies: human disorders of ribosome dysfunction. Blood *115*, 3196-3205.

Nie, M., and Boddy, M.N. (2016). Cooperativity of the SUMO and Ubiquitin Pathways in Genome Stability. Biomolecules *6*, 14.

Nomura, M., Nogi, Y., and Oakes, M. (2004). Transcription of rDNA in the yeast *Saccharomyces cerevisiae*. In Nucleolus, M.O.J. Olson, ed. (Georgetown: Landes Bioscience/Eurekah.com), pp. 128-153.

O'Donohue, M.F., Choesmel, V., Faubladier, M., Fichant, G., and Gleizes, P.E. (2010). Functional dichotomy of ribosomal proteins during the synthesis of mammalian 40S ribosomal subunits. J. Cell Biol. *190*, 853-866.

Ohtake, F., and Tsuchiya, H. (2017). The emerging complexity of ubiquitin architecture. J Biochem *161*, 125-133.

Özkaynak, E., Finley, D., Solomon, M.J., and Varshavsky, A. (1987). The yeast ubiquitin genes: a family of natural gene fusions. EMBO J. *6*, 1429-1439.

Panasenko, O.O., and Collart, M.A. (2012). Presence of Not5 and ubiquitinated Rps7A in polysome fractions depends upon the Not4 E3 ligase. Mol. Microbiol. *83*, 640-653.

Pausch, P., Singh, U., Ahmed, Y.L., Pillet, B., Murat, G., Altegoer, F., Stier, G., Thoms, M., Hurt, E., Sinning, I.*, et al.* (2015). Co-translational capturing of nascent ribosomal proteins by their dedicated chaperones. Nat. Commun. *6*, 7494.

Peng, J., Schwartz, D., Elias, J.E., Thoreen, C.C., Cheng, D., Marsischky, G., Roelofs, J., Finley, D., and Gygi, S.P. (2003). A proteomics approach to understanding protein ubiquitination. Nat Biotechnol *21*, 921-926.

Peña, C., Hurt, E., and Panse, V.G. (2017). Eukaryotic ribosome assembly, transport and quality control. Nat. Struct. Mol. Biol. *24*, 689-699.

Peña, C., Schütz, S., Fischer, U., Chang, Y., and Panse, V.G. (2016). Prefabrication of a ribosomal protein subcomplex essential for eukaryotic ribosome formation. eLife *5*, e21755.

Pérez-Fernández, J., Román, A., de las Rivas, J., Bustelo, X.R., and Dosil, M. (2007). The 90S preribosome is a multimodular structure that is assembled through a hierarchical mechanism. Mol. Cell. Biol. *27*, 5414-5429.

Peroutka Iii, R.J., Orcutt, S.J., Strickler, J.E., and Butt, T.R. (2011). SUMO fusion technology for enhanced protein expression and purification in prokaryotes and eukaryotes. Methods Mol. Biol. *705*, 15-30.

Pertschy, B., Schneider, C., Gnadig, M., Schafer, T., Tollervey, D., and Hurt, E. (2009). RNA helicase Prp43 and its co-factor Pfa1 promote 20 to 18 S rRNA processing catalyzed by the endonuclease Nob1. J. Biol. Chem. *284*, 35079-35091.

Pickart, C.M. (2001). Mechanisms underlying ubiquitination. Annu. Rev. Biochem. *70*, 503-533.

Pickart, C.M., and Eddins, M.J. (2004). Ubiquitin: structures, functions, mechanisms. Biochim Biophys Acta *1695*, 55-72.



Pillet, B., García-Gómez, J.J., Pausch, P., Falquet, L., Bange, G., de la Cruz, J., and Kressler, D. (2015). The dedicated chaperone Acl4 escorts ribosomal protein Rpl4 to its nuclear pre-60S assembly site. PLoS Genet. *11*, e1005565.

Pillet, B., Mitterer, V., Kressler, D., and Pertschy, B. (2017). Hold on to your friends: Dedicated chaperones of ribosomal proteins: Dedicated chaperones mediate the safe transfer of ribosomal proteins to their site of pre-ribosome incorporation. Bioessays *39*, 1-12.

Rabl, J., Leibundgut, M., Ataide, S.F., Haag, A., and Ban, N. (2011). Crystal structure of the eukaryotic 40S ribosomal subunit in complex with initiation factor 1. Science *331*, 730-736.

Rodríguez-Galán, O., García-Gómez, J.J., and de la Cruz, J. (2013). Yeast and human RNA helicases involved in ribosome biogenesis: current status and perspectives. Biochim. Biophys. Acta-Gene Regulatory Mechanisms *1829*, 775-790.

Rodríguez-Galán, O., García-Gómez, J.J., Kressler, D., and de la Cruz, J. (2015). Immature large ribosomal subunits containing the 7S pre-rRNA can engage in translation in *Saccharomyces cerevisiae*. RNA Biol. *12*, 838-846.

Rosado, I.V., Dez, C., Lebaron, S., Caizergues-Ferrer, M., Henry, Y., and de la Cruz, J. (2007). Characterization of *Saccharomyces cerevisiae* Npa2p (Urb2p) reveals a low-

molecular-mass complex containing Dbp6p, Npa1p (Urb1p), Nop8p, and Rsa3p involved in early steps of 60S ribosomal subunit biogenesis. Mol. Cell. Biol. *27*, 1207-1221.

Rout, M.P., Blobel, G., and Aitchison, J.D. (1997). A distinct nuclear import pathway used by ribosomal proteins. Cell *89*, 715-725.

Salas-Marco, J., and Bedwell, D.M. (2005). Discrimination between defects in elongation fidelity and termination efficiency provides mechanistic insights into translational readthrough. J. Mol. Biol. *348*, 801-815.

Sambrook, J., Fritsch, E.F., and Maniatis, T. (1989). Molecular cloning: a laboratory manual, 2nd edn (Cold Spring Harbor, N. Y.: Cold Spring Harbor Laboratory Press).

Sarkar, A., Pech, M., Thoms, M., Beckmann, R., and Hurt, E. (2016). Ribosome-stalk biogenesis is coupled with recruitment of nuclear-export factor to the nascent 60S subunit. Nat. Struct. Mol. Biol. *23*, 1074-1082.

Scaiola, A., Pena, C., Weisser, M., Bohringer, D., Leibundgut, M., Klingauf-Nerurkar, P., Gerhardy, S., Panse, V.G., and Ban, N. (2018). Structure of a eukaryotic cytoplasmic pre-40S ribosomal subunit. EMBO J *37*.

Schäfer, T., Maco, B., Petfalski, E., Tollervey, D., Bottcher, B., Aebi, U., and Hurt, E. (2006). Hrr25-dependent phosphorylation state regulates organization of the pre-40S subunit. Nature *441*, 651-655.

Schäfer, T., Strauss, D., Petfalski, E., Tollervey, D., and Hurt, E. (2003). The path from nucleolar 90S to cytoplasmic 40S pre-ribosomes. EMBO J. *22*, 1370-1380.

Schmeing, T.M., and Ramakrishnan, V. (2009). What recent ribosome structures have revealed about the mechanism of translation. Nature *461*, 1234-1242.

Schütz, S., Fischer, U., Altvater, M., Nerurkar, P., Pena, C., Gerber, M., Chang, Y., Caesar, S., Schubert, O.T., Schlenstedt, G.*, et al.* (2014). A RanGTP-independent mechanism allows ribosomal protein nuclear import for ribosome assembly. eLife *3*, e03473.

Seiser, R.M., Sundberg, A.E., Wollam, B.J., Zobel-Thropp, P., Baldwin, K., Spector, M.D., and Lycan, D.E. (2006). Ltv1 is required for efficient nuclear export of the ribosomal small subunit in Saccharomyces cerevisiae. Genetics *174*, 679-691.



Sengupta, J., Bussiere, C., Pallesen, J., West, M., Johnson, A.W., and Frank, J. (2010). Characterization of the nuclear export adaptor protein Nmd3 in association with the 60S ribosomal subunit. J. Cell Biol. *189*, 1079-1086.

Sharma, S., and Lafontaine, D.L. (2015). 'View From A Bridge': A New Perspective on Eukaryotic rRNA Base Modification. Trends Biochem. Sci. *40*, 560-575.

Sibbald, S.J., Hopkins, J.F., Filloramo, G.V., and Archibald, J.M. (2019). Ubiquitin fusion proteins in algae: implications for cell biology and the spread of photosynthesis. BMC Genomics *20*, 38.

Sikorski, R.S., and Hieter, P. (1989). A system of shuttle vectors and yeast host strains designed for efficient manipulation of DNA in *Saccharomyces cerevisiae*. Genetics *122*, 19-27.

Simon, J.R., Treger, J.M., and McEntee, K. (1999). Multiple independent regulatory pathways control UBI4 expression after heat shock in Saccharomyces cerevisiae. Mol Microbiol *31*, 823-832.

Soudet, J., Gelugne, J.P., Belhabich-Baumas, K., Caizergues-Ferrer, M., and Mougin, A. (2010). Immature small ribosomal subunits can engage in translation initiation in *Saccharomyces cerevisiae*. EMBO J. *29*, 80-92.

Steffen, K.K., McCormick, M.A., Pham, K.M., Mackay, V.L., Delaney, J.R., Murakami, C.J., Kaeberlein, M., and Kennedy, B.K. (2012). Ribosome deficiency protects against ER stress in *Saccharomyces cerevisiae*. Genetics *191*, 107-118.

Strunk, B.S., Loucks, C.R., Su, M., Vashisth, H., Cheng, S., Schilling, J., Brooks, C.L., III., Karbstein, K., and Skiniotis, G. (2011). Ribosome assembly factors prevent premature translation initiation by 40S assembly intermediates. Science *333*, 1449-1453.

Strunk, B.S., Novak, M.N., Young, C.L., and Karbstein, K. (2012). A translation-like cycle is a quality control checkpoint for maturing 40S ribosome subunits. Cell *150*, 111-121.

Sun, Q., Zhu, X., Qi, J., An, W., Lan, P., Tan, D., Chen, R., Wang, B., Zheng, S., Zhang, C*., et al.* (2017). Molecular architecture of the 90S small subunit pre-ribosome. eLife *6*.

Sung, M.K., Porras-Yakushi, T.R., Reitsma, J.M., Huber, F.M., Sweredoski, M.J., Hoelz, A., Hess, S., and Deshaies, R.J. (2016a). A conserved quality-control pathway that mediates degradation of unassembled ribosomal proteins. eLife *5*, e19105.

Sung, M.K., Reitsma, J.M., Sweredoski, M.J., Hess, S., and Deshaies, R.J. (2016b). Ribosomal proteins produced in excess are degraded by the ubiquitin-proteasome system. Mol. Biol. Cell *27*, 2642-2652.

Swindle, J., Ajioka, J., Eisen, H., Sanwal, B., Jacquemot, C., Browder, Z., and Buck, G. (1988). The genomic organization and transcription of the ubiquitin genes of Trypanosoma cruzi. EMBO J *7*, 1121-1127.

Sykes, M.T., and Williamson, J.R. (2009). A complex assembly landscape for the 30S ribosomal subunit. Annu. Rev. Biophys. *38*, 197-215.

Synetos, D., Frantziou, C.P., and Alksne, L.E. (1996). Mutations in yeast ribosomal proteins S28 and S4 affect the accuracy of translation and alter the sensitivity of the ribosomes to paromomycin. Biochim. Biophys. Acta *1309*, 156-166.

Tabb, A.L., Utsugi, T., Wooten-Kee, C.R., Sasaki, T., Edling, S.A., Gump, W., Kikuchi, Y., and Ellis, S.R. (2001). Genes encoding ribosomal proteins Rps0A/B of *Saccharomyces cerevisiae* interact with *TOM1* mutants defective in ribosome synthesis. Genetics *157*, 1107-1116.

Teng, T., Thomas, G., and Mercer, C.A. (2013). Growth control and ribosomopathies. Curr. Opin. Genet. Dev. *23*, 63-71.

Thomas, B.J., and Rothstein, R. (1989). Elevated recombination rates in transcriptionally active DNA. Cell *56*, 619-630.

Thoms, M., Thomson, E., Bassler, J., Gnadig, M., Griesel, S., and Hurt, E. (2015). The Exosome Is Recruited to RNA Substrates through Specific Adaptor Proteins. Cell *162*, 1029-1038.

Thomson, E., and Tollervey, D. (2010). The final step in 5.8S rRNA processing is cytoplasmic in *Saccharomyces cerevisiae*. Mol. Cell. Biol. *30*, 976-984.

Trapman, J., and Planta, R.J. (1976). Maturation of ribosomes in yeast. I. Kinetic analysis by labelling of high molecular weight rRNA species. Biochim. Biophys. Acta *442*, 265-274.

Treger, J.M., Heichman, K.A., and McEntee, K. (1988). Expression of the yeast *UB14* gene increases in response to DNA-damaging agents and in meiosis. Mol. Cell. Biol. *8*, 1132-1136.

Tye, B.W., Commins, N., Ryazanova, L.V., Wuhr, M., Springer, M., Pincus, D., and Churchman, L.S. (2019). Proteotoxicity from aberrant ribosome biogenesis compromises cell fitness. Elife *8*.

Udem, S.A., and Warner, J.R. (1973). The cytoplasmic maturation of a ribosomal precursor ribonucleic acid in yeast. J. Biol. Chem. *248*, 1412-1416.

Ulbrich, C., Diepholz, M., Bassler, J., Kressler, D., Pertschy, B., Galani, K., Bottcher, B., and Hurt, E. (2009). Mechanochemical removal of ribosome biogenesis factors from nascent 60S ribosomal subunits. Cell *138*, 911-922.

van der Veen, A.G., and Ploegh, H.L. (2012). Ubiquitin-like proteins. Annu. Rev. Biochem. *81*, 323-357.

Varshavsky, A. (2012). The ubiquitin system, an immense realm. Annu Rev Biochem *81*, 167-176.

Venema, J., Planta, R.J., and Raué, H.A. (1998). *In vivo* mutational analysis of ribosomal RNA in *Saccharomyces cerevisiae*. In Protein synthesis: Methods and Protocols, R. Martin, ed. (Totowa, N. J.: Humana Press), pp. 257-270.

Vilardell, J., and Warner, J.R. (1997). Ribosomal protein L32 of *Saccharomyces cerevisiae* influences both the splicing of its own transcript and the processing of rRNA. Mol. Cell. Biol. *17*, 1959-1965.

Wang, F., Liu, M., Qiu, R., and Ji, C. (2011). The dual role of ubiquitin-like protein Urm1 as a protein modifier and sulfur carrier. Protein Cell *2*, 612-619.

Warner, J.R. (1999). The economics of ribosome biosynthesis in yeast. Trends Biochem. Sci. *24*, 437-440.

Warner, J.R., Mitra, G., Schwindinger, W.F., Studeny, M., and Fried, H.M. (1985). *Saccharomyces cerevisiae* coordinates accumulation of yeast ribosomal proteins by modulating mRNA splicing, translational initiation, and protein turnover. Mol. Cell. Biol. *5*, 1512-1521.

Wawiorka, L., Molestak, E., Szajwaj, M., Michalec-Wawiorka, B., Molon, M., Borkiewicz, L., Grela, P., Boguszewska, A., and Tchorzewski, M. (2017). Multiplication of Ribosomal P-Stalk Proteins Contributes to the Fidelity of Translation. Mol. Cell. Biol. *37*.

Wells, G.R., Weichmann, F., Colvin, D., Sloan, K.E., Kudla, G., Tollervey, D., Watkins, N.J., and Schneider, C. (2016). The PIN domain endonuclease Utp24 cleaves pre-ribosomal RNA at two coupled sites in yeast and humans. Nucleic Acids Res *44*, 5399-5409.

Wilson, D.N., and Doudna Cate, J.H. (2012). The structure and function of the eukaryotic ribosome. Cold Spring Harb. Perspect. Biol. *4*, a011536.



Wilson, V.G. (2017). Introduction to Sumoylation. Adv Exp Med Biol *963*, 1-12.

Woodson, S.A. (2008). RNA folding and ribosome assembly. Curr. Opin. Chem. Biol. *12*, 667-673.

Wool, I.G. (1979). The structure and function of eukaryotic ribosomes. Annu. Rev. Biochem. *48*, 719-754.

Woolford, J.L., Jr., and Baserga, S.J. (2013). Ribosome biogenesis in the yeast *Saccharomyces cerevisiae*. Genetics *195*, 643-681.

Wostmann, C., Liakopoulos, D., Ciechanover, A., and Bakker-Grunwald, T. (1996). Characterization of ubiquitin genes and -transcripts and demonstration of a ubiquitin-conjugating system in Entamoeba histolytica. Mol Biochem Parasitol *82*, 81-90.

Wu, S., Tutuncuoglu, B., Yan, K., Brown, H., Zhang, Y., Tan, D., Gamalinda, M., Yuan, Y., Li, Z., Jakovljevic, J.*, et al.* (2016). Diverse roles of assembly factors revealed by structures of late nuclear pre-60S ribosomes. Nature *534*, 133-137.

Yaffe, M.P., and Schatz, G. (1984). Two nuclear mutations that block mitochondrial protein import in yeast. Proc Natl Acad Sci U S A *81*, 4819-4823.

Yu, H., Kago, G., Yellman, C.M., and Matouschek, A. (2016). Ubiquitin-like domains can target to the proteasome but proteolysis requires a disordered region. EMBO J. *35*, 1522-1536.

Yusupova, G., and Yusupov, M. (2014). High-resolution structure of the eukaryotic 80S ribosome. Annu. Rev. Biochem. *83*, 467-486.

Zhang, J., Harnpicharnchai, P., Jakovljevic, J., Tang, L., Guo, Y., Oeffinger, M., Rout, M.P., Hiley, S.L., Hughes, T., and Woolford, J.L., Jr. (2007). Assembly factors Rpf2 and Rrs1 recruit 5S rRNA and ribosomal proteins rpL5 and rpL11 into nascent ribosomes. Genes Dev. *21*, 2580-2592.



Zhang, Y., Sinning, I., and Rospert, S. (2017). Two chaperones locked in an embrace: structure and function of the ribosome-associated complex RAC. Nat. Struct. Mol. Biol. *24*, 611-619.

Zhou, Y., Musalgaonkar, S., Johnson, A.W., and Taylor, D.W. (2019). Tightly-orchestrated rearrangements govern catalytic center assembly of the ribosome. Nat. Commun. *10*, 958.

Zientara-Rytter, K., and Subramani, S. (2019). The Roles of Ubiquitin-Binding Protein Shuttles in the Degradative Fate of Ubiquitinated Proteins in the Ubiquitin-Proteasome System and Autophagy. Cells *8*.

Zuin, A., Isasa, M., and Crosas, B. (2014). Ubiquitin signaling: extreme conservation as a source of diversity. Cells *3*, 690-701.